The role of the periplasmic chaperones SurA, Skp and DegP in fitness, outer membrane integrity, antibiotic susceptibility and virulence of *Acinetobacter baumannii*: same-same, but different?

Dissertation
der Mathematisch-Naturwissenschaftlichen Fakultät
der Eberhard Karls Universität Tübingen
zur Erlangung des Grades eines
Doktors der Naturwissenschaften
(Dr. rer. nat.)

vorgelegt von
Karolin Birkle (geb. Leibiger)
aus Ludwigsburg

Tübingen 2021

Gedruckt mit Genehmigung der Mathematisch-Naturwissenschaftlichen Fakultät der Eberhard Karls Universität Tübingen.

Tag der mündlichen Qualifikation:	11.06.2021
Dekan:	Prof. Dr. Thilo Stehle
1. Berichterstatter:	PD Dr. Monika Schütz
2. Berichterstatter:	Prof. Dr. Samuel Wagner

Für meine Familie

Table of contents

Abbreviations

Acinetobacter baumannii	*Ab*
Acinetobacter calcoaceticus - Acinetobacter baumannii complex	Acb
Aminoglycoside modifying enzymes	AMEs
Antimicrobial peptides	AMPs
β-barrel assembly machinery	BAM
Dithiothreitol	DTT
Ethylenediaminetetraacetate	EDTA
Escherichia coli	*Ec*
Inner membrane	IM
Intensive care units	ICUs
Lipooligosaccharide	LOS
Lipopolysaccharide	LPS
Mass spectrometry	MS
Membrane fractions	MEM
Multidrug-resistant	MDR
Neisseria meningitidis	*Nm*
Optical density at 600 nm	OD_{600nm}
Outer membrane	OM
Outer membrane proteins	OMPs
Outer membrane vesicles	OMVs
Over night	ON
Polymerase chain reaction	PCR
Pseudomonas aeruginosa	*Pa*
Phosphate buffered saline	PBS

Resistance-nodulation-division family	RND
Real time PCR	RT-PCR
Seventeen kilodalton protein	Skp
Sodiumdodecylsulfate	SDS
Survival protein A	SurA
Tris(hydroxymethyl)aminomethane	Tris
Type 4 pili	T4P
Type II secretion system	T2SS
Type VI secretion system	T6SS
Whole cell lysate	WCL
World health organization	WHO
Yersinia enterocolitica	*Ye*

Summary

The number of nosocomial infections with multidrug-resistant (MDR) strains of *Acinetobacter baumannii* (*Ab*) rises worldwide. Hence, MDR *Ab* became the leading pathogen for which the development of novel antibiotics is of utmost importance. The extreme antibiotic resistance of *Ab* is especially provided by the composition of its outer membrane (OM). Tightly regulated and specific outer membrane proteins (OMPs) contribute to the efficient barrier function as well as the virulence of *Ab*. Upon biogenesis, nascent OMPs are guided through the periplasm to the β-barrel assembly machinery (BAM) by periplasmic chaperones. The BAM finally enables insertion of OMPs into the OM. In most Gram-negative bacteria SurA, Skp and DegP represent the major periplasmic chaperones. In *Escherichia coli* (*Ec*), *Yersinia enterocolitica* (*Ye*) as well as *Pseudomonas aeruginosa* (*Pa*) a reduced OM integrity, as well as an increased susceptibility against antibiotics could be observed upon the deletion of SurA. Therefore, the aim of this work was to determine the relevance of SurA and the two other periplasmic chaperones, Skp and DegP in *Ab*. Markerless single gene knockout mutants for *surA*, *skp* and *degP* were created in AB5075, a highly virulent MDR *Ab* strain, and analyzed with regards to consequences on OM integrity, antibiotic susceptibility and virulence. In contrast to what has been observed for other Gram-negative pathogens, in *Ab* only weak phenotypes resulted. Also, the concurrent lack of *surA* + *skp*, *surA* + *degP*, and *skp* + *degP*, which is lethal in *Ec*, was tolerated well by AB5075. Most surprisingly, even a triple knockout strain, lacking all three periplasmic chaperones was viable. A mass spectrometric analysis revealed no significant reduction in the abundance of the major OMPs of *Ab* including OmpA and CarO. Thus, our findings suggest the existence of mechanisms that allow *Ab* to tolerate or compensate for the concurrent lack of the three periplasmic chaperones SurA, Skp and DegP.

Zusammenfassung

Die Zahl der Pathogene die gegen nahezu alle kommerziell verfügbaren Antibiotika resistent sind, ist in den letzten Jahren weltweit gestiegen. Vor allem für das multiresistente Bakterium *Acinetobacter baumannii* (*Ab*) ist die Entwicklung neuer Antibiotika oder alternative therapeutische Optionen dringend notwendig. Insbesondere in Krankenhäusern verursachen multiresistente Stämme von *Ab* eine große Anzahl an schwer therapiebaren Infektionen. Wichtige Faktoren, die zur Virulenz, Resistenz und der schwierigen Therapierbarkeit von *Ab* beitragen sind die geringe Permeabilität der äußeren Membran sowie zahlreiche Außenmembranfaktoren, die direkt oder indirekt mit der Resistenz bzw. Virulenz von *Ab* verknüpft sind. Während ihrer Biogenese werden äußere Membranporteine mit Hilfe periplasmatischer Chaperone, zu einem in der Außenmembran verankerten Multiproteinkomplex, dem BAM-Komplex (**β**-barrel **a**ssembly **m**achinery (BAM)) transportiert, der ihre Insertion in die äußere Membran katalysiert. In Gram-negativen Bakterien repräsentieren SurA, Skp sowie DegP die wichtigsten periplasamtischen Chaperone. Durch eine Deletion von SurA wurden in *Escherichia coli* (*Ec*), *Yersinia enterocolitica* (*Ye*) und *Pseudomonas aeruginosa* (*Pa*) eine stark beeinträchtigte Außenmembranintegrität sowie eine erhöhte Sensitivität gegenüber Antibiotika verursacht. Das Ziel dieser Arbeit war daher, die Relevanz der periplasmatischen Chaperone SurA, Skp und DegP für die Virulenz und Antibiotikaresistenz von *Ab* zu untersuchen. Dafür wurden genomische Knockouts für *surA*, *skp* und *degP* generiert. Diese Knockout-Mutanten wurden anschließend bezüglich ihrer Außenmembranintegrität, ihrer Sensitivität gegenüber Antibiotika, bezüglich ihrer Virulenz analysiert. Im Gegensatz zu den starken Phänotypen, die bei Einzelmutanten in anderen Gram-negativen Pathogenen beobachtet wurden, gab es in *Ab* nur sehr schwach ausgeprägte Phänotypen. Selbst die gleichzeitige Deletion von *surA* + *skp*, *surA* + *degP* und *skp* + *degP* führte in *Ab* nur zu vergleichsweise schwachen Effekten. In *Ec* dagegen ist bekannt, dass ein Doppel-Knockout letal ist. Überraschenderweise war in *Ab* sogar eine Triple-Mutante, in der alle der drei periplasmatischen Chaperone gleichzeitig deletiert wurden, lebensfähig. Massenspektrometrische Analysen zeigten in dieser Triplemutante keine signifikante Reduktion der wichtigsten äußeren Membranproteine von *Ab*, darunter OmpA und CarO. Zusammenfassend, weisen die Daten in dieser Arbeit darauf hin, dass in *Ab* ein Mechanismus existiert, der dazu führt, dass *Ab*, die simultane Deletion von SurA, Skp und DegP tolerieren bzw. kompensieren kann.

1 Introduction

1.1 *Acinetobacter baumannii,* rise of the most successful nosocomial pathogen

The discovery of the antibacterial activity of penicillin in 1928 can be considered as the starting point of the golden era of antibiotics (Fleming, 2001; Zaffiri et al., 2012). It initiated the revolution of modern medicine and in the following, a variety of antimicrobial substances were discovered. Infectious diseases, including tuberculosis and pneumonia, that previously caused high morbidity and mortality, could now be successfully treated (Zaffiri et al., 2012). However, shortly after the commencing use of penicillin antibiotic resistant bacteria arose (Abraham and Chain, 1940). In the following years, bacteria evolved resistance mechanisms against almost any newly developed antimicrobial agent, and antibiotic resistance was soon recognized as a global problem (Cohen, 1992; Kunin, 1983; Neu, 1992). Especially bacteria concurrently resistant to a variety of antibiotics, so called multidrug-resistant bacteria (MDR), challenge the global health system (Calvert et al., 2018). At the same time, the development of new antimicrobial agents decreased significantly in the past decades (Boucher et al., 2009). These days, MDR bacteria rank among the major threats for human health (Calvert et al., 2018). The European Union in 2017 recorded 25.000 deaths per year due to infections with MDR (Asokan et al., 2019). Economically, the treatment of diseases caused by MDR results in excess costs due to prolonged hospital stays as well as the use of more expensive antibiotics (Peleg et al., 2008; Sipahi, 2008; Spellberg and Rex, 2013). Thus, it is a tremendous challenge for the global health system to invent new antimicrobial agents and antibiotics active against MDR. In 2017 the world health organization (WHO) published a list with 12 MDR species categorized as critical, high or medium resistant against antibiotics. The list prioritized the pathogens according to the urgency with which research and development of new antibiotics needs to be carried out. Top-listed was the carbapenem-resistant pathogen *Acinetobacter baumannii* (*Ab*) (Tacconelli et al., 2018). *Ab* has evolved a variety of resistance mechanisms as well as different strategies to persist in the hospital environment (Ayoub Moubareck and Hammoudi Halat, 2020; Dijkshoorn et al., 2007). Because of its tremendous adaptability, *Ab* is justifiably considered as ´priority 1´ by the WHO (Tacconelli et al., 2018). Aim of the work presented herein was therefore to validate novel drug targets previously identified in other Gram-negative pathogens in *Ab*.

1.1.1 Origin and characteristics

The genus *Acinetobacter* comprises strictly aerobic, Gram-negative, non-motile coccobacilli (Peleg et al., 2008). After a long history of taxonomic studies, *Acinetobacter* species currently are specified as members of the γ-*Proteobacteria* belonging to the family of *Moraxellaceae* (Rossau et al., 1991). The first strain of *Acinetobacter* was isolated by Martinus Willem Beijernick from soil in 1911. At this time, *Acinetobacter* was termed *Micrococcus calcoaceticus* (Beijerinck, 1911). Decades later, Brisou and Prévot proposed a novel genus *Acinetobacter* to discriminate between non-motile and motile bacteria within the genus *Achromobacter* (Brisou and Prevot, 1954). Performing DNA hybridization studies in 1986, Bouvet and Grimont could distinguish 12 species within the genus *Acinetobacter*, including *Ab* and *Acinetobacter calcoaceticus* (Bouvet and Grimont, 1986). To date, over 50 *Acinetobacter* species are designated. Most of them are nonpathogenic species living in natural reservoirs like wetlands, wastewater and ponds (Al Atrouni et al., 2016; Harding et al., 2018). However, the genus *Acinetobacter* also comprises pathogenic species, like *Ab*, currently challenging the global health system (Higgins et al., 2010a; Perez et al., 2007). In contrast to other pathogenic *Acinetobacter* species, *Ab* is primarily a nosocomial pathogen and has no known natural habitat (Peleg et al., 2008). Between 2003 and 2005 *Ab* was repeatedly isolated from wounds of US soldiers involved in military operations in Iraq. It was speculated that the source of these infections was contaminated soil (Camp and Tatum, 2010; Davis et al., 2005). However, later it was demonstrated that the increased infection rate of soldiers in Iraq with *Ab* was caused by contaminated field hospitals and health-care facilities (Scott et al., 2007).

1.1.2 Clinical importance

In the 1960s *Ab* did not receive much attention when it was isolated from clinical samples, and was generally considered as a low-grade pathogen. However, over the years the clinical importance of *Ab* infections has increased tremendously (Bergogne-Berezin and Joly-Guillou, 1991; Bergogne-Berezin and Towner, 1996; Joly-Guillou, 2005). The most pertinent health care-associated pathogens are included in the *Acinetobacter calcoaceticus - Acinetobacter baumannii* complex (Acb), compromising the closely related species *A. baumannii*, *A. calcoaceticus*, *A. nosocomialis, A. pittii*, *A. seifertii*, and *A. dijkshoornia* (Bernards et al., 1996; Cosgaya et al., 2016; Gerner-Smidt, 1992; Gerner-Smidt et al., 1991; Nemec et al., 2015; Nemec et al., 2011). Because of the high similarity in genotype and phenotype, the distinction of the Acb complex is limited to detection of species-specific gene cluster using PCR-based methods (Higgins et al., 2010b; Higgins et al., 2007; Turton et al., 2006). Followed by *A. pittii* and *A. nosocomialis*, *Ab* represents the most considerable pathogen associated with nosocomial infections (Chuang et al., 2011; Chusri et al., 2014; Fitzpatrick et al., 2015; Lee et al., 2011; Wisplinghoff et al., 2012). Additionally, *Ab* strains appear to be more virulent compared to other *Acinetobacter* species (Wong et al., 2017).

Especially the rapid increase of MDR *Ab* strains has led to an upsurge of nosocomial infections and severe restriction of therapeutic options (Bergogne-Berezin and Towner, 1996; Joly-Guillou, 2005; Peleg et al., 2008). In comparison to other *Acinetobacter* species, or other Gram-negative pathogens like *Pseudomonas aeruginosa* (*Pa*), the number of MDR *Ab* strains is significantly higher (Chuang et al., 2011; Giammanco et al., 2017; Wisplinghoff et al., 2012). From 2004 to 2014 the number of isolated MDR strains rose by 40% (Giammanco et al., 2017). Nowadays, the majority of *Ab* strains isolated worldwide is resistant against almost the entire repertoire of accessible antibiotics excluding those that have shown a decreased effect or a higher toxicity, and are thus called extreme drug- resistant (XDR) (Infectious Diseases Society of, 2012; Wong et al., 2017).

Considering the ability to "escape" the bactericidal effects of antibiotics, *Ab* was grouped among other pathogens in the so called ESKAPE group, comprising ***E****nterococcus faecium*, ***S****taphylococcus aureus,* ***K****lebsiella pneumoniae,* ***A****cinetobacter baumannii,* ***P****seudomonas aeruginosa*, and ***E****nterobacter* species. In addition to the increased resistance against antibiotics, pathogens of the ESKAPE group are responsible for the majority of nosocomial infections worldwide (Boucher et al., 2009; Rice, 2008). *Ab* causes various nosocomial infections including pneumonia, meningitis, and endocarditis as well as infections of soft-tissues, the bloodstream or the urinary-tract (Dijkshoorn et al., 2007). Usually, *Ab* poses no danger to people with a fully functional immune system. Risk factors predisposing for an *Ab* infection include a prolonged stay in the hospital, immunosuppression, or exposure to contaminated medical equipment like catheters or ventilators (Garcia-Garmendia et al., 1999; Garcia-Garmendia et al., 2001; Gomez et al., 1999; Mulin et al., 1995; Wisplinghoff et al., 1999). As an opportunistic nosocomial pathogen, *Ab* mainly affects immunocompromised or critically ill patients in intensive care units (ICUs) (Dijkshoorn et al., 2007). In 2009, *Ab* accounted for 3.7% to 19.2% of infections in ICUs worldwide, depending on the geographical region that was analyzed (Vincent et al., 2009). In ICUs, *Ab* most frequently causes central-line associated bloodstream infections or ventilator-associated pneumonia caused by contaminated medical equipment (Bernards et al., 2004; Sievert et al., 2013; Weiner et al., 2016). These infections are often associated with the ability of *Ab* to persist on different surfaces over an extended period of time (Getchell-White et al., 1989; Giannouli et al., 2013; Jawad et al., 1998; Wendt et al., 1997). Additionally, many *Ab* stains show a significantly reduced susceptibility against commonly used disinfectants (Martro et al., 2003; Wisplinghoff et al., 2007). In sum, the development of manifold mechanisms to resist the bactericidal environment in a hospital, including the use of disinfectants and antibiotics, make *Ab* to the most successful nosocomial pathogen of these days.

1.2 Model strain *Ab* AB5075

For the present study the MDR *Ab* strain AB5075 was used. AB5075 was isolated in 2008 from an U.S American soldier suffering from osteomyelitis of the tibia (Jacobs et al., 2014). AB5075 is a highly virulent global clone 1 strain. It is well characterized and sequenced, making it a suitable tool for studies using *Ab* (Gallagher et al., 2015; Jacobs et al., 2014; Zurawski et al., 2012). Gallagher et al. created an accessible, comprehensive transposon mutant library for AB5075 (http://tools.uwgenomics.org/tn_mutants/) (Gallagher et al., 2015). Also the periplasmic proteome of AB5075 in absence and presence of the antibiotic imipenem has been characterized (Scribano et al., 2019). AB5075 carries three plasmids named p1AB5075, p2AB5075, and p3AB56075 consisting of 83.6 kb, 8.7 kb and 1.9 kb respectively (Gallagher et al., 2015). The large plasmid p1AB5075 harbors several resistance genes, especially mediating resistance to aminoglycosides (see also chapter resistance mechanisms) (Anderson et al., 2018; Gallagher et al., 2017; Gallagher et al., 2015). One remarkable characteristic of the strain AB5075 is its ability to switch between different phenotypes by phase variation (Tipton et al., 2015). Phase variation of AB5075 implies a rapid and reversible switch of gene expression, resulting in a heterogeneous population consisting of two phenotypical variants, macroscopically identifiable by differences in appearance (opaque and translucent colonies on specific solid media) and several virulence-associated traits (Andrewes, 1922; Henderson et al., 1999) such as biofilm and capsule formation, motility, resistance, and persistence. It could be shown that opaque variants display a more virulent and resistant phenotype compared to the translucent variants (Chin et al., 2018; Tipton et al., 2015; Tipton and Rather, 2017). The exact cues and the regulatory machinery inducing and facilitating a phase switch of *Ab* have not yet been clarified in detail. However, a high cell density and the accumulation of extracellular signaling molecules could be associated with phase variation (Tipton et al., 2015) and orthologues of the *ompR-envZ* two-component system have been identified as regulators for phase variation (Tipton and Rather, 2017). During routine overnight culturing AB5075 typically undergoes a phase variation. The result is a mixed culture of two phenotypically different populations of *Ab* characterized by different properties (Chin et al., 2018; Tipton et al., 2015; Tipton and Rather, 2017). Therefore, it is important for interpretation and reproducibility of experimental results to use pure or at least highly enriched cultures consisting of only one phase type. The usage of mixed populations containing both variants often leads to a high variability in assay outcomes. Since the opaque phase represents the variant with the higher resistance and virulence and presumably is more relevant in the host (Chin et al., 2018; Tipton et al., 2015; Tipton and Rather, 2017), only this phase was used in this work, if technically feasible. The variants can be distinguished by plating of an AB5075 culture on a special solid medium (Tipton et al., 2015). Translucent variants appear more transparent, by holding the plate against light, whereby opaque colonies appear non-transparent.

Because opaque cells generate more capsule, the variants can additionally be differentiated by performing a Maneval´s capsule stain (Hughes, 2019; Maneval, 1941).

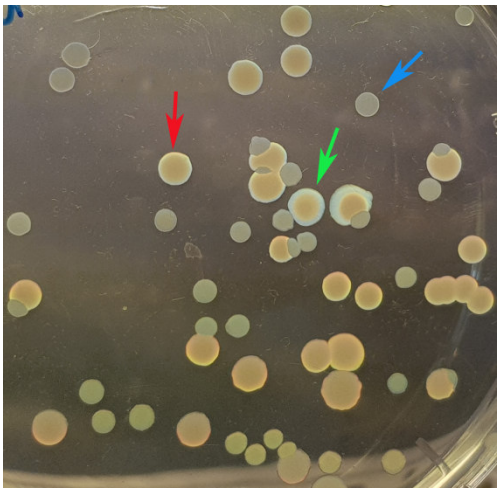

Figure 1 Mixed culture of two phenotypically different populations of *Ab* AB5075, plated on 0.5 x LB agar as described in Tipton et al. 2015. Opaque colonies are indicated by the red arrow. Translucent colonies are indicated by the blue arrow. Colonies which are currently undergoing phase switch are indicated by the green arrow

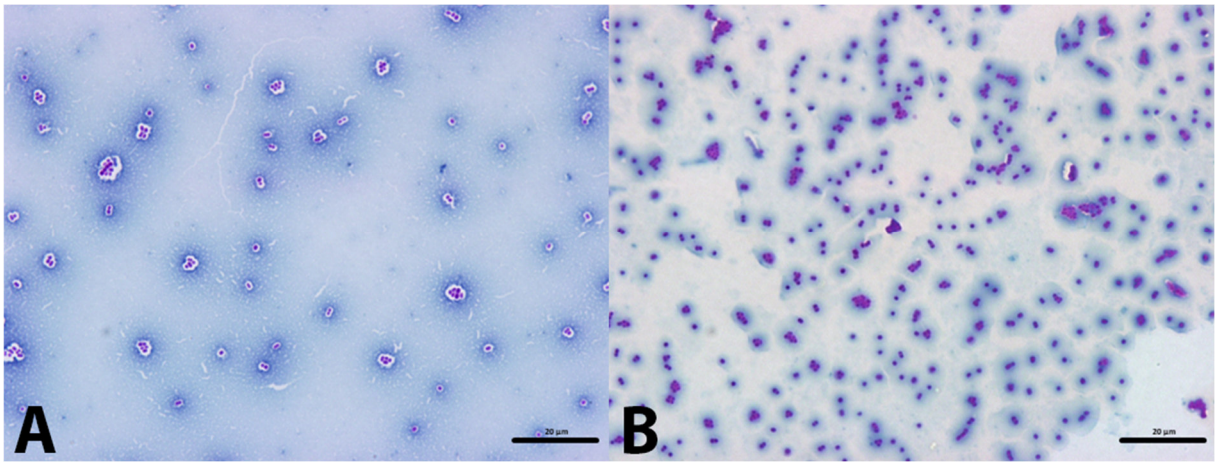

Figure 2 Maneval´s capsule stain of two phenotypically different populations of *Ab* AB5075. (A) Opaque cells with a clearly pronounced capsule surrounding the cells, visible as a halo around the pink cell. The blue background staining is excluded by the capsule, whereby the capsule appears to be white in the picture. (B) Translucent cells without a capsule. Because of the missing capsule the cells are directly surrounded by blue background.

1.3 Resistance mechanisms

The ability of *Ab* to resist the treatment with antibiotics and other bactericidal agents is accomplished by a plethora of intrinsic and acquired mechanisms (Lee et al., 2017; Vila et al., 2007). At genomic level MDR *Ab* strains possess large resistance islands (RI), integrated into their chromosomes. RIs typically comprise genes encoding for multiple resistance mechanisms (Pagano et al., 2016). As the Ab strain AYE and several others, AB5075 harbors a RI, named TnAbaR1, which is integrated into the *comM* gene (Adams et al., 2008; Gallagher et al., 2015; Kochar et al., 2012; Rose, 2010). TnAbaR1 of AB5075, however, is much shorter (13.5 kb compared to ~ 85 kb in strain AYE). Nevertheless, the RI carries several genes encoding for resistance against heavy metals as well as antibiotics (Gallagher et al., 2015). The second RI of AB5075 is present on its largest of three plasmids, p1AB5075. This RI harbors genes mediating resistance against aminoglycosides, chloramphenicol, and trimethoprim (Gallagher et al., 2015). In a mutant lacking both RIs in parallel, Gallagher et al. identified paralogs of genes on the chromosome that became essential for normal growth. This indicates that the RIs not only carry resistance genes, but also genes which can compensate the loss of essential core genes (Gallagher et al., 2017). Besides RIs, many *Ab* strains harbor insertion sequences (IS) in their genome. IS are transposable elements of 0.5 to ~ 2 kb, that enhance the expression as well as the spread of resistance genes (Pagano et al., 2016). In AB5075, four IS elements are integrated into the chromosome (IS*Aba1*, IS*Aba13*, IS*Aba113*, and IS*Ppu12*), and one (IS*Aba125*) in the p1AB5075 plasmid (Gallagher et al., 2015). Apart from these intrinsic resistance mechanisms, *Ab* is capable to acquire additional resistance genes via natural transformation or horizontal gene transfer (Ramirez et al., 2010; Valenzuela et al., 2007; Wilharm et al., 2013).

1.3.1 OM β-barrel proteins: crucial factors shaping OM permeability and susceptibility to antibiotic treatment

At the cellular level, the high intrinsic resistance of *Ab* is facilitated by a very low permeability of its OM (Vila et al., 2007; Zgurskaya et al., 2015). Because of the high prevalence of small and only minor active porins, the permeability of *Ab* for specific antibiotics is about 100-fold lower compared to *Ec* (Sugawara and Nikaido, 2012). The most abundant and best characterized OMP of *Ab* is $OmpA_{AB}$, a homolog to the OM protein F (OprF) of *Pa* and the OM protein A (OmpA) of *Ec* (Gribun et al., 2003; Jyothisri et al., 1999). Despite the large size (28-36 kDa, eight-stranded β-barrel) of the $OmpA_{AB}$ channel, the permeation rate is low, defining $OmpA_{AB}$ as a “slow porin” (Sugawara and Nikaido, 2012). Because of the high similarity to OprF of *Pa* it is assumed that $OmpA_{AB}$ is also able to switch between an open and closed conformation, whereby the closed formation is more frequently adopted (Nestorovich et al., 2006; Sugawara et al., 2006; Sugawara and Nikaido, 2012).

The carbapenem-associated OM porin (CarO, 29-kDa) was identified as the second most abundant OMP in *Ab* (Vashist et al., 2010).

Although contrary results have been published (Siroy et al., 2005; Zahn et al., 2015), the deletion or disruption of the *carO* gene was associated with resistance to the carbapenem imipenem in many strains of *Ab* (Catel-Ferreira et al., 2011; Limansky et al., 2002; Mussi et al., 2005). However, in *Ab* also other OMPs, like the 33- to 36 kDa OM protein (Omp33-36) have been associated with resistance to carbapenem antibiotics, especially imipenem (Clark, 1996; del Mar Tomas et al., 2005).

In *Pa*, the porin OprD is associated with resistance towards imipenem (Hancock and Brinkman, 2002). However, in *Ab* it is still under debate whether OprD is associated with imipenem uptake (Dupont et al., 2005; Zahn et al., 2016) or not (Catel-Ferreira et al., 2012; Smani and Pachon, 2013). Recently, Zahn et al. solved the crystal structure of OprD of the *Ab* strain AB307-0294 and renamed it to OM carboxylate channel *Ab* 1 (OccAB1). Compared to other Occ proteins, OccAB1 has a large pore-size and facilitates a relatively high uptake of small-molecules including antibiotics. Besides OccAB1 they solved the crystal structure of three further Occ proteins, which they renamed (former designations in parentheses) to OccAB2 (HcaE), OccAB3 (VanP), and OccAB4 (BenP). The fifth Occ, OccAB5, shares a significantly high similarity to OccAB4 and was not further investigated. The small pore size of OccAB2-4 could also contribute to the low permeability of *Ab* (Zahn et al., 2016). Another OM channel is represented by the OMP DcaP, which was first described in 2001 (Parke et al., 2001). Recently, the X-ray crystal structure of DcaP was solved, uncovering a trimeric porin-like structure. DcaP is involved in the uptake of substrates such as succinate, but also in the uptake of β-lactamase inhibitors including tazobactam and sulbactam. Furthermore, during infection DcaP is highly abundant in the OM (Bhamidimarri et al., 2019).

Taken together, pathogenic *Ab* species possess several OM porins which are involved in the low permeability of the OM but also in resistance against antibiotics.

1.3.2 Expression of efflux pumps

In addition to the low influx of antimicrobials or other bactericidal agents, *Ab* maintains its high resistance due to the expression of efflux pumps (Abdi et al., 2020; Vila et al., 2007). The major clinically relevant efflux pumps expressed by MDR *Ab* strains, AdeABC, AdeDE and AdeIJK belong to the resistance-nodulation-division (RND) family (Chau et al., 2004; Damier-Piolle et al., 2008; Magnet et al., 2001; Tseng et al., 1999). RND efflux pumps typically represent tripartite structures composed of an OM channel protein (AdeC and AdeK), a membrane fusion protein (MFP) (AdeA and AdeI) and a multidrug transporter (AdeB and AdeJ) facilitating the efflux of antimicrobial agents across the inner and outer membrane (Eswaran et al., 2004; Tseng et al., 1999; Zgurskaya and Nikaido, 2000).

In several studies it has been shown, that the overproduction of these efflux pumps is associated with resistance to multiple antibiotics including aminoglycosides, β-lactams, tetracyclines, carbapenems and cephalosporins (Chau et al., 2004; Damier-Piolle et al., 2008; Hou et al., 2012; Magnet et al., 2001).

1.3.3 Aminoglycoside modifying enzymes (AMEs)

Antimicrobials able to pass the OM barrier of *Ab* may be degraded by different enzymes. One of the major reasons for e.g aminoglycoside resistance of MDR *Ab* strains is the expression of AMEs, classified into acetyltransferases, nucleotidyltransferases and phosphotransferases (Benveniste and Davies, 1973; Shaw et al., 1993). These enzymes modify functional groups of aminoglycosides, resulting in decreased binding efficiency to the bacterial ribosomes, where the antibiotics act by disrupting protein synthesis (Ramirez and Tolmasky, 2010). However, extremely resistant *Ab* strains express various AMEs or even a combination of different AME classes (Nemec et al., 2004; Zhu et al., 2009).

1.3.4 Resistance to β–lactam antibiotics

Apart from aminoglycosides, MDR *Ab* strains are also often resistant to antibiotics, belonging to the class of β-lactams, such as carbapenems (Jeon et al., 2015). This resistance is facilitated by the expression of a variety of hydrolytic enzymes, so called β–lactamases (Jeon et al., 2015). There are four groups of β-lactamases (A-D), whereof three are metal-independent (A, C and D) and one is metal-dependent (B) (Ambler, 1980). Recently, Wu et al. demonstrated a direct interaction of the class D β-lactamase OXA-23 with OM porins like OmpA and CarO *in vivo*. The authors assume that this interaction keeps the enzymes near the porins where the penetration of antibiotics takes place and provides a fast enzymatic elimination of antimicrobial agents (Wu et al., 2016). This illustrates how multifactorial antibiotic resistance is facilitated in *Ab*.

In sum, the high intrinsic resistance of MDR *Ab* is facilitated by the interplay of a low permeability, the presence of aminoglycoside-modifying enzymes or β-lactamases and the constant efflux of antimicrobial agents (Fernandez-Cuenca et al., 2003; Wong et al., 2017).

1.3.5 Desiccation resistance

Besides the high resistance against a wide variety of antibiotics, a decisive factor for the clinical importance of MDR *Ab* is its ability to persist in the bactericidal environment of the hospital. In 1978, Buxton et al. revealed *Ab´*s extreme resistance against desiccation by recovering it from a contaminated washcloth after seven days (Buxton et al., 1978). Since then, many experiments demonstrated the ability of *Ab* to resist desiccation over a long period in a strain-dependent manner (Getchell-White et al., 1989; Giannouli et al., 2013; Jawad et al., 1998; Wendt et al., 1997).

The exact mechanism of desiccation tolerance is still not fully understood. However, different factors like stress-response mechanisms (Aranda et al., 2011; Farrow et al., 2018), capsule formation (Tipton et al., 2018), parts of the OM, like hepta-acylated lipid A (Boll et al., 2015) and biofilm formation (Espinal et al., 2012; Gayoso et al., 2014) could be identified as factors contributing to desiccation tolerance.

Taken together, MDR *Ab* rates among the most successful nosocomial pathogens worldwide because it has evolved multiple mechanisms mediating resistance against antibiotics or bactericidal environments (Peleg et al., 2008).

1.4 Virulence factors

Like mentioned before, *Ab* is highly virulent and more often causative for infections compared to other species of the genus *Acinetobacter* (Wong et al., 2017). Virulence of *Ab* is facilitated by manifold factors and mechanisms.

1.4.1 OM porins

Apart from functioning as selective porins, *Ab* OMPs have also been identified as virulence factors (Lee et al., 2017). In several studies, the major OMP of *Ab*. $OmpA_{AB}$, could be associated with biofilm formation (Gaddy et al., 2009), induction of cell apoptosis (Choi et al., 2005; Gaddy et al., 2009; Lee et al., 2010) and binding and invasion of host epithelial cells (Choi et al., 2008; Gaddy et al., 2009; Smani et al., 2012). Additionally, Omp33-36 (Rumbo et al., 2014; Smani et al., 2013), CarO and an OprD-like protein (Fernandez-Cuenca et al., 2011) were associated with virulence.

1.4.2 Pili and other adhesins (adhesion, motility, natural competence and biofilm formation)

MDR *Ab* strains express different types of pili to interact with biotic and abiotic surfaces, to mediate host cell invasion, to facilitate motility or to enable the formation of biofilms (Harding et al., 2018). In 1975, Henrichsen and Blom were the first to discover long polar fimbriae on the surface of an A. *baylyi* strain (Henrichsen and Blom, 1975). Nowadays, several types of pili are described as virulence factors of *Ab* (Harding et al., 2018). In spite of the lack of flagella, *Ab* is able to move across wet surfaces in a type 4 pili (T4P)-dependent manner. This movement is called twitching motility and is facilitated by the extension and retraction of T4P (Harding et al., 2013; Henrichsen, 1983; Wilharm et al., 2013). T4P are assumed to be associated also with DNA-uptake, mediating the high natural competence of *Ab* (Harding et al., 2013; Herzberg et al., 2000; Porstendorfer et al., 1997; Porstendorfer et al., 2000; Wilharm et al., 2013). Recently, Ronish et al. described differences in the surface chemistry of the T4P protein PilA within two *Ab* strains, leading to a phenotype favoring twitching motility or biofilm formation. They assumed that the tradeoff between the two phenotypes is driven by the presence of either single pili or pilus bundling in microcolonies (Ronish et al., 2019). Because of the complexity of biofilm formation, pilus bundling, however, is only one factor favoring the formation of biofilms. In some *Ab* strains the type I chaperone-usher pilus system, encoded by six genes (*csuA/BABSDE*), is crucial for biofilm formation (Tomaras et al., 2003). However, the presence of the *csuA/BABSDE* operon does not necessarily lead to the formation of Csu type pili (McQueary and Actis, 2011). McQueary et al. examined structurally different pili in clinical isolates harboring the *csuA/BABSDE* operon.

They found that a variety of types of pili is expressed by *Ab* during biofilm formation (McQueary and Actis, 2011). Additionally, it was shown that type I pili are not involved in the adherence to epithelial cells, exemplifying the complexity of *Ab* virulence (de Breij et al., 2009).

For adhesion to collagen I, III, IV and V as well as to other extracellular matrix components, a trimeric autotransporter, belonging to the type Vc secretion system, was found to be responsible (Bentancor et al., 2012). The *Acinetobacter* trimeric autotransporter (Ata) consists of a transporter domain, integrated in the OM, and a surface exposed passenger domain (Bentancor et al., 2012; Harding et al., 2018). Ata is also involved in virulence, apoptosis, adhesion to human epithelial cells and biofilm formation in *Ab* (Bentancor et al., 2012; Weidensdorfer et al., 2015; Weidensdorfer et al., 2019).

1.4.3 Secreted virulence factors

Further secretion systems have been characterized, secreting proteins including toxins, lipases or proteases which promote virulence and persistence of *Ab* (Weber et al., 2017). The lipases LipA and LipH as well as the metallopeptidase CpaA represent effectors secreted by the type II secretion system (T2SS) (Harding et al., 2016; Johnson et al., 2015). T2SSs are widely expressed among Gram-negative bacteria and were identified in *Ab* in 2014 (Eijkelkamp et al., 2014; Sandkvist, 2001). This protein complex is built up by a platform anchored to the IM, an outer-membrane complex, a pseudopilus which is evolutionary related to T4P and an ATPase as driving force (Campos et al., 2013; Korotkov et al., 2012). Proteins comprising a T2SS are encoded by 12 – 16 general secretion pathway genes (gsp) (Douzi et al., 2012). However, the exact function and interplay of the gsp genes is not fully understood. In *Ab* ATCC 17978 and *A. nosocomialis* M2 the necessity of some gsp genes (*gspD*, *gspE1* and *lipA*) for virulence as well as LipA secretion could be demonstrated using different infection models using (Harding et al., 2016; Johnson et al., 2015). Nevertheless, virulence and the secretion of LipA in mutants lacking *gspN* and *gspE2* were not affected, indicating a dispensable or different role for these genes in T2SS (Johnson et al., 2015; Wang et al., 2014). Interestingly, for processing of the pseudopili T2SSs share the prepilin peptidase PilD with T4P, demonstrating their close evolutionary relationship (Harding et al., 2016).

For interaction and killing of competing bacteria *Ab* encodes a type VI secretion system (T6SS), secreting effectors like antibacterial toxins (Carruthers et al., 2013; Fitzsimons et al., 2018; Lewis et al., 2019; Weber et al., 2013). The secretion apparatus of T6SSs is closely related and similar to the injection system of bacteriophage T4 (Brunet et al., 2014). A protein complex located in the IM (TssAEFGK), stabilized by the proteins TssMJK, serves as the baseplate of the T6SS apparatus. The effectors are bound to an injectable tube surrounded by a contractile sheath (TssBC) that is assembled by hemolysin co-regulated proteins (Hcp), proline-alanine-alanine-arginine proteins (PAAR) and valine-glycine-arginine G proteins (VgrG) at the tip. After secretion, the contracted sheath is disassembled and recycled by an ATPase (ClpV) (Zoued et al., 2014).

As mentioned above, it was suggested that T6SSs are primary used for interspecies killing in competitive environments. However, studies have shown that the expression of T6SSs is tremendously decreased, or even abrogated in MDR *Ab* strains. Thus it was assumed that MDR *Ab* strains favor the evolutionary more advantageous expression of resistance genes than the high energy consuming expression of T6SS (Repizo et al., 2015; Weber et al., 2015; Wright et al., 2014).

1.4.4 Outer membrane vesicles (OMVs)

Another strategy of *Ab* to interact with host cells and to take advantage in a competitive environment is the secretion of outer membrane vesicles. OMVs are spherical nanoparticles of a size between 20 and 300 nm, composed of lipopolysaccharides (LPS), OMPs, phospholipids, DNA or RNA and other proteins driving from the OM and periplasmic space (Kulp and Kuehn, 2010; Weber et al., 2017). The previously mentioned virulence factor $OmpA_{AB}$ represents the most abundant OMP in OMVs, and is able to induce apoptosis in host cells (Choi et al., 2005; Jin et al., 2011; Moon et al., 2012). Recently, Moon et al. demonstrated that the virulence factor Omp_{AB} is also involved in OMV biogenesis (Moon et al., 2012). In several proteomic studies, also other virulence-associated effectors could be identified in OMVs of *Ab* (Kwon et al., 2009; Li et al., 2015; Mendez et al., 2012). Interestingly, also AmpC-like as well as carbapenem-hydrolyzing class D β-lactamases, able to reduce the extracellular concentrations of antibiotics, could be detected in OMVs (Jin et al., 2011; Liao et al., 2015). Originally, the formation of OMVs has been reported as an important virulence trait, but more recently, they were repeatedly considered as a novel therapeutic strategy to prevent or ameliorate *Ab* infections. Actually, in murine sepsis infection models the vaccination with OMVs produced a strong humoral immune response and resulted in an increased survival of mice (Huang et al., 2016; Huang et al., 2014; McConnell et al., 2011).

1.4.5 Specialized systems for the acquisition of iron and other essential nutrients

During infection, essential nutrients are scarce, especially iron (Weinberg, 2009). To overcome iron limitations, Gram-negative bacteria have an effective iron homeostasis, which means the regulation of iron acquisition, storage and the expression of iron-containing proteins (Andrews et al., 2003). *Ab* possesses different iron acquisition systems (Eijkelkamp et al., 2011; Runci et al., 2019; Zimbler et al., 2009). The secretion of small proteins with a high affinity to iron, so called siderophores, is one mechanism shared by many aerobic bacteria (Saha et al., 2013).

In *Ab*, three siderophore-mediated iron acquisition systems have been identified, whereof acinetobactin is the best characterized (Dorsey et al., 2003; Mihara et al., 2004; Penwell et al., 2015; Proschak et al., 2013; Yamamoto et al., 1994). Gaddy et al. demonstrated the dependence of a functional acinetobactin expression for the persistence of the *Ab* strain ATCC 19606 in human alveolar epithelial cells. In infection models using *Galleria mellonella* caterpillars or mice, acinetobactin dependent killing was demonstrated, indicating the importance of acinetobactin not only for survival in the host but also for virulence (Gaddy et al., 2012).

Additionally, systems for zinc (Hood et al., 2012; Lonergan et al., 2019; Mortensen et al., 2014; Nairn et al., 2016) and manganese (Green et al., 2020; Juttukonda et al., 2016) acquisition have been identified and were associated with virulence.

Taken together, the high pathogenicity of MDR *Ab* strains is facilitated by multiple virulence factors. Thus, not only the development of new therapeutics that are able to kill MDR *Ab*, but also of therapeutics reducing the virulence, and thus capable to ameliorate or support the clearance of infections with *Ab*, would be highly desirable.

1.5 The cell envelope of Gram-negative bacteria

As mentioned before, the high resistance against antibiotics and bactericidal environments of *Ab* is primarily facilitated by the bacterial cell envelope and its composition. In contrast to Gram-positive bacteria, the cell envelope of Gram-negative bacteria is composed of two membranes (the inner, IM; and outer membrane, OM) (Nikaido, 2003). The IM separating the cyto- from the periplasm is a symmetric phospholipid bilayer with integral proteins or lipoproteins anchored to the inner leaflet. Besides mediating protein translocation, integral membrane proteins are involved in lipid biosynthesis and oxidative phosphorylation, both of which are usually performed by organelles in eukaryotic cells (Ruiz et al., 2006). The periplasm separates the IM and OM (Silhavy et al., 2010). Despite the lack of ATP, protein transport of nascent OMPs to the OM as well as protein degradation of misfolded proteins take place in the periplasm (Bos et al., 2007). Furthermore, the periplasm harbors a peptidoglycan layer, serving as an additional exoskeleton for stabilization of the bacterial cell (Vollmer and Holtje, 2004). A special characteristic of the OM is its asymmetry. Similar to the IM, the inner leaflet is composed of phospholipids, but the outer leaflet is mainly composed of lipopolysaccharide (LPS) or lipooligosaccharide (LOS) (Funahara and Nikaido, 1980; Kamio and Nikaido, 1976; Mühlradt and Golecki, 1975). LPS is composed of an acylated glucosamine disaccharide (lipid A), a core oligosaccharide, and a polysaccharide chain (O-antigen) varying in length (Raetz and Whitfield, 2002). LOS are composed analogous to LPS, but lack the O-antigen polymer (Preston et al., 1996).

In many bacteria, LPS or LOS are essential for cell viability and contribute both to resistance and pathogenicity (Raetz and Whitfield, 2002). Furthermore, the inhibition of LPS biosynthesis leads to the accumulation of toxic intermediates generated during LPS biosynthesis, which cannot be tolerated by many bacteria (Yuasa et al., 1969; Zhang et al., 2013). However, *Ab* (Bojkovic et al., 2015; Moffatt et al., 2010), *Neisseria meningitidis* (*Nm*) (Steeghs et al., 1998) as well as *Moraxella catarrhalis* (Peng et al., 2005) are able to compensate the loss of LPS. In *Nm*, it was first assumed that LPS deficiency was compensated by the expression of capsular polysaccharides (Steeghs et al., 2001). This theory was refuted, however, by the generation of double mutants in *Nm* lacking proteins involved in the synthesis of LPS and capsule formation (Bos and Tommassen, 2005).

The exact mechanism of how *Ab*, *Nm* and other species survive without LPS/LOS is still not understood. However, in contrast to other bacteria, *Nm* (Bos et al., 2004) and *Ab* (Bojkovic et al., 2015; Richie et al., 2016; Wei et al., 2017) are able to somehow tolerate the accumulation of toxic intermediates or may have evolved mechanisms to efficiently remove them.

A large portion of the OM composition is comprised of integral membrane proteins, so called OMPs. These OMPs typically are β–barrel proteins, and are mainly responsible for virulence and resistance (Koebnik et al., 2000; Schulz, 2002). Despite the efficient barrier function of the OM, it facilitates the import of nutrients as well as the export of toxic components by OMPs (Silhavy et al., 2010).

1.5.1 Biogenesis of outer membrane proteins

After biogenesis in the cytoplasm, nascent OMPs are guided to the Sec by the holdase SecB or by the signal recognition particle (SRP) (Tsirigotaki et al., 2017). This is facilitated by an N-terminal signal sequence. The Sec machinery itself is built up by several integral membrane proteins (SecY, SecG, SecE, SecF, SecD and YajC) mediating an efficient translocation (Mori and Ito, 2001). Sec-mediated protein translocation across the IM into the periplasm is energized by the ATPase SecA. The majority of proteins destined to the periplasm follow the Sec pathway as described, however, some proteins are translocated SecB-independently (Kihara and Ito, 1998) and the translocation of already folded proteins is mediated by the twin arginine translocation (Tat) system, encoded by the *tatABCD* operon (Frain et al., 2019). After translocation and cleavage of the signal sequence by a signal peptidase, periplasmic chaperone proteins bind the precursor OMPs to prevent aggregation and misfolding (Rollauer et al., 2015). Next, the chaperones guide the nascent OMPs through the periplasm to the β-barrel assembly machinery (BAM) which mediates the folding and insertion into the OM (Knowles et al., 2009; Noinaj et al., 2017). In *Ec*, survival factor A (SurA), the seventeen kilodalton protein (Skp) and the high temperature requirement A (HtrA) or DegP protein represent the best studied periplasmic chaperones (Goemans et al., 2014). Originally, described as a protein essential for bacterial survival during stationary phase, later on a chaperone function of SurA, important for OMP biogenesis was recognized (Lazar and Kolter, 1996; Rouviere and Gross, 1996; Tormo et al., 1990). SurA belongs to the family of peptidyl-prolyl *cis-trans* isomerase (PPIase), catalyzing cis-trans transformation in peptide bonds (Behrens et al., 2001; Rahfeld et al., 1994). It is composed of two parvulin-like PPIase domains (P1 and P2) embraced by the N- and C-terminal domain, whereby the PPIase activity was shown to exclusively reside in the P2 domain, and the specific peptide binding activity in the P1 domain (Behrens et al., 2001; Bitto and McKay, 2002; Xu et al., 2007). More recent studies revealed that SurA cycles between distinct conformational and functional states during the OMP assembly process and that both P1 and P2 are involved in regulation of these states (Calabrese et al., 2020; Jia et al., 2020).

SurA is thought to be the primary periplasmic chaperone involved in the periplasmic transport of a wide range of proteins (Goemans et al., 2014).

The deletion of *surA* led to a decreased abundancy of many OMPs, including OmpA, OmpF, OmpX, and LamB, however, often indirectly via the induction of a periplasmic stress response and subsequent downregulation of the expression of major OMPs (Rouviere and Gross, 1996; Sklar et al., 2007b; Vertommen et al., 2009; Weirich et al., 2017). Nevertheless, for some proteins like LptD and FhuA a direct SurA-dependency could be shown (Sklar et al., 2007b; Vertommen et al., 2009; Weirich et al., 2017).

In addition to SurA, other proteins with PPIase activity, namely PpiA, PpiD and FkpA, have been identified in the periplasm (Bos et al., 2007). Although a double knockout of *ppiD* and *surA* is lethal in *Ec*, a direct association of the mentioned PPIases with OMP biogenesis has not been drawn (Bos et al., 2007; Dartigalongue and Raina, 1998).

Skp is composed of a β-barrel core domain that mediates trimerisation of three α-helices, and leads to the formation of a `jellyfish`-like architecture (Korndorfer et al., 2004; Walton and Sousa, 2004). Because of significant structural similarities to the eukaryotic holdase prefoldin, it was suggested that Skp also is a chaperone belonging to the holdase family (Walton and Sousa, 2004). While the substrate-binding cavity of Skp is comparably small, a large substrate-profile including several OM proteins as well as periplasmic proteins could be detected (Chen and Henning, 1996; Jarchow et al., 2008; Walton and Sousa, 2004). In contrast to *Ec*, with SurA playing the major role in OMP biogenesis, in *Nm* Skp seems to be the most relevant periplasmic chaperone (Volokhina et al., 2011).

Belonging to the HtrA serine proteases family, DegP was first initially described as a periplasmic protease essential for survival of *Ec* at higher temperatures (Lipinska et al., 1989; Lipinska et al., 1990; Skorko-Glonek et al., 1995; Strauch et al., 1989). DegP contains a N-terminal catalytic domain linked to two PDZ domains at the C terminus (Krojer et al., 2002). The proteolytic activity of DegP could be linked to the PDZ1 domain, whereas the PDZ2 domain was not essential for protease activity (Jomaa et al., 2007; Spiess et al., 1999). Structural analyses have shown that in absence of substrates DegP forms a homohexamer assembled by two trimeric rings (Krojer et al., 2002). However, after binding to a substrate DegP is capable to form higher-order oligomers (12-mer and 24-mer), providing a large catalytic cavity (Jiang et al., 2008; Krojer et al., 2008). The expression of DegP is regulated by the σ^E and Cpx signaling pathways, primarily responding to envelope stress (Alba and Gross, 2004; Danese et al., 1995). Using the native substrate MalS, first evidence for an additional chaperone activity of DegP in a temperature-dependent fashion was provided (Spiess et al., 1999). As for Skp and SurA several OMPs, including OmpA, OmpF and LamB, could be identified as substrates of DegP (Krojer et al., 2008).

A model for the transport of nascent OMPs by the main periplasmic chaperones SurA, Skp and DegP, has been proposed. In this model, SurA acts as the primary chaperone, and Skp and DegP act together in a parallel pathway, but play a minor role in OMP biogenesis in *Ec* (Rizzitello et al., 2001; Sklar et al., 2007b).

After the transport through the periplasm, nascent OMPs are assembled and integrated in the OM, by the BAM. In *Ec* the complex is assembled by the β-barrel protein BamA, containing five polypeptide transport-associated (POTRA) domains, and the four lipoproteins BamBCDE (Noinaj et al., 2017). BamA and BamD are essential components of the BAM in *Ec* (Malinverni et al., 2006; Wu et al., 2005) as well as in *Nm* (Volokhina et al., 2011). The deletion of the other components of the BAM is not lethal, but the loss of BamB eventually results in reduced OM density (Malinverni et al., 2006; Onufryk et al., 2005; Sklar et al., 2007a; Sklar et al., 2007b; Wu et al., 2005). This could also be demonstrated for *Ye* (Weirich et al., 2017). Although the existence of an open and closed confirmation of BamA could be demonstrated, the exact mechanism of protein assembly and OM integration is not fully understood yet (Wu et al., 2020). However, different models for OMP assembly by the BAM have been proposed (Noinaj et al., 2017; Wu et al., 2020). The first model, describes the multiprotein complex as a trafficking complex, whereby the insertion of the OMPs is only assisted by the BAM. Here, BamA leads to a destabilization of the OM where nascent or pre-folded OMPs, guided by SurA, are directly inserted in the OM. In the second model, the BAM complex systematically folds the OMPs in the OM strand by strand by the formation of a BamA-OMP hybrid barrel. Afterwards the newly synthesized OMPs are separated from BamA in a budding-like mechanism (Wu et al., 2020). Recently, a variation of this model has been proposed in which the OMP is assembled at the interphase of the OM and the separation from BamA is facilitated by swinging motions of BamA (Doyle and Bernstein, 2019).

1.5.2 Periplasmic chaperones as new drug targets?

The composition of the OM is responsible for the tight barrier function of Gram-negative bacteria. Since periplasmic chaperones decisively influence the composition of the OM, the interest in assessing their potential to serve as new drug targets in different pathogens is increasing (Justice et al., 2006; Klein et al., 2019; Watts and Hunstad, 2008; Weirich et al., 2017).

Because SurA is the primary chaperone for many OMPs in *Ec*, its deletion leads to a reduced abundance of several OMPs and results in a profound rearrangement of the OM composition. Effects of a lack of a SurA can either be mediated directly, e.g. if OM proteins are inserted into the OM strictly SurA-dependent, or also indirectly as is the case e.g. for LPS. The OMP LptD, which is crucial for LPS insertion into the OM, is one of the strictly SurA-dependent proteins in *Ec* and also *Ye* and *Pa*. Therefore, a lack of SurA indirectly induces changes in LPS assembly and insertion by impairment of LptD biogenesis. As a consequence of OM rearrangements, the sensitivity against detergents like bile salts increases in *surA* mutant strains (Lazar and Kolter, 1996; Rouviere and Gross, 1996; Sklar et al., 2007b). Interestingly, in *Pa* the deletion of SurA seems to be even lethal. However, experiments using a conditional knockout of SurA showed a reduction of OM integrity, resistance against human serum and antibiotics, and virulence (Klein et al., 2019).

A decreased virulence upon a lack of SurA could also be observed in species of the genus *Yersinia*, including *Ye* (Weirich et al., 2017), *Yersinia pestis* (Southern et al., 2016) and *Yersinia pseudotuberculosis* (Obi et al., 2011) as well as in *Shigella flexneri* (Purdy et al., 2007), *Salmonella enterica* (Sydenham et al., 2000; Tamayo et al., 2002), and especially in uropathogenic *Ec* (Hunstad et al., 2005; Justice et al., 2006; Watts and Hunstad, 2008).

Playing only a minor role in the biogenesis of OMPs in *Ec* and *Pa*, the deletion of *skp* results in less significant phenotypes (Klein et al., 2019; Sklar et al., 2007b). However, for some OMPs (OmpA, OmpC, OmpF, and LamB) a decreased abundancy could be detected in mutants lacking Skp (Chen and Henning, 1996). In *Ye* the deletion of *skp* led to increased susceptibility towards treatment with human serum and a reduced virulence in a mouse infection model, albeit to a lesser extent compared to the deletion of *surA* (Weirich et al., 2017). A knockout of the *skp* gene led to a reduction of virulence in *Salmonella Typhimurium* (Rowley et al., 2011). In *Nm*, in which Skp seems to be the major chaperone, the lack of Skp leads to reduced levels of the OMPs PorA and PorB (Volokhina et al., 2011). Very recently, it could be shown that the deletion of *skp* leads to a hyposensitivity against antimicrobial peptides (AMPs) in *Salmonella Typhimurium* (Kapach et al., 2020).

An effect on virulence could be also demonstrated upon the deletion of *degP* in several species, including *Ec* (Redford and Welch, 2006), *Klebsiella pneumoniae* (Cortés et al., 2002), *Salmonella Typhimurium* (Mo et al., 2006), and *Pa* (Yorgey et al., 2001). In *Shigella flexneri*, the loss of DegP results in a reduced intracellular spread, which represents an important virulence trait (Purdy et al., 2007; Purdy et al., 2002). Furthermore, Fu et al. demonstrated the importance of DegP in bacterial acid resistance in *Ec* (Fu et al., 2018).

The knockout of *surA* and *skp* or *surA* and *degP* in parallel is not tolerated by *Ec*. This demonstrates not only functional redundancy, but also emphasizes the potential of periplasmic chaperones as novel drug targets. (Rizzitello et al., 2001).

Apart from the periplasmic chaperones, also components of the BAM complex could be considered as potential new drug targets. A variety of novel compounds, including JB-95 (Urfer et al., 2016), MRL-494 (Hart et al., 2019), darobactin (Imai et al., 2019), as well as the antibody MAB1 (Storek et al., 2018), were found to inhibit BamA function and thereby induced a reduction of membrane barrier function or even acted bactericidal.

In *Ye*, the deletion of *bamB* led to comparable phenotypes compared to that caused by the deletion of *surA* including reduced abundance of specific OMPs, increased susceptibility towards complement induced killing, decreased sensitivity toward specific antibiotics, as well as decreased virulence (Weirich et al., 2017).

Taken together, the disruption and deletion of the OMP biogenesis machinery lead to significant changes in antibiotic resistance, OM integrity and composition as well as virulence. For this reason, the components of OMP biogenesis, especially periplasmic chaperones, represent promising novel drug targets for the treatment of infections caused by MDR Gram-negative pathogens.

2. Aim of the thesis

Infections with MDR *Ab* strains have become a major health problem worldwide. Especially the capability of *Ab* to colonize and persist on items in the hospital environment and the lack of adequate treatment options is very challenging. Since the frequency of infection rises, and consequently also the number of fatal cases new therapeutic options need to be developed. One strategy that became more popular in the recent years is not to aim at the killing of pathogens (which exerts high selection pressure and thereby fosters the rise and spread of resistance), but to disarm them, or to re-sensitize them to antibiotic treatment. To disarm means to reduce the virulence of pathogens by specifically blocking the function or biogenesis of virulence factors. Thereby the host can be enabled to clear infections by itself. Re-sensitization means to circumvent resistance mechanisms, e.g. by blocking antibiotic inactivating enzymes, as is already done by using combinations of beta-lactam antibiotics and beta-lactamase inhibitor. Re-sensitization, however, could also be achieved by enhancing the entry of antibiotics into the bacterial cells, e.g. by impairing the OM barrier function. Previously, the potential of the periplasmic chaperones SurA, Skp and DegP in *Ye* and *Pa* to serve as novel targets for therapeutics has been tested. Both a reduction of virulence and/or a break of antibiotic resistance could be demonstrated. Especially a knockout of SurA reduced virulence in both *Ye* and *Pa*, and moreover, re-sensitized a multidrug-resistant clinical bloodstream isolate of *Pa* to antibiotic treatment (Klein et al., 2019; Weirich et al., 2017).

Therefore, the aim of this work was to examine the potential of the periplasmic chaperones SurA, Skp and DegP to serve also as antivirulence/resistance breaker targets in *Ab*.

To achieve this, the following tasks were to be fulfilled:

(1) Creation and verification of deletion mutants lacking SurA, Skp or DegP in the highly virulent MDR strain *Ab* AB5075. Therefore, a protocol for efficient creation of marker-less gene knockouts had to be established.

(2) Phenotypic characterization of the created mutant strains with regards to general fitness and the desired phenotypes (membrane integrity, antibiotic susceptibility, virulence associated traits and virulence in an infection model).

(3) Assessment of changes in the OMP composition caused by the deletion of the periplasmic chaperones by mass spectrometric analyses (MS).

(4) Assessment of virulence-associated phenotypes and virulence in an infection model (*Galleria mellonella*).

Declaration of contributions

Parts of this thesis will be published in the paper "An unprecedented tolerance to deletion of the periplasmic chaperones SurA, Skp and DegP in the nosocomial pathogen *Acinetobacter baumannii"* by Birkle et al.. The following table lists the authors of the paper as well as their contributions. Additionally, in each chapter a declaration of contributions of the authors are written.

Author	**Author position**	**Scientific ideas %**	**Data generation %**	**Analysis & Interpretation %**	**Paper writing %**
Karolin Birkle	1	15	80	15	40
Fabian Renschler	2	5	5	5	5
Angel Angelov	3	0	5	5	5
Gottfried Wilharm	4	0	0	5	0
Mirita Franz-Wachtel	5	0	5	5	5
Boris Maček	6	0	5	5	0
Erwin Bohn	7	30	0	20	0
Monika Schütz	8	50	0	40	45
Titel of paper:	An unprecedented tolerance to deletion of the periplasmic chaperones SurA, Skp and DegP in the nosocomial pathogen *Acinetobacter baumannii*				
Status in publication process:	Submitted to: International Journal of Medical Microbiology (21.01.2021) Status: „Under Review "				

3. Materials

Declaration of contributions

The plasmids and strains ("Table *1*) of section 3.1 as well as the oligonucleotides ("Table *4*) of section 3.4 are the same to be published in Birkle et al. (manuscript submitted). The tables are literally taken from Birkle et al. (manuscript submitted) and are highlighted with quotation marks as well as written in italics. The manuscript Birkle et al. (manuscript submitted) was mainly written by PD Dr. Monika Schütz and me.

"3.1. Plasmids and strains"

"Table 1: Plasmids and strains used in this study."

Plasmid	***Resistance marker***	***Cassette for counter selection***	***Parent plasmid***	***Strains generated with***	***Source of plasmid***
pVT77	*tellurite*	*$lacI_q$-P_{trc}-lacO-tdk*	*-*	*-*	*GenScript / (7)*
surA_pVT77	*tellurite*	*$lacI_q$-P_{trc}-lacO-tdk*	*pVT77*	*AB5075_ΔsurA* *AB5075_ ΔsurA / ΔdegP* *AB5075_ ΔsurA / Δskp* *AB5075_ΔsurA/Δskp/ΔdegP*	*GenScript*
skp_pVT77	*tellurite*	*$lacI_q$-P_{trc}-lacO-tdk*	*pVT77*	*AB5075_Δskp* *AB5075_ΔsurA/ Δskp* *AB5075_Δskp/ ΔdegP* *AB5075_ΔsurA/Δskp/ΔdegP*	*This study*
degP_pVT77	*tellurite*	*$lacI_q$-P_{trc}-lacO-tdk*	*pVT77*	*AB5075_ΔdegP* *AB5075_ΔsurA/ ΔdegP* *AB5075_Δskp/ ΔdegP* *AB5075_ΔsurA/Δskp/ΔdegP*	*This study*

3.2 Culture Media for Bacteria

Table 2: Liquid and solid culture media for bacteria used in this study

Culture medium	Ingredients
Liquid culture media	
LB Broth (Miller)	10 g tryptone 10 g NaCl 5 g yeast extract ad 1 l ddH_2O
Mueller Hinton Broth II (MHB II)	3 g beef extract 1.5 g starch 17.5 g acid hydrolysate of casein ad 1 l ddH_2O
Solid culture media	
Luria Bertani (LB) agar (Miller)	10 g tryptone 5 g yeast extract 10 g NaCl 15 g agar ad 1 l ddH_2O
Agar for transformation via twitching motility	2,5 g tryptone 1,25 g NaCl 2,5 g agar ad 500 ml ddH_2O
0,5 x Agar for visualization of phase variation	5 g tryptone 2,5 g NaCl 2,5 g yeast extract 8 g agar ad 1 l ddH_2O

3.3 Buffers and solutions

Table 3: Buffers and solutions used in this study

Buffer/solution	Ingredients
5 x SDS running buffer	60.4 g Tris base 288 g Glycine 20 g SDS ad 2 l ddH_2O
5 x TBE electrophoresis buffer	54 g Tris base 27.5 g boric acid 20 ml 0.5 M EDTA (pH 8) ad 1 l ddH_2O
10 x Western blot transfer buffer	60.4 g Tris base 288 g Glycine ad 2 l ddH_2O
10 x Western- wash buffer	24.2 g Tris base 180 g NaCl 100 ml Tween 20

	adjust to pH 7.4 with HCl ad 2 l ddH_2O
Blocking buffer	0.3 g BSA ad 10 ml PBS
Extraction buffer	50 mM Tris 10 mM MgCl2 2% TritonX-100
HPLC solvent A	0.1% formic acid
HPLC solvent B	80% acetonitrile 0.1% formic acid
Lysis buffer	10 mM Tris 1 mM MgCl2 5 mM EDTA 0.2 mM DTT pH 7,5
PBS-T 0.1 %	100 µl Tween 20 ad 100 ml PBS
Resuspending buffer	0.2 M Tris 1 M Sucrose 1 mM EDTA pH 8.4
TE buffer	0.2 ml Tris-HCl 1 M (pH8) 0.04 ml EDTA 0.5 M (pH8) ad 20 ml ddH_2O

“3.4 Oligonucleotides”

“Table 4: Oligonucleotides used in this study”

Gene	Name	Sequence (5´-3´)	Expected size of PCR product (bp)
Oligonucleotides used for amplification of up- and downstream flanking regions of target genes			
skp	*skp_Up_fwd*	*AGTCAACGGCTGATATCCATTGCTGTTGACCGAAGCTGAATGATGACTATAAC*	*1165*
	skp_Up_rev	*TTATTTCATTGAATTAACCTTTTGTATCATCCCTAACATTAATTTATTTAATTTATTCATGT*	
	skp_Down_fwd	*ATGAATAAATTAAATAAATTAATGTTAGGGATGATACAAAAGGTTAATTCAATGAAATAAA*	*1178*
	skp_Down_rev	*GGATCCCCGGGTACCGAGCTCGAATTCCTCCGGTCATAATATTCTATTTACGCAAA*	
degP	*degP_Up_fwd*	*ATTCGGAACCCAGCATGATATTCCGGAAATACAAGAAAGAACGTGCTTGCGGATG*	*1077*
	degP_Up_rev	*CATTTTTATAATATTTTACTGAATACGTAAATAGCGAGATTTCATTCGGTGCTCACC*	
	degP_Down_fwd	*GTGGGTGAGCACCGAATGAAATCTCGCTATTTACGTATTCAGTAAAATATTATAAAAATGAACC*	*1072*
	degP_Down_rev	*CCGCAAGCTTCCTGCAGGCTCTAGAGGATCAGTTAAGCTGATATTCCTGCCCG*	
Oligonucleotides used for sequencing of target region after knockout			
surA	*seq_ΔSurA_FWD*	*ATTGCTGCCAACTCGGCCTG*	*WT: 2363 Mutant: 1082*
	seq_ΔSurA_REV	*CAATTGCTGTAGGTACTTCACACG*	
skp	*seq_ΔSkp_fwd*	*GGTGACTGGACTCGACAAG*	*WT: 1061 Mutant: 617*
	seq_ΔSkp_rev	*GCTGCGGTAACAATGTAAGC*	
degP	*seq_ΔDegP_fwd*	*AACACCACCTTGTGCATAGAAG*	*WT: 1989 Mutant: 642*
	seq_ΔDegP_rev	*GCATCCACTGGACATACATTAC*	
Oligonucleotides used for verification of deletion (inside primers; bind in the region intended to be deleted)			

surA	*Validation_ΔSurA_negative_fwd*	*CAAACGATACAGGTTCAGCAC*	*WT: 515* *Mutant: -*
	Validation_ΔSurA_rev	*GTACAGCTGGTAATGCTGACAAG*	
skp	*Validation_ΔSkp_negative_fwd*	*CAGCAAGGCTTACAGTCAAGAG*	*WT: 607* *Mutant: -*
	Validation_ΔSkp_rev	*CGCCAACTACACAATTCTCAC*	
degP	*Validation_ΔDegP_negative_fwd*	*CGGTAATCAAGCCTCTGCTTC*	*WT: 626* *Mutant: -*
	Validation_ΔDegP_rev	*CTTTACGGTATTGCACATGGTG*	
Oligonucleotides used for the detection of specific gene transcripts by RT-PCR			
surA	*RT-PCR_ΔSurA_FWD*	*TCCGAAGTGGTAAGCCCTGA*	*82*
	RT-PCR_ΔSurA_REV	*TAGCGAAATCTTCACCCGCT*	
skp	*RT-PCR_ΔSkp_FWD*	*ACGTCAAGCGCAGACTCAA*	*113*
	RT-PCR_ΔSkp_REV	*ACTGTAAGCCTTGCTGTGTTG*	
degP	*RT-PCR_ΔDegP_FWD*	*CCACAGCAACAAGGTCCTCA*	*116*
	RT-PCR_ΔDegP_REV	*ATACTGATGCGGGAAGCGTT*	

3.5 Kits

Table 5: Kits used in this study

Product	Manufacturer
MiSeq v2 reagent kit	Illumina, San Diego
Nextera DNA Flex Library Prep Kit	Illumina, San Diego
Plasmid Miniprep Kit II, peqGOLD	Peqlab, Erlangen
QIAamp DNA Mini Kit	Qiagen, Hilden
Wizard AV Gel and PCR Clean up System	Promega, Mannheim

3.6 Reagents and chemicals

Table 6: Reagents and chemicals used in this study

Product	Manufacturer
1-N-phenylnaphthylamine (NPN)	Acros organics / Thermo Fisher, Schwerte
Agar	Roth, Karlsruhe
Agarose, SeaKem	Lonza, Rockland (USA)
Azido-3'-deoxythymidine (AZT)	Jena Bioscience, Jena
Bile salts	Sigma-Aldrich, Taufkirchen
Clarity Western ECL Blotting Substrates	Bio-Rad, München
Congo Red solution (1%)	Carolina, New York
Descosept	Dr. Schumacher, Malsfeld
dNTP Mix (10 mM each)	Thermo Fisher, Schwerte
DpnI restriction enzyme	Thermo Fisher, Schwerte
Dithiothreitol (DTT)	Applichem, Darmstadt
Ethylenediaminetetraacetic acid (EDTA)	Merck, Darmstadt
Gene Ruler 1 kb plus DNA Ladder	Thermo Fisher, Schwerte
Glycine	Applichem, Darmstadt
Glycerol	Applichem, Darmstadt
HEPES	Roth, Karlsruhe
IPTG	Peqlab, Erlangen
KOD Hot Start DNA Polymerase (Novagen)	Merck, Darmstadt
Laemmli buffer 5x	Bio-Rad, München

Lysozyme	Sigma-Aldrich, Taufkirchen
Magnesium chloride ($MgCl_2$)	Applichem, Darmstadt
Maneval´s stain	Carolina, New York
Mercaptoethanol	Applichem, Darmstadt
Methanol	Applichem, Darmstadt
Orange G	Sigma-Aldrich, Taufkirchen
Phosphate buffered saline (PBS)	Gibco/ Thermo Fisher, Schwerte
PAGE Ruler prestained Protein Ladder (10 – 180 kDA)	Thermo Fisher, Schwerte
Polymyxin B (PMB)	Merck, Darmstadt
Protease inhibitor	Sigma-Aldrich, Taufkirchen
RNase-free water	Thermo Fisher, Schwerte
RNA storage solution	Thermo Fisher, Schwerte
Roti®-Blue Colloidal Coomassie Staining solution	Roth, Karlsruhe
Roti-Histol	Roth, Karlsruhe
Sodium chloride (NaCl)	Merck, Darmstadt
Sodium dodecyl sulfate (SDS)	Roth, Karlsruhe
Sucrose	Sigma-Aldrich, Taufkirchen
SYBR Safe DNA gel stain	Thermo Fisher, Schwerte
Tellurit	Sigma-Aldrich, Taufkirchen
Tris base	Applichem, Darmstadt
Tris(hydroxymethyl)aminomethane (Tris)	Sigma-Aldrich, Taufkirchen
Triton X-100	Applichem, Darmstadt
TRIzolTM Reagent	Thermo Fisher, Schwerte
Trularv™ *Galleria mellonella* larvae	BioSystems Technology, Crediton (England)
Tryptone	Applichem, Darmstadt
Tween 20	Merck, Darmstadt
Yeast extract	Roth, Karlsruhe

3.7 Consumables

Table 7: Consumables used in this study

Product	Manufacturer
Blotting paper sheets	Bio-Rad
Cuvettes	Sarstedt, Nümbrecht
Erlenmeyer flasks	DWK Life Scences, Mainz
E-test stripe (vancomycin)	Liofilchem, Roseto degli Abruzzi (Italy)
Glass bottles	DWK Life Scences, Mainz
Glass spatulas	WU, Mainz
Gloves (Peha-soft nitrile)	Hartmann, Heidenheim
Inoculation loops (1 µl, 10 µl)	Greiner, Frickenhausen
Lightcyler 480 multiwell plates, 96 wells	Roche, Rotkreuz (CH)
Lightcycler 480 sealing foils	Roche, Rotkreuz (CH)
Microfine insulin syringe	BD Bioscience, Heidelberg
Micronaut-S AST plates	Merlin Diagnostika, Bornheim-Hersel
Microtiter plates (polystyrene, 24 well)	Greiner, Frickenhausen
Microtiter plates (polystyrene, 96 well)	Greiner, Frickenhausen
Microtiter plates (polystyrene, 96 well, F-bottom, non-binding)	Greiner, Frickenhausen
Mueller-Hinton Broth agar plate	Oxoid/ Thermo Fisher, Schwerte
Nitrocellulose membrane (0.45 µm pore size)	GE Healthcare, Freiburg
non-breathable seal for Micronaut plates	Merlin Diagnostika, Bornheim-Hersel
PCR reaction tubes (0.2 ml)	Sarstedt, Nümbrecht
Parafilm	Brand, Wertheim
Petri dishes	Greiner, Frickenhausen
Pipettes (5 ml, 10 ml, 25 ml, 50 ml)	Corning, Amsterdam (NL)
Pipette tips (10 µl)	Brand, Wertheim
Pipette tips (200 µl)	Sarstedt, Nümbrecht
Pipette tips (1000 µl)	Greiner, Frickenhausen
Pipette tips, filter tips, sterile	STARLAB, Hamburg
Reaction tubes (1.5 ml, 2 ml)	Greiner, Frickenhausen
Reaction tubes (15 ml, 50 ml)	Greiner, Frickenhausen
Round-bottom tubes (5 ml, 14 ml)	Greiner, Frickenhausen
SDS gels, Mini-Protean TGX Precast Gel, 10%	Bio-Rad, München

3.8 Technical Equipment

Table 8: Technical equipment used in this study

Equipment	Type	Manufacturer
Analytical scale	L 2200 S	Sartorius, Göttingen
Centrifuge	5417R	Eppendorf, Hamburg
Centrifuge	Optima LE-80K	Beckmann Coulter, Krefeld
Centrifuge	Optima MAX-XP	Beckmann Coulter, Krefeld
Centrifuge	Multifuge 3S-R	Heraeus, Hanau
Electrophoresis system	Mini PROTEAN Tetra Cell	Bio-Rad, München
French Press	FA-032	Thermo Fisher, Schwerte
Gel electrophoresis chamber	Mini-Sub Cell GT	Bio-Rad, München
Gel documentation system	BioDoc Analyze	Biometra, Göttingen
Heating block	Thermomixer comfort	Eppendorf, Hamburg
Ice machine	AF 20	Scotsman, Vernon Hills (USA)
Incubator for agar plates	B6420	Heraeus, Hanau
Laminar flow safety cabinet	BDK-S 1200, 1300	Weiss, Sonnenbühl
Magnetic stirring hotplate	MR 3002	Heidolph, Schwabach
Mass spectrometer	LTQ Orbitrap Elite	Thermo Fisher, Schwerte
Microscope	BX51	Olympus, Hamburg
Microwave	Micromat	AEG, Frankfurt a.M.
NGS DNA Sequencer	MiSeq	Illumina, San Diego
Photometer	Bio Photometer	Eppendorf, Hamburg
Pipettes (2,5 µl, 10 µl, 100 µl, 200 µl, 1000 µl)	Reference; Research plus	Eppendorf, Hamburg
Pipetting aid	Easypet	Eppendorf, Hamburg
Power supply	PowerPac 200/300	Bio-Rad, München
Quantitative realtime PCR system	Lightcycler 480	Roche, Rotkreuz (CH)
Rocking shaker	Assistant RM5	Karl Hecht, Sondheim
Shaking incubator	HT	Infors, Bottmingen
Spectral photometer	NanoDrop One	Thermo Fisher, Schwerte
Tecan microplate reader	Infinite M200 Pro	Tecan,Crailsheim
Thermal cycler	C1000 Touch	Bio-Rad, München
Vortexer	Vortex Genie 2	Scientific Industries, New York (USA)

Water bath	WB 10	Memmert, Schwabach

3.9 Software and programs

Table 9: Software and programs used in this study

Software/Program	Manufacturer/Reference
Acrobat X Pro	Adobe Systems, San Jose (USA)
Adobe Photoshop CS6	Adobe Systems, San Jose (USA
BLAST (2.10.0+)	Altschul et al. 1997
ClustalΩ	Sievers et al. 2011, Zimmermann et al. 2018
DEP package ver 1.10.0	Zhang et al. 2018
EndNote X7	Clarivate Analytics, Philadelphia (USA)
Ggplot2 ver 3.3.2	Wickham et al. 2016
Glimma package ver 1.16.0	Su et al. 2017
GraphPad Prism 7.04	GraphPad Software, San Diego
ImputeLCMD package ver 2.0	Lazar, 2015
Jalview	Waterhouse et al. 2009
LightCycler 480 SW 1.5.0	Roche, Rotkreuz (CH)
Limma package ver 3.44.3	Ritchie et al. 2015
MaxQuant software package version 1.6.7.0	(Cox and Mann, 2008)
Microsoft Office 2019	Microsoft, Redmond (USA)
Nf-core/bacass pipeline	Ewels et al. 2020
SnapGene software	GSL Biotech, Chigcago (USA)
UpSetR ver 1.4.0	Conway et al. 2017
Vsn package ver 3.56.0	Huber et al. 2002

4. Methods

Declaration of contributions

The section methods including all figures and the corresponding signatures are literally taken from Birkle et al. (manuscript submitted) and are highlighted with quotation marks as well as written in italics. The numbering of the figures and tables were adjusted to this thesis.
The manuscript Birkle et al. (manuscript submitted) was written by PD Dr. Monika Schütz and me.

The “Library Preparation, Sequencing and Genome Assembly” described in chapter 4.4 as well as the section “Differential Expression Analysis of Proteomics Data” in chapter 4.15.2 was performed and written by the co-author of Birkle et al. (manuscript submitted) Dr. Angel Angelov from the NGS Competence Center Tübingen (NCCT).

The “NanoLC-MS/MS Analysis” described in chapter 4.15.1 was performed and written by the co-authors of Birkle et al. (manuscript submitted) Dr. Mirita Franz-Wachtel and Prof. Boris Maček from the Proteome Center Tübingen.

"*4.1 Cultivation of Bacteria in liquid and on solid Media*"

"AB5075 was routinely grown in LB (Miller) medium without supplements. Overnight cultures were inoculated from glycerol stocks and grown overnight without shaking at room temperature (RT) to keep the strain in an opaque state (Tipton et al., 2015). Every culture was routinely tested for the presence of a capsule as an indicator for the strain being in an opaque state by a Maneval's stain before being used for experiments. For growth on LB agar (e.g. after mutagenesis) bacteria were incubated at 37°C for 18 h with supplements if indicated. Strains and supplements used are listed in "Table 1."

"*4.2 Generation of Knockout Mutants of AB5075*"

"To generate markerless single gene deletion mutants, a plasmid harboring a knockout cassette having an appropriate selection marker (Tellurite^{Res}) was created. For amplification of the up- and downstream regions of the gene to be deleted, genomic DNA of AB5075 was isolated using the QIAamp DNA Mini Kit (Qiagen). The flanking regions of genes of interests comprising ~ 1000 bp of the 3´- and 5´- ends and a scar sequence encoding a small peptide of 30 aa (first 15 and last 15 amino acids including the start and stop codon of the gene to be deleted) were amplified by PCR using genomic DNA as template. The plasmid pVT77 (Trebosc et al., 2016) synthesized by GenScript; GenBank: KX397287.1) was linearized also by PCR and purified using the Promega Wizard SV Kit (Promega). Amplified up- and downstream fragments were fused with the linearized and purified plasmid pVT77 by Gibson assembly. Successful insertion of the KO-cassette was verified by PCR amplification and sequencing of the insert region. All oligonucleotides used for the described PCR amplifications are listed in "Table 4.

Next, AB5075 was transformed by exploiting its capacity to take up DNA while moving along a surface. Therefore, a three-streak plate of AB5075 was prepared and incubated overnight at 37°C. For transformation, the knockout plasmid to be transformed (total amount 4-8 µg) was adjusted to a volume of 20 µl in sterile phosphate buffered saline (PBS) (GibcoTM) in a 1.5 ml reaction tube. Then a single colony of AB5075 was picked from the plate prepared the day before using a sterile pipette tip and resuspended in the 20 µl knockout plasmid DNA in PBS. The DNA/AB5075 mixture was pipetted up and down several times using a sterile 100 µl pipet tip. Finally, a motility agar plate (5 g/l tryptone, 2.5 g/l of NaCl, and 5 g/l of agarose) was inoculated by stabbing and pipetting 2 µl of the mixture into the agar (7 times). Plates were closed with a lid, sealed with parafilm and incubated right side up for 18 h at 37°C. Next day, 1 ml PBS was used to wash off the colonies growing on the surface of the agar. Another 1 ml PBS was used to harvest the cells from the space between plate and agar by stabbing into the agar and dispensing the PBS several times to harvest as much of the bacteria as possible. After harvest, 100 µl bacterial suspension was plated onto LB agar containing tellurite (30 mg/l for pVT77) (Sigma Aldrich) as a selective agent.

The remaining cells were spun down in a tabletop centrifuge (5.000 x g for 5 min) (Eppendorf 5417R, rotor: F45-30-11) and the supernatant was discarded. Pelleted bacteria were resuspended in 100 µl PBS and spread onto a second LB agar plate also containing tellurite as a selective agent. Both plates were incubated upside down for 18 h at 30°C. Next day, single colonies were picked to perform colony PCR using the oligonucleotide pairs listed in "Table 4 to detect whether the KO plasmid had been taken up. Colonies that were tested positive for the presence of the KO plasmid were used to inoculate 2 ml fresh LB broth containing 1 mM IPTG (Peqlab) (without further supplements) to induce expression of the heterologous thymidine kinase encoded on the pVT77 plasmid. Thymidine kinase triggers cytotoxicity in the presence of 3'-azido-3'-deoxythymidine (AZT) (Jena Bioscience). Then bacteria were allowed to grow for 3 h at 37°C with shaking. Afterwards, bacteria were streaked on selective agar (containing 200 µg/ml AZT) using a 10 µl inoculation loop and incubated overnight at 37°C. To test whether the target gene had been replaced by the KO cassette via homologous recombination, a PCR was carried out using oligonucleotide pairs flanking the corresponding gene using genomic DNA as a template ("Table 4). Colonies tested positive for the deletion of the target gene were additionally tested with another colony PCR using an oligonucleotide pair where the 5' primer was placed upstream of the target gene and the 3' primer was placed in the deleted region ("Table 4). No PCR product was detected in colonies where the KO was successful. Additionally, the regions containing the gene deletion were verified by sequencing. For the double and triple KO strains, also a qualitative RT-PCR was carried out to test for the presence of mRNA transcripts."

"4.3 *Isolation of genomic DNA*"

"Genomic DNA, used for the validation of gene deletion as well as for sequencing, was isolated as follows: 5 ml overnight culture was prepared at 37°C and with shaking at 200 rpm. DNA isolation was performed using the QIAamp DNA mini Kit (Qiagen) according to the manufacturer's instructions. Genomic DNA was stored at -20 °C until use."

"4.4 *Library Preparation, Sequencing and Genome Assembly*"

"Libraries for Illumina sequencing were prepared with Nextera DNA Flex Library Prep Kit (Illumina), using as input 500 ng of genomic DNA for each mutant strain. Sequencing was performed on an Illumina MiSeq sequencer using a MiSeq v2 reagent kit (300 cycles) in paired-end mode (2 x 150). In order to verify the expected genome edits in the deletion mutants, we performed de novo assemblies using the nf-core/bacass pipeline (Ewels et al., 2020). The gene deletions in each strain were validated by inspecting the respective genomic regions in the assemblies."

"4.5 *Isolation of RNA and RT-PCR*"

"For RNA isolation 5 × 10^9 bacteria were harvested from an overnight culture and resuspended in 1 ml TRIzolTM Reagent (Thermo Fisher Scientific). RNA isolation and DNase digestion were carried out as described previously (Klein et al., 2019). The resulting RNA was stored at a concentration of 0.1 µg/µl in RNA storage solution (Invitrogen) at -80°C until use. To carry out RT-PCR, RNA was thawed on ice and diluted 1:10 using RNase-free water (Ambion). mRNA expression of mutant strains in comparison to wild type was analyzed qualitatively by RT-PCR using the QuantiFast SYBR Green qRT-PCR Kit (Qiagen) according to the manufacturer's instructions. The resulting PCR products were analyzed by agarose gel electrophoresis and staining of the gel with SYBR Safe (Thermo Fisher Scientific). Primers used are listed in "Table 4."

"4.6 *Generation of pure Stocks of opaque Cells*"

"AB5075 can undergo a phase switch which is induced by a high density of cells in the growing culture. This phase switch is associated with a number of phenotypic changes that also influence virulence (Tipton et al., 2015). To generate homogenous opaque state glycerol stocks, a mixed culture was plated on 0.5 x LB agar as described in Tipton et al. (2015) and grown overnight at 37°C (Tipton et al., 2015). Essentially, opaque colonies were identified by oblique lighting and single colonies were used for a three-phase streak on LB agar plates. After 6-8 h of growth at 37°C several single opaque colonies were picked using a dissecting microscope and used to inoculate 2 ml LB medium each. The cultures were then grown overnight at RT. Purity was again assessed by streaking on 0.5 x LB agar plates. The remaining cultures were used to prepare glycerol stocks that were flash-frozen and stored until use at -80°C. Only cultures that had an estimated purity of 99% or greater were used for further experiments. Purity was additionally assessed by performing a Maneval's capsule stain. For the following experiments overnight cultures were grown at RT and without shaking to obtain AB5075 wild type and the regarding mutant strains in the opaque phase only. Regularly, the opaque state was confirmed by plating the cells on 0.5 x LB agar as well as performing Maneval's capsule stain."

See Figure 1 as an example of the visual sorting of opaque and translucent cells.

"4.7 *Maneval's Capsule Stain*"

"A single colony was resuspended in 10 µl PBS. 5 µl of this suspension was pipetted onto the left side of a glass slide for microscopy. A drop of 1% Congo Red solution (Carolina) was added and mixed with the bacteria. Then a smear was prepared by evenly distributing the mixture across the entire slide using a clean glass slide. The smear was allowed to air-dry. Next, 3 drops of Maneval's stain (Carolina) were placed on parafilm and the slide was placed upside down into the staining solution.

After a 2 min incubation at RT excess staining solution was removed by tilting the slide on Whatman paper. The slide was then air-dried, embedded with Roti-Histol (Carl Roth) and sealed with a coverslip. Samples were then analyzed with an upright light microscope using the 63x lens and oil immersion. Only capsule positive bacteria were characterized by a distinct halo around the bacterial cells."
See Figure 2 as an example of the Maneval´s capsule stain of opaque and translucent cells.

"*4.8 Growth Curves*"

"Growth curves were recorded to monitor potential differences in growth between the wild type strain and the knockout mutants. First, overnight cultures were prepared. Next day, the OD_{600nm} *was measured and cultures were adjusted to 1 x* 10^7 *cells/ml using fresh LB. In a 24 well plate (Greiner Bio-One), 1 ml of bacterial suspension was added per well. Plates were incubated with a lid and with shaking at 300 rpm at 37°C or 42°C for 14 or 24 h, as indicated. All growth curves were recorded in triplicates and in three independent experiments using an Infinite® PRO 200 plate reader (Tecan)."*

"*4.9 Bile Salts Assay*"

"5 ml overnight cultures were grown at RT without shaking. Next day all samples were adjusted to 1 x 10^7 *bacteria/ml using PBS and a 10-fold serial dilution using PBS was prepared in a 96-well plate. 5 µl of each sample and dilution were spotted on LB agar plates containing 0.3% bile salts (Sigma Aldrich). Plates were incubated right side up overnight at 37°C and pictures were taken the next day using a digital camera. The bile salts assay was performed three times."*

"*4.10 NPN Assay*"

"Membrane integrity was analyzed as described before (Klein et al., 2019; Konovalova et al., 2016) using the hydrophobic fluorescent 1-N-phenylnaphthylamine (NPN) (Acros organics). Briefly, overnight cultures of each strain, grown at RT without shaking, were harvested by centrifugation for 5 min at 5.000 x g (Heraeus Multifuge 3 S-R, rotor: 6445). The pellets were resuspended with 2 ml 5 mM HEPES buffer (pH 7.2) and centrifuged for 10 min at 5.000 x g (Heraeus Multifuge 3 S-R, rotor: 6445). This washing step was repeated once. Afterwards cells were adjusted to an OD_{600nm} *of 0.5 with 5 mM HEPES buffer (pH 7.2) and NPN was added to a final concentration of 10 µM. 200 µl of the solution was transferred to a 96-well, black, F-bottom and nonbinding plate (Greiner Bio-One) in triplicates. Fluorescence was measured immediately (excitation: 350 nm, emission: 420 nm) using an Infinite® PRO 200 plate reader (Tecan). As a positive control, Polymyxin B (PMB) (Merck) was added to the WT strain/NPN solution to a final concentration of 8 µg/ml and measured at the same conditions. Additionally, 200 µl of 5 mM HEPES buffer was used as a negative control and subtracted from the values of the sample data. Three independent assays were performed. Relative fluorescence was calculated by using the AB5075 wild type strain as a reference. Significant differences were analyzed by a two-way ANOVA analysis."*

"*4.11 Antibiotic Susceptibility Testing (AST) with Broth Microdilution*"

"To obtain an AB5075 culture in opaque state, 5 ml overnight cultures were inoculated from a frozen opaque stock and grown without shaking at RT. Bacteria were harvested by centrifugation for 5 min at 5.000 x g (Heraeus Multifuge 3 S-R, rotor: 6445), resuspended in 500 µl 0.9% NaCl and adjusted to a 0.5 McFarland standard. To prepare the inoculum for AST testing, 62.5 µl of the suspension were mixed with 15 ml of cation-adjusted Mueller-Hinton Broth (Biotrading). Micronaut-S AST plates (MERLIN Diagnostika) were inoculated with 100 µl of bacteria per well according to the manufacturer instructions. Plates were sealed with a non-breathable seal (MERLIN Diagnostika) and incubated for 18 hours at 37°C. Subsequently the seal was removed and the OD_{600nm} was determined using an Infinite® PRO 200 plate reader (Tecan). Additionally, plates were visually inspected for growth using a special mirror system."

"*4.12 E-tests for Vancomycin*"

"As described above, bacteria were adjusted to a McFarland standard of 0.5. Using a sterile cotton swab, the bacteria suspension was distributed evenly on a Mueller-Hinton Broth agar plate (Oxoid). Then, a vancomycin E-test stripe (Liofilchem) was placed in the centre of the agar plate and the plate was incubated right side up for 18 h at 37°C. After that the inhibition zones were measured. The assay was repeated in two independent experiments."

"*4.13 Preparation of Samples for Mass spectrometric Analysis*"

"To examine changes in the protein expression of the ΔsurAΔskpΔdegP mutant strain compared to the wild type a MS analysis was performed, using whole cell lysates (WCL). For the generation of WCL, the OD_{600nm} of 20 ml overnight cultures of each strain was measured in a 1:20 dilution using LB. After centrifugation for 5 min at 5.000 x g (Heraeus Multifuge 3 S-R, rotor: 6445) the supernatant was removed. Next, 100 µl sterile distilled water was added per OD_{600nm} of 0.1 of the diluted sample and the protein concentration was determined using the Pierce® BCA protein assay kit (Thermo Fisher Scientific). Afterwards, 100 µl 4x Lämmli buffer (Bio-Rad) per OD_{600nm} of 0.1 containing 10% β-Mercaptoethanol (AppliChem) were added. The samples were boiled at 95°C for 5 min. 13 µg protein per lane were loaded on a 10% Mini-PROTEAN® TGX™ Precast Protein Gel (Bio-Rad) and the samples were allowed to enter the gel by applying a current of 100V for 2 mins. Next, the Gel was stained with Roti®-Blue Colloidal Coomassie Staining solution (Carl Roth) containing 20% methanol (AppliChem)."

"*4.14 Preparation of Membrane Fractions*"

"For a more precise proteomic analysis, an additional MS analysis was performed using membrane fractions. Subcellular fractionation was performed as described before (Oberhettinger et al., 2015) with slight modifications. For each strain 50 ml overnight culture was prepared at RT without shaking. Cells were pelleted by centrifugation for 5 min at 5.000 x g (Heraeus Multifuge 3 S-R, rotor: 6445).

After one single washing step with sterile PBS, cells were resuspended in 500 µl resuspending buffer (0.2 M Tris, 1 M Sucrose and 1 mM EDTA, pH 8.4). Additionally, resuspension buffer was supplemented with 1 mg/ml Lysozyme and protease inhibitors (Sigma Aldrich). The suspension was incubated for 10 min at RT, whereby after 5 min 3.2 ml distilled water was added. By centrifugation for 45 min at 16.000 x g (Beckman Coulter Optima LE-80K, rotor: SW 41 Ti) and 4°C, the membrane fraction was separated from other remaining components of the cell. The harvested pellet was resuspended in 2.5 ml lysis buffer (10 mM Tris, 1 mM MgCl2, 5 mM EDTA and 0.2 mM DTT, pH 7,5) and lysed using a french press (Thermo Fisher Scientific). Unlysed cells were removed by centrifugation for 10 min at 5.000 x g (Heraeus Multifuge 3 S-R, rotor: 6445) at 4°C. By another centrifugation step at 290.000 x g (Beckman Coulter Optima MAX-XP, rotor: TLA 100.3) for 60 min at 4°C the membrane fraction was pelletized and separated from the cytosolic fraction. The pellet was resuspended in 2 ml extraction buffer (50 mM Tris, 10 mM MgCl2, 2% TritonX-100) and incubated for 30 min at 4°C. Then, the suspension was centrifuged for 40 min at 84.000 x g (Beckman Coulter Optima MAX-XP, rotor: TLA 100.3) at 4°C, followed by 3 washing steps with water and centrifugation for 20 min at 84.000 x g (Beckman Coulter Optima MAX-XP, rotor: TLA 100.3). The final pellet containing the membrane fraction was resuspended in 100 µl water and prepared for MS analysis as described before."

"*4.15 NanoLC-MS/MS Analysis and Data Processing*"

"*4.15.1 NanoLC-MS/MS Analysis*"

"NanoLC-MS/MS Analysis and Data Processing was essentially carried out as described in Klein et al. (Klein et al., 2019) with the following modifications: peptide mixtures were separated using either a 57 or 127 min segmented gradient (10-33-50-90%) of HPLC solvent B (80% acetonitrile in 0.1% formic acid) in HPLC solvent A (0.1% formic acid) at a flow rate of 200 nl/min. The 7 or 12 most intense precursor ions were sequentially fragmented in each scan cycle using higher energy collisional dissociation (HCD) fragmentation. In all measurements, sequenced precursor masses were excluded from further selection for 30 s. The target values for MS/MS fragmentation were 10^5 charges and 3 x 10^6 charges for the MS scan. MaxQuant software package version 1.6.7.0 was used. Database search was performed against a target-decoy Acinetobacter baumannii database obtained from UniProt, containing 3,839 protein entries and 286 commonly observed contaminants. Endoprotease trypsin was defined as protease with a maximum of two missed cleavages. Oxidation of methionine and N-terminal acetylation were specified as variable modifications, and carbamidomethylation on cysteine was set as fixed modification. Initial maximum allowed mass tolerance was set to 4.5 parts per million (ppm) for precursor ions and 20 ppm for fragment ions. The iBAQ (Intensity Based Absolute Quantification) and LFQ (Label-Free Quantification) algorithms were enabled, as was the "match between runs" option (Luber et al., 2010; Schwanhäusser et al., 2011)"

"4.15.2 Differential Expression Analysis of Proteomics Data"

"The analysis was performed with the DEP package ver 1.10.0 (Zhang et al., 2018) in R, using three replicates for each strain. The default workflow was applied, using filtering for proteins which have maximum of one missing value in at least one condition, variance-stabilizing transformation with the vsn package ver 3.56.0 (Huber et al., 2002) and MNAR imputation of missing values using the imputeLCMD package ver 2.0 (Lazar, 2015). Differential enrichment analysis was performed with the limma package ver 3.44.3 (Ritchie et al., 2015), the volcano and upset plots were generated with the ggplot2 ver 3.3.2 (Wickham, 2016) and UpSetR ver 1.4.0 (Conway et al., 2017) packages respectively. Interactive volcano plots, available at https://bit.ly/379SM6R (WCL) and https://bit.ly/35kHHNV (MEM), were produced with the Glimma package ver 1.16.0 (Su et al., 2017)."

"4.16 Galleria mellonella Infection"

"Galleria mellonella larvae were infected to examine the virulence of the knockout mutants in comparison to the wild type strain. 5 ml overnight culture of each strain was prepared at RT without shaking. Bacteria were harvested by centrifugation for 5 min at 5.000 x g (Heraeus Multifuge 3 S-R, rotor: 6445). The supernatant was discarded and bacteria were resuspended in 5 ml PBS. The OD_{600nm} of overnight cultures was measured and cells were adjusted to 1 x 10^7 bacteria/ml using PBS. 10 µl of the bacteria suspension was injected into 10 Trularv™ larvae (BioSystems Technology) per strain using a microfine insulin syringe (BD Bioscience). After infection the larvae were incubated at 37°C for 6 days and inspected regularly. Larvae were defined to be dead when no movement occurred after touching them gently for several times with forceps. To determine the actual inoculum, a 10-fold serial dilution of the suspension used for infection of larvae was prepared using sterile PBS. 100 µl of the dilutions 10^4, 10^3 and 10^2 were plated on LB agar and incubated overnight at 37°C. Next day, colonies were counted and the actual infection dose was calculated. In total, in six independent experiments 30 larvae per strain were infected with 9 x 10^4 - 2.3 x 10^5 bacteria. As a negative control, larvae were injected with 10 µl PBS only. For statistical analysis a log rank test (Mantel-Cox test) was performed."

“*5. Results*”

Declaration of contributions

The section results, including all figures and the corresponding signatures are literally taken from Birkle et al. (manuscript submitted) and are highlighted with quotation marks as well as written in italics. The numbering of the figures and tables were adjusted to this thesis.

“Figure *10* “Overview of proteins that showed statistically significant changes in label-free quantification (LFQ) intensities” was generated by Dr. Angel Angelov from the NGS Competence Center Tübingen (NCCT).

The manuscript Birkle et al. (manuscript submitted) was mainly written by PD Dr. Monika Schütz and me.

"5.1 Creation of markerless Deletions of Genes encoding for the periplasmic Chaperones SurA, Skp and DegP in AB5075"

"To determine the role of periplasmic chaperones in Ab we used a MDR strain, AB5075, which has been sequenced, is well characterized and genetically accessible (Gallagher et al., 2015; Jacobs et al., 2014). To generate single gene deletion mutants for surA, skp and degP we used pVT77 as a markerless genome-editing tool (Trebosc et al., 2016). All deletions were verified by PCR ("Figure 3) and by sequencing of the scar regions.

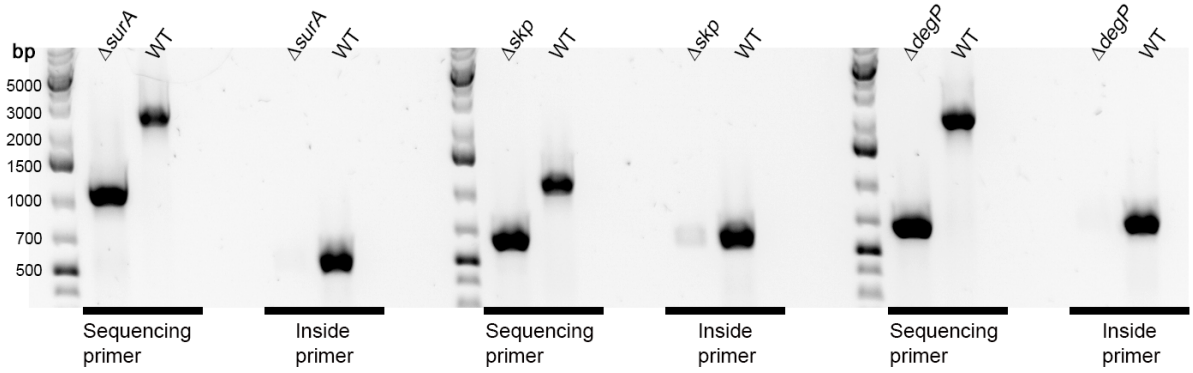

"Figure 3 PCR verification of single knockout mutants Deletion of the target genes was verified by PCRs using genomic DNA of the mutants as a template. *One PCR was carried out using the same primer pair as used for sequencing of the target region after mutagenesis. These primers anneal to the flanking regions of the gene and result in a larger PCR product for the wild type (WT) than the mutant in case of successful deletion. Additionally, "nested primers" were used. These primers can only anneal to the unmodified wild type gene, resulting in a PCR product only for the wild type. For a list of primers used and the expected size of the PCR products please refer to "Table **4**."*

First, we analyzed whether the knockout strains have any defects with regards to growth ("Figure 4). None of the single gene knockout mutants displayed a growth defect at either 37°C or 42°C in LB medium. However, the mutant lacking DegP reached a higher maximum OD_{600nm} value than the other mutants at both temperatures. At 42°C the OD_{600nm} of all strains started to decline upon reaching the stationary phase."

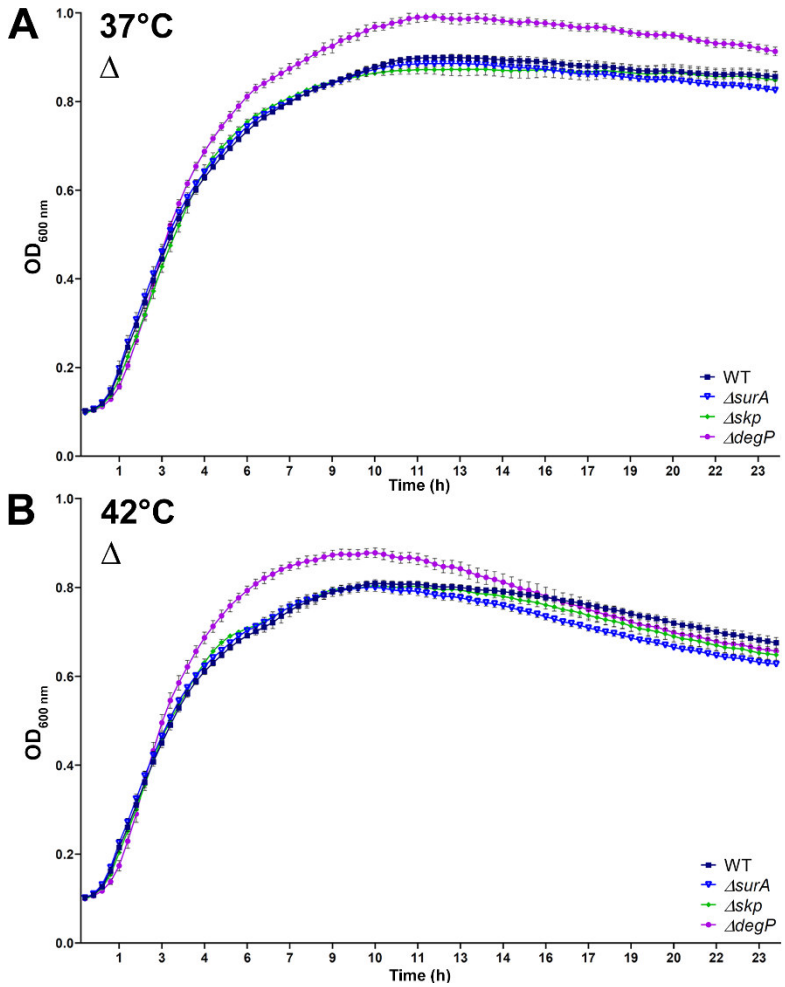

"Figure 4 Effect of single chaperone gene deletions on the growth of AB5075. *(A) To monitor the growth behavior of the indicated single null mutant strains in comparison to the wild type strain (WT), growth curves were recorded in quadruplicate and 3 independent experiments. The initial inoculum was adjusted to 1 x 10^7 cells per ml and cells were grown with shaking at 37°C or (B) 42°C in a 24-well plate."*

"5.2 Effects on the OM Integrity of AB5075"

"As deletion of SurA has previously been associated with OM integrity defects (Klein et al., 2019; Lazar and Kolter, 1996; Rouviere and Gross, 1996; Weirich et al., 2017), we tested the susceptibility of the strains towards bile salts. To this end, we spotted serial dilutions of cultures on solid LB, as a control, and on solid LB supplemented with 0.3% bile salts (a condition that barely allowed growth of the wild type). Only the ΔdegP strain was impaired in growth in presence of bile salts, whereas the ΔsurA and the Δskp strain grew like the wild type ("Figure 5). This was in contrast to our previous analyses in Ye and Pa (Klein et al., 2019; Weirich et al., 2017) in which we detected sensitivity towards bile salts only in absence of SurA. Therefore, we investigated whether the Ab periplasmic chaperones may differ in relevance and function when compared to those of Ye and Pa."

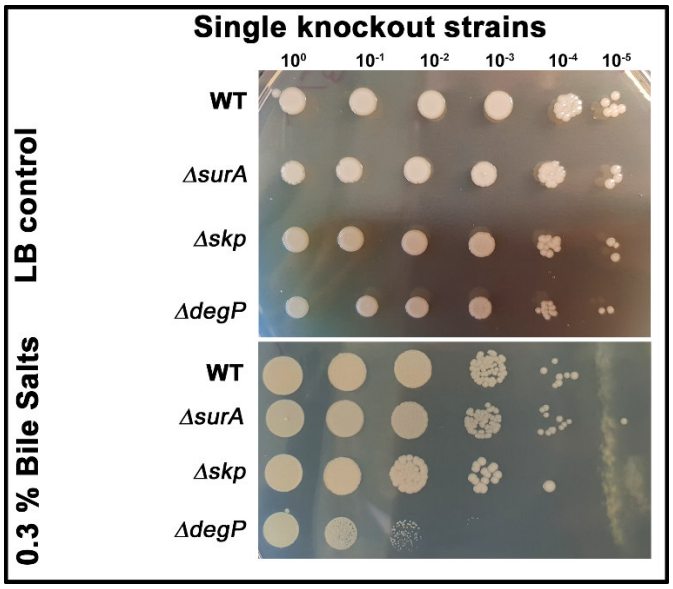

"Figure 5 Relevance of the periplasmic chaperones SurA, Skp and DegP for growth in the presence of bile salts. *The growth behavior of the wild type (WT) and the single null strains in the absence and presence of bile salts was compared. The indicated strains were adjusted to 1 x 10^7 bacteria/ml, serially diluted, and spotted onto LB agar or LB agar containing 0.3% bile salts. At least three experiments were performed. Pictures were taken after an overnight incubation at 37°C (please note: different spot size of the control and treatment group result from different spacing of spots and different spreading behavior of liquid on the plates)."*

"5.3 Apparent redundant Functions for the periplasmic Chaperones SurA, Skp and DegP in AB5075"

"In Ec SurA, Skp and DegP are -at least partially- redundant. Simultaneous disruption of the chaperoning pathway maintained by SurA, and the alternative pathway dependent on Skp/DegP, results in synthetic phenotypes (Rizzitello et al., 2001; Sklar et al., 2007b). Therefore, we tested whether the concomitant deletion of two of the periplasmic chaperones might have a similar effect in AB5075. To this end, we generated different combinations of double mutants, and succeeded also in generating a triple knockout strain lacking surA, skp and degP without any problems. All deletions were verified by PCR, sequencing of the scar region, and by RT-PCR ("Figure 6).

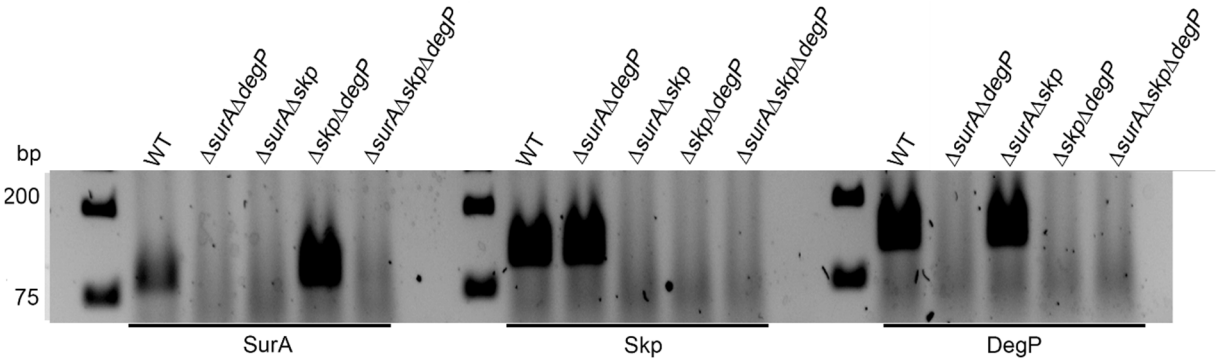

"Figure 6 Qualitative RT-PCR validation of double and triple knockout strains. *To check for the absence of mRNA of the genes that were knocked out qualitative RT-PCR was carried out. Total RNA was isolated from the wild type (WT), the double and triple knockout strains as indicated, reverse transcribed and amplified using primer pairs for surA, skp and degP. The primers used are listed in "Table **4**. A stained agarose gel of PCR products is shown."*

Moreover, we performed whole genome sequencing of the parent strain as well as of the double and triple mutants confirming the target deletion of the chaperone encoding genes (data available at the European Nucleotide Archive (ENA), study ID PRJEB40766). Again, we recorded growth curves at 37°C and 42°C ("Figure 7). At 37°C the ΔsurAΔskp, ΔskpΔdegP and the triple knockout strains grew slower than the wild type strain and the triple mutant displayed the most pronounced growth defect. At 42°C we saw the strongest phenotypes for the ΔsurAΔdegP and the ΔsurAΔskpΔdegP strain."

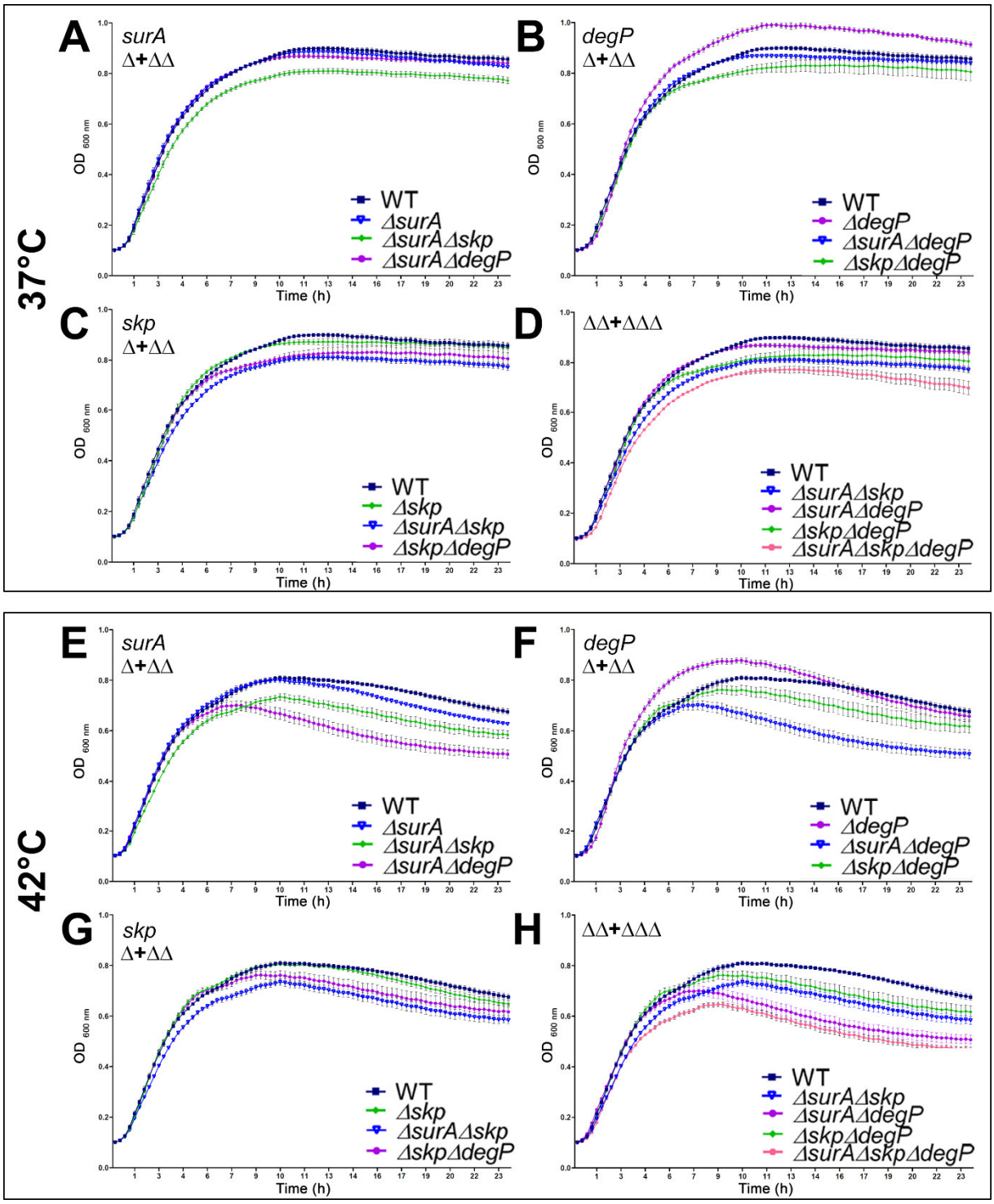

"Figure 7 Effect of double and triple chaperone gene deletions on the growth of AB5075. *To monitor the growth behavior of the double and triple mutant strains in comparison to the wild type (WT) strain, growth curves were recorded in quadruplicate and three independent experiments. The initial inoculum was adjusted to 1 x 10^7 cells per ml and cells were grown with shaking at (A-D) 37°C or (E-H) 42°C in a 24-well plate."*

"5.4 Phenotyping the double and triple periplasmic Chaperone Mutants of AB5075 with respect to:"

"5.4.1 OM Integrity"

Our initial hypothesis was that the deletion of the periplasmic chaperones will induce changes in the OM composition. Therefore, we assessed OM integrity, again using a bile salts assay ("Figure 8). Of note, only the strain lacking both Skp and DegP displayed a reduced growth whereas further deletion of SurA rescued the growth defect of the ΔskpΔdegP mutant strain.

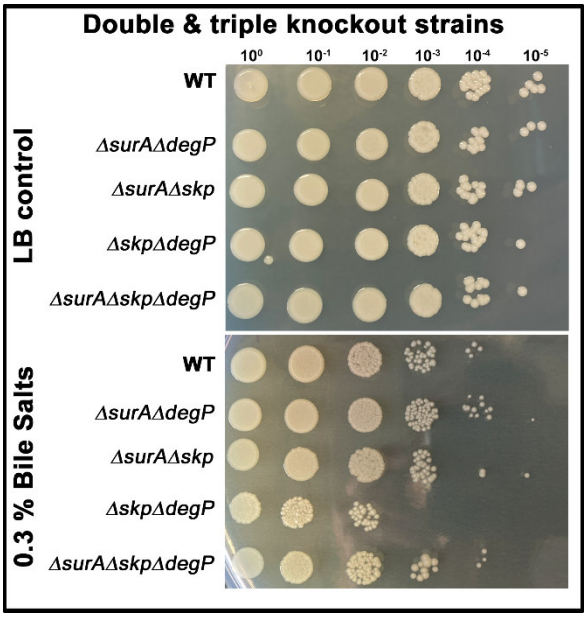

"Figure 8 Relevance of the periplasmic chaperones SurA, Skp and DegP for growth in the presence of detergent. *The growth behavior of double and triple knockout strains for the periplasmic chaperones SurA, Skp and DegP in the absence and presence of bile salts was compared to that of the parent strain AB5075 (WT). The indicated strains were adjusted to 1 x 10^7 bacteria/ml, serially diluted, and spotted onto LB agar and LB agar containing 0.3% bile salts. The dilution factor is indicated on top of the photograph. At least three experiments were performed. Pictures were taken after an overnight cultivation at 37°C."*

To corroborate these interesting but unexpected results, we probed membrane integrity with another assay, i.e. the 1-N-phenylnaphthylamine (NPN)-assay ("Figure 9). NPN is fluorescent only in hydrophobic environments. If the integrity of the OM is compromised, NPN can reach the phospholipid bilayer of the inner OM leaflet more efficiently (Konovalova et al., 2016). Higher fluorescence therefore indicates a reduced OM integrity. Essentially, we found that all single, double and the triple mutant strains displayed a slight, but statistically significant increase in uptake of NPN, being most pronounced in the ΔsurAΔskp mutant strain. Only the ΔsurAΔdegP mutant strain did not show a significant change in the fluorescence signal. These results do not match those of the bile salts assay, probably indicating that the two assays detect different modifications of the OM."

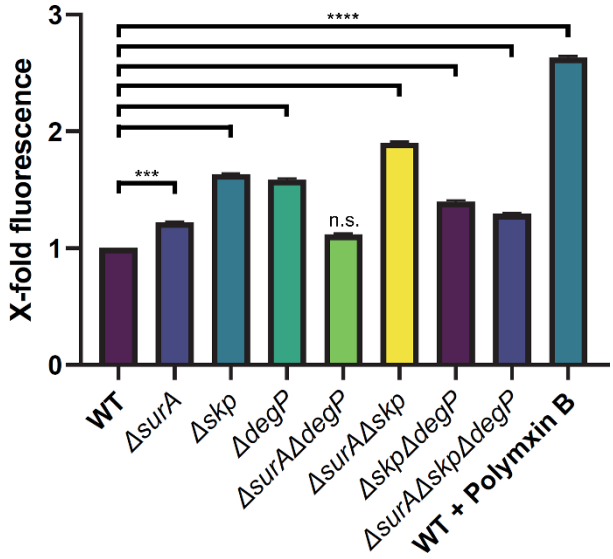

"Figure 9 Probing membrane integrity of knockout strains with the 1-N-phenylnaphthylamine (NPN) assay. *(A) 1-N-phenylnaphthylamine (NPN) assay. The wild type (WT), single, double and triple knockout strains were incubated in presence of NPN which emits fluorescence only in hydrophobic environments. Higher fluorescence therefore indicates a reduced OM integrity. Treatment with polymyxin B was used as a positive control. Data show means of three independent experiments. Statistical analysis was performed using two-way ANOVA analysis. Asterisks designate significant differences (****p < 0.0001 or ***p < 0.0008)."*

"5.4.2 Antibiotic Susceptibility"

"Since SurA, Skp and DegP decisively shape the composition of the OM, we investigated the impact of their single, double and triple deletion on antibiotic susceptibility. To this aim, we performed microbroth dilution assays with a set of antibiotics relevant for the treatment of infections caused by Ab according to the European Committee on Antimicrobial Susceptibility Testing (EUCAST) (http://www.eucast.org) or to the Clinical & Laboratory Standards Institute (CLSI) (http://em100.edaptivedocs.net/dashboard.aspx) for piperacillin/tazobactam. Additionally, we tested some antibiotics typically not used for therapy of Ab (thus no breakpoints were available) and vancomycin as an indicator of OM permeability ("Table 10).

"Table 10 Influence of knockouts on susceptibility against common antibiotics. *Antibiotic susceptibility of AB5075 wild type (WT) compared to the periplasmic chaperone deletion mutants was assessed by microbroth dilution and E-test. A red background indicates a decreased MIC value that is still above the breakpoint. A green background labels MIC values that dropped below the breakpoint. A gray background indicates a reduction of the MIC of less than 2-fold or unchanged MIC. Increased MIC values are labeled with an exclamation mark. Asterisks mark where colonies appearing in the inhibition zone in E-tests."*

MIC-plates		MIC Breakpoints		WT	Single K.O.			Double K.O.			Triple K.O.
		S ≤	R >		*ΔsurA*	*Δskp*	*ΔDegP*	*ΔsurAΔdegP*	*ΔsurAΔskp*	*ΔskpΔdegP*	*ΔsurAΔskpΔdegP*
Aminoglycosides	AMK	8	16	32	16	8	>32!	32	8	32	4
	GEN	4	4	>32	32	>32	>32	32	8	>32	16
	TOB	4	4	8	2	16!	16!	2	2	8	1
Carbapenems	IMP	2	4	>8	8	8	8	8	4	4	4
	MER	2	8	16	16	16	16	16	2	4	4
Penicillins	PIT	16	64	>128	>128	128	>128	>128	16	128	64
Cephalosporins	CTA	-	-	>8	>8	>8	>8	>8	1	>8	8
	CAA	-	-	>8	2	2	>8	4	1	4	1
Fluoroquionolone	LEV	0,5	1	4	4	4	8!	4	2	4	4
E-tests											
Vancomycin	VAN	-	-	>256	48	96*	128	96	12*	64	24

Taken together, we found rather subtle changes in antibiotic susceptibility of the single knockout mutants compared to the wild type strain. All double mutant strains showed increased susceptibility to a broader panel of antibiotics compared to wild type and the single mutants. Interestingly, the ΔsurAΔskp mutant strain was more susceptible to all tested antibiotics compared to the wild type strain. However, the most striking finding was that lack of SurA re-sensitized AB5075 to treatment with the aminoglycoside tobramycin since the MIC for tobramycin dropped below the EUCAST breakpoint for resistance (http://www.eucast.org) in all the mutants lacking SurA. The ΔsurAΔskpΔdegP strain showed an even lower MIC for tobramycin suggesting a synergistic impact of all three chaperones on tobramycin as well as amikacin resistance.

With respect to vancomycin, all mutant strains were more sensitive than the wild type. The most pronounced effect was observed in the ΔsurAΔskp mutant strain. Of note, only with this mutant we frequently observed some colonies within the zone of inhibition (values labeled with asterisks in "Table 10). After re-growth of some of these colonies we repeated the vancomycin E-test. The isolated clones were sensitive to vancomycin, but still more resistant compared to the ΔsurAΔskp parent strain (32 mg/l).

All in all, the lack of individual periplasmic chaperones had only a mild effect on antibiotic susceptibility. However, the deletion of surA, skp and degP synergistically enables a break of resistance against two of the three tested aminoglycosides, indicating an indirect or even direct role of these chaperones in aminoglycoside resistance and specifically an important role of SurA in tobramycin resistance."

“5.4.3 Comparative Mass spectrometric Analyses of AB5075 wild type and ΔsurAΔskpΔdegP Proteomes”

“To identify changes in the proteome of the triple mutant that might help to interpret the altered phenotypes we observed, we carried out mass spectrometric (MS) analyses of whole cell lysates (WCL) of the wild type strain and the triple knockout mutant lacking SurA, Skp and DegP. Additionally, we analyzed by MS a membrane-enriched fraction (MEM) to catch also membrane proteins with low abundance. We then performed a differential expression analysis comparing the label-free quantification (LFQ) intensity values of proteins identified in the ΔsurAΔskpΔdegP mutant strain samples to that of the wild type strain by employing the DEP package (Zhang et al., 2018) (“Figure 10). Results were then filtered for observations that had at least a 2-fold change in mean LFQ intensity and an adjusted p-value of at least 0.05 (corresponds to (-log10) of a p-value of 1.30). We found that ~ 74% of the proteins that showed a statistically significant change of LFQ intensities (160 in total) were less abundant in the triple mutant (119/160) in either of the datasets (WCL or MEM) (“Figure 10; interactive volcano plots for WCL https://bit.ly/379SM6R and MEM https://bit.ly/35kHHNV).

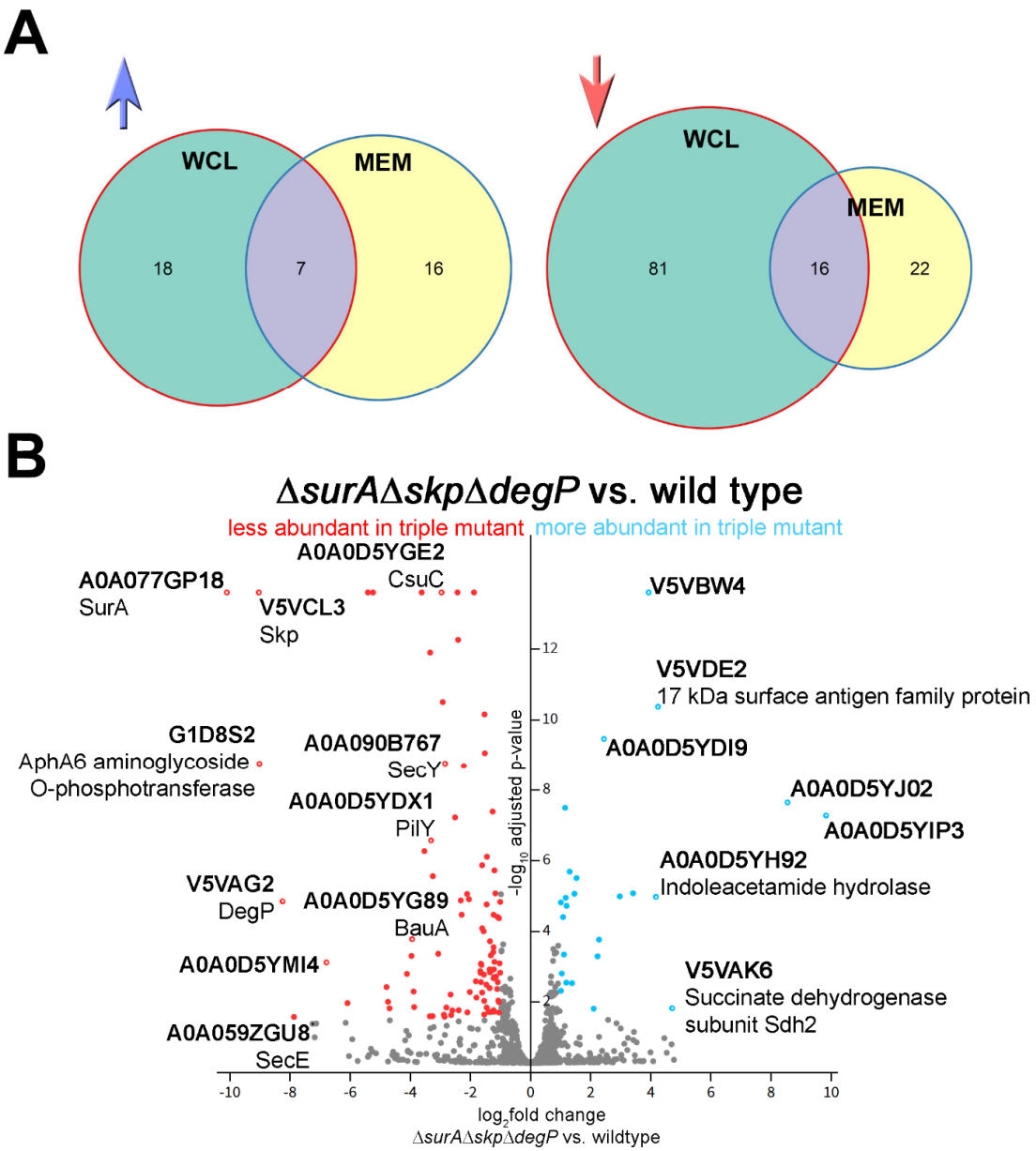

"Figure 10 Overview of proteins that showed statistically significant changes in lable-free quantification (LFQ) intensities. *(A) Venn diagrams visualize the number of proteins that were less (red arrow) or more abundant (blue arrow) in the samples of the ΔsurAΔskpΔdegP mutant strain compared to wild type. Both, proteins from whole cell lysates (WCL) or membrane fractions (MEM) fraction are shown. Overlapping areas indicate that proteins were detected in both fractions. (B) Volcano plot showing statistical significance (-log10 of p-values) versus magnitude of change (log2-fold change) of all detected proteins in WCL samples. Colored dots indicate statistically significant differences. Grey dots indicate proteins that were not significantly altered in the triple mutant strain compared to wild type. Selected proteins that were mentioned in the manuscript are labeled with a white dot in the center and UniProt ID and protein name (if available)."*

A selection of proteins previously observed to be affected in other species, or being significantly changed in the ΔsurAΔskpΔdegP mutant strain is shown in "Table 11. For a comprehensive overview of all proteins the abundance of which was significantly changed at least 2-fold in WCL and/or MEM refer to"Table 15.

"Table 11 List of selected proteins significantly altered in the ΔsurAΔskpΔdegP (ΔΔΔ) mutant strain compared to the Ab wild type strain (WT) (upper part), or not showing significant alteration (lower part). *The latter proteins were included because they are known to be affected by the lack of SurA in other species or might be of interest in other respect. All samples for MS analyses were prepared independently and analyzed in three replicates. The upper part of the table includes proteins that revealed a statistically significant change (p-value ≤ 0.05) when comparing the means of LFQ intensities of three sample replicates of WCL or MEM (for details of analysis please refer to the methods section). Log2-fold changes in LFQ intensities of ΔsurAΔskpΔdegP/wild type were calculated for easier comparison. These entries were colored by using the conditional formatting option of excel, assigning colors according to cell values by using a heat map ranging from blue (high values) over white to red (low values). Additionally, the corresponding -log10 adjusted pvalues for all changes are shown. Entries for SurA, Skp and DegP are boldface. Color code for entries is as follows: green: pil proteins, red: proteins associated with a function in antibiotic drug resistance, blue: proteins involved in iron acquisition; n.a. = gene name not available"*

Gene ID	UniProt Entry	Gene Name, Synonym	Function	log2-fold change LFQ ΔΔΔ/WT	-log10 adjusted p-value ΔΔΔ/WT	log2-fold change LFQ ΔΔΔ/WT	-log10 adjusted p-value ΔΔΔ/WT
				WCL		MEM	
ABUW_2034	A0A0D5YIP3	*n.a.*	Uncharacterized	9,83	7,05		
ABUW_1997	A0A0D5YJ02	*n.a.*	Uncharacterized	8,55	7,42		
ABUW_0869	V5VAK6	*sdhD*	Succinate dehydrogenase hydrophobic membrane anchor subunit	4,71	1,60		
ABUW_1563	V5VDE2	*n.a.*	17 kDa surface antigen family protein	4,24	10,15	2,88	3,18
ABUW_0607	A0A0D5YDI9	*n.a.*	Uncharacterized	2,44	9,24	1,79	4,58
ABUW_1298	A0A059ZT62	*n.a.*	Uncharacterized	2,10	1,59		
ABUW_2165	A0A0D5YJ17	*fhuE_1*	Outer-membrane receptor for Fe(III)-coprogen,Fe(III)-ferrioxamine B and Fe(III)-rhodotrulic acid	1,46	4,84	6,22	1,56
ABUW_3362	Q2FD52	*macA*	Efflux transporter, RND family, MFP subunit	1,20	4,50	1,53	4,74
ABUW_3730	V5VJ35	*n.a.*	Lipoprotein	1,19	2,33		

ABUW_1070	G1C763	*dacD*	Beta-lactamase enzyme family protein	1,11	3,12		
ABUW_3364	A0A0D5YL63	*adeC*	AdeC/AdeK/OprM family multidrug efflux complex outer membrane factor	1,04	2,58	1,66	2,93
ABUW_1902	A0A0D5YIN1	*sndH2*	L-sorbosone dehydrogenase	1,01	2,10		
ABUW_1907	A0A0D5YIN6	*gdhB1*	Quinoprotein glucose dehydrogenase	1,01	4,59		
ABUW_0679	V5V9M9	*pilH*	Type IV pilus response regulator protein	-1,46	1,62		
ABUW_0291	A0A0D5YCR0	*pilN, comN*	Fimbrial assembly protein	-2,64	1,41		
ABUW_1631	V5VC75	*csuB_2*	Csu pilus subunit CsuB	-2,80	1,62		
ABUW_0426	A0A090B767	*secY*	Protein translocase subunit	-2,84	8,54		
ABUW_1632	A0A0D5YGE2	*csuC*	Type I pilus chaperone usher secretion system	-2,96	13,38		
ABUW_0317	A0A0D5YDX1	*pilY1*	Pilus assembly protein tip-associated adhesin	-3,31	6,35		
ABUW_0682	A0A0D5YFD1	*pilL*	Type IV pilus hybrid sensor kinase/response regulator PilL	-3,89	2,07		
ABUW_1177	A0A0D5YG89	*bauA*	Ferric acinetobactin receptor	-3,94	3,55		
ABUW_3032	A0A086HYC5	*pilU*	Type IVa pilus ATPase	-4,11	2,57		
ABUW_3549	A0A0D5YLN2	*pulE, pilB*	Type IV-A pilus assembly ATPase	-4,69	1,60		
ABUW_0304	A0A0D5YCX7	*pilA*	Type IV pilin structural subunit	-5,41	13,38	-5,87	11,61
ABUW_0294	A0A0D5YCW8	*pilQ, comQ*	Fimbrial assembly protein	-6,09	1,75	-5,10	1,35
ABUW_0916	A0A0D5YFJ5	*n.a.*	Biofilm-associated protein	-7,87	1,36		
ABUW_1027	**V5VAG2**	***mucD_1, degP***	**Periplasmic serine endoprotease DegP-like**	-8,25	4,62	-4,32	6,72
ABUW_4087	G1D8S2	*aphA6*	APH(3')-VI family aminoglycoside O-phosphotransferase	-9,02	8,53		

ABUW_1742	**V5VCL3**	***skp***	**OmpH family outer membrane protein**	-9,04	13,38	-3,69	4,10
ABUW_2268	**A0A077GP18**	***surA***	**Unfolded protein binding**	-10,10	13,38		
ABUW_3583	A0A0D5YMU6	*n.a.*	OmpW family protein			-1,28	2,13
ABUW_0293	A0A0D5YDP9	*pilP, comL*	Pilus assembly protein			-2,28	1,38
ABUW_0292	V5V999	*pilO, comO*	Pilus assembly protein			-2,42	1,41
ABUW_0681	V5VA86	*pctA, pilJ*	Chemotaxis protein			-5,59	5,77
ABUW_1976	A0A0D5YIU4	*adeC*	Multidrug efflux RND transporter outer membrane channel subunit AdeC	0,75	1,14	0,94	0,57
ABUW_1218	A0A0D5YGS6	*algW, degS*	Probable periplasmic serine endoprotease DegP-like	0,18	0,11	0,06	0,06
ABUW_1015	C0L0K5	*carO*	Carbapenem-associated resistance protein (CarO)	-0,07	0,07	0,08	0,06
ABUW_2828	A0A0D5YKZ4	*fhuA*	TonB-dependent receptor	-0,25	0,10	-0,04	0,06
ABUW_0649	W6RU67	*ompA*	OmpA family protein	-0,12	0,08	-0,04	0,06
ABUW_2267	A0A0D5YI30	*ostA, lptD*	LPS-assembly protein LptD	-0,44	0,37	-0,41	0,21
ABUW_2197	A0A0E1JKW1	*ppiD*	Peptidyl-prolyl cis-trans isomerase	-0,03	0,06	-0,42	0,13
ABUW_0629	A0A0D8GEK5	*secA*	Protein translocase subunit	0,29	0,09	0,74	0,46
ABUW_3371	V5VIB6	*secB*	Protein translocase subunit	0,05	0,06		
ABUW_3596	A0A059ZGU8	*secE*	Protein translocase subunit	-7,25	1,16		
ABUW_0166	A0A0B9W7U0	*n.a.*	Omp25	0,13	0,07	0,14	0,07
ABUW_1741	A0A0D8F481	*bamA*	Outer membrane protein assembly factor BamA	0,24	0,11	0,36	0,17
ABUW_3374	V5VGU9	*bamB*	Outer membrane protein assembly factor BamB	0,30	0,12	0,20	0,08

ABUW_0060	V5V8H7	*bamC, nlpB*	Outer membrane protein assembly factor BamC	0,22	0,09	0,01	0,05
ABUW_3087	A0A0C2LLC6	*bamD*	Outer membrane protein assembly factor BamD	0,30	0,21	0,22	0,11
ABUW_3034	A0A1A9L379	*bamE, smpA*	Outer membrane protein assembly factor BamE	0,20	0,09	-0,16	0,08
ABUW_1590	A0A0D5YHE7	*tamA, bamA_2*	Autotransporter assembly factor TamA	-0,01	0,06	-0,01	0,05
ABUW_1591	A0A0D5YH88	*tamB*	DUF490 domain-containing protein	0,10	0,07	0,26	0,09

Next, we asked whether representatives of the OMP family were affected in the triple mutant strain. Neither of the typically highly abundant OMPs OmpA (W6RU67), Omp25 (A0A0B9W7U0), CarO (C0L0K5) or AdeC (A0A0D5YIU4) showed a significant change. Interestingly, also LptD (A0A0D5YI30) and FhuA (A0A0D5YKZ4), the OM insertion of which is strongly SurA-dependent in Ec (Vertommen et al., 2009), Ye (Weirich et al., 2017) and Pa (Klein et al., 2019), did not exhibit significant changes in protein levels. Our findings thus indicate that the triple knockout does not induce a global reduction in OMP abundance and does not impact specific proteins found to be SurA-dependent in other Gram-negative bacteria. However, we observed a specific and significant reduction of other OMPs, such as the acinetobactin receptor BauA (A0A0D5YG89). Also, several proteins assigned to the subcategory type IV pili (A0A0D5YCR0, A0A0D5YDX1, A0A0D5YFD1, V5V9M9, A0A086HYC5, A0A0D5YLN2, A0A0D5YCX7, A0A0D5YCW8, A0A0D5YDP9, V5V999, V5VA86), as well as a number of uncharacterized proteins were significantly less abundant. Two components of the type I chaperone-usher pilus system, CsuB (V5VC75) and CsuC (A0A0D5YGE2) were also less abundant in the triple mutant. We also found the aminoglycoside inactivating enzyme APH(3')-VI family aminoglycoside O-phosphotransferase (G1D8S2) (Ramirez and Tolmasky, 2010), below detection limit in the triple mutant strain, but well expressed in the wild type strain. This could possibly explain our previous finding of reduced resistance towards tobramycin in the triple mutant.

Another remarkable observation was that the protein translocase subunit SecY (A0A090B767) appeared to be significantly less abundant in the triple mutant. As a part of the general secretion pathway (Sec), SecY is involved in the process of translocation of nascent proteins, including OMPs, into the periplasm (Mori and Ito, 2001).

Of course, we cannot discern whether the observed changes are directly or indirectly linked to the lack of SurA, Skp and DegP. Still, we conclude that if SurA, Skp and DegP were to have the same role in Ab as that in Ec, Ye and Pa, there have to exist mechanisms that can compensate for the concurrent lack of SurA, Skp and DegP.

Next, we searched our dataset for proteins that were not or only weakly expressed in the wild type and significantly more abundant in the triple mutant. We identified 25 such proteins in the WCL of the triple mutant strain. Assuming that factors that compensate for the lack of periplasmic chaperones should also act in the periplasm, we then filtered out cytoplasmic proteins. Of the remaining 14 non-cytoplasmic candidate proteins five are uncharacterized (A0A0D5YIP3, A0A0D5YJ02, A0A059ZT62, A0A0D5YDI9, V5VJ35), three are associated with antibiotic resistance (G1C763, Q2FD52, A0A0D5YL63), three are classified as dehydrogenases of different substrates (A0A0D5YIN6, A0A0D5YIN1, V5VAK6), one is the outer membrane iron receptor FhuE_1 (A0A0D5YJ17), and one is classified as member of the 17kD surface antigen family (V5VDE2). As none of these candidates obviously qualified as periplasmic chaperone we had a closer look at the poorly annotated proteins.

A0A0D5YIP3 and A0A0D5YJ02 are encoded in the genome of AB5075 several times (3x and 7x, respectively). Their genomic context and BLAST searches suggest they are both phage-derived. A0A059ZT62 has been annotated as a L-2,4-diaminobutyrate decarboxylase in the Ab strain NCGM 237. This enzyme is part of the biosynthetic pathway for the production of the polyamine 1,3-diaminopropane which has been linked to surface-associated motility and virulence of Ab (Skiebe et al., 2012). A0A0D5YDI9 and V5VJ35 are lipoproteins of unknown function. V5VDE2 has been annotated in other Ab strains as a glycine-zipper containing OmpA-like membrane domain protein, but also this protein is uncharacterized.

Taken together, we found numerous changes in the proteome of the triple mutant strain. However, they do not obviously explain how Ab manages to cope with the absence of SurA, Skp and DegP. Proteins that were more abundant in the triple mutant strain are either of unknown function, or their suggested function is not associated with specific phenotypes. Therefore, especially the so-far uncharacterized candidates need further investigation which has been initiated already and will be addressed in the near future. Even if we finally could not answer the question of how Ab can live in the absence of SurA, Skp and DegP, we investigated how the observed proteomic changes influence specific virulence-associated phenotypes of Ab and translate into overall virulence in an infection model."

"5.5 In vivo Virulence"

"We assessed virulence of the different strains in the Galleria mellonella infection model. To this end, we injected 30 larvae with 1.1 x 10^5 – 2.3 x 10^5 cells of the wild type strain and the single mutant strains, respectively. The survival of the larvae was monitored over 6 days ("Figure 11A). All larvae infected with the wild type died within 96 hours. However, larvae infected with the single mutants had a significantly enhanced survival rate. The deletion of Skp resulted in the highest survival rate (53.3%, $p < 0.0001$) followed by the ΔdegP (36.7%, $p < 0.0001$) and the ΔsurA strain (13.33%, $p < 0.0078$), indicating a more critical role of Skp than SurA in virulence. Next, we analyzed the effect of the double and triple knockouts compared to the wild type strain ("Figure 11B). Please note that the experiments shown in "Figure 11A and "Figure 11B were carried out independently because of technical reasons. Again, 30 larvae were injected with 9 x 10^4 - 1.12 x 10^5 cells of the respective strains and survival at 37°C was monitored for 6 days after injection. All larvae infected with the wild type died within 48 hours. The simultaneous knockout of Skp and SurA, induced the greatest reduction of virulence (86.7%, $p < 0.0001$). The ΔskpΔdegP (73.3%, $p < 0.0001$) and the triple knockout mutant strain (70%, $p < 0.0001$) resulted in comparably enhanced survival rates. However, the growth defect of the ΔsurAΔskpΔdegP mutant strain (see "Figure 7) could also have contributed to its decrease in virulence. The injection of larvae with the ΔsurAΔdegP strain produced the lowest survival rate (6.7%, $p < 0.0233$). Taken together, all strains that lacked Skp either individually or in combination with other chaperones, were reduced in virulence, while in contrast to Ye and Pa SurA plays only a minor role for virulence."

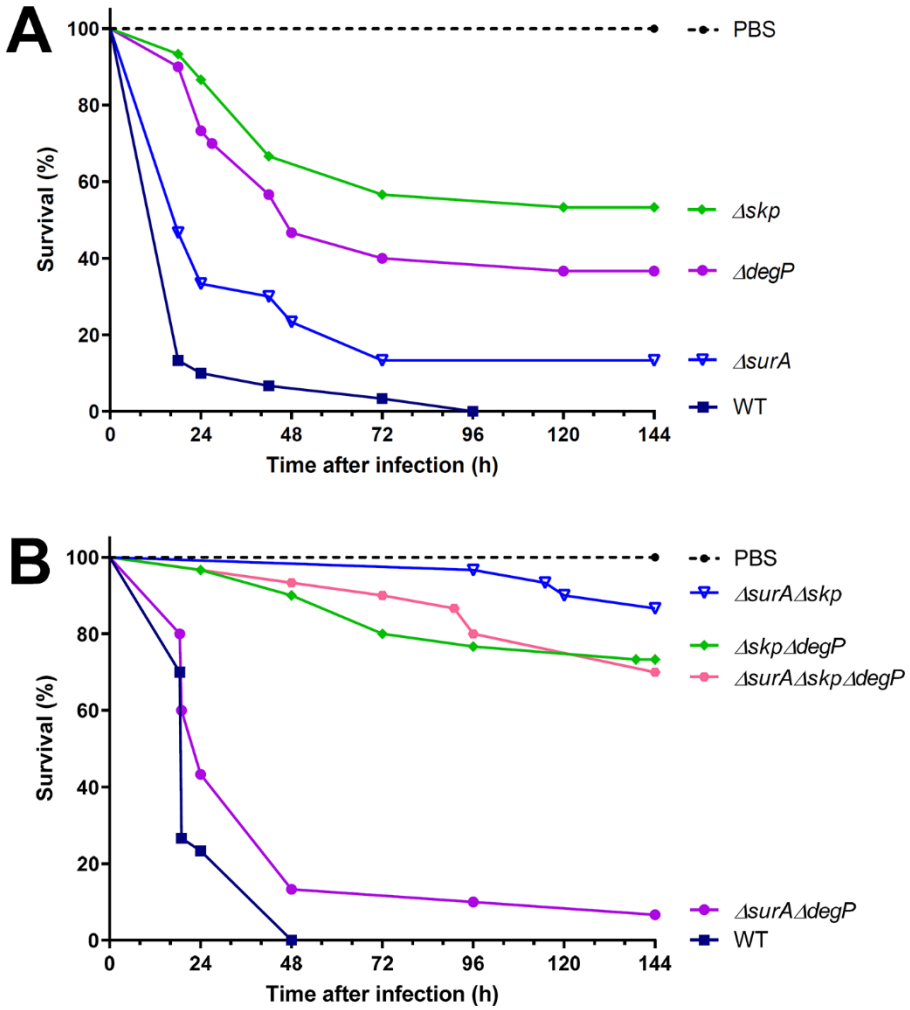

"Figure 11 Assessment of virulence of AB5075 wild type and mutant strains in the Galleria mellonella infection model. *The infection of 30 Galleria mellonella larvae per strain was performed to study the role of periplasmic chaperones for virulence. The larvae were injected with the indicated strains in three independent experiments and incubated at 37°C for 6 days. Larvae were recorded as dead when no movement occurred after cautious touching with forceps. (A) Survival of single knockout strains compared to wild type (WT). (B) Survival of double and triple knockout strains compared to wild type. Statistical analysis was performed using a log rank test (Mantel-Cox test). A significant difference between wild type and all mutant strains was observed. The p-value was < 0.0001 for wild type vs. Δskp, ΔdegP, ΔsurAΔskp, ΔskpΔdegP and ΔsurAΔskpΔdegP. For wild type vs. ΔsurAΔdegP we observed a p-value of 0.0233 and for wild type vs. ΔsurA a p-value of 0.0056."*

6. Discussion

Declaration of contributions

“Table ***12*** and “Figure *12* as well as the corresponding text in chapter 6.3 are literally taken from Birkle et al. (manuscript submitted) and are highlighted with quotation marks as well as written in italics.
The discussion concerns the experimental results of Birkle et al. (manuscript submitted).
“Table *13* as well as the figure text which is mentioned in chapter 6.3.1 and can be found in the appendix was generated and written by the co-author Dr. Fabian Renschler.
The manuscript Birkle et al. (manuscript submitted) was mainly written by PD Dr. Monika Schütz and me.

6.1 Generation and phenotypical characterization of single gene knockout mutants for *surA*, *skp* and *degP* in *Ab* AB5075

Nowadays, *Ab* represents one of the major nosocomial pathogens challenging the healthcare system worldwide. The enormous adaptability of *Ab* to its environment as well as many intrinsic and acquired resistance mechanisms urgently demands the development of new therapeutics (Dijkshoorn et al., 2007). Like in other pathogens, the OM of *Ab* provides a tight barrier for antimicrobial agents. Especially, the specific peculiarities of integral OMPs impede the influx or ensure the active efflux of antibiotics (Vila et al., 2007; Zgurskaya et al., 2015). One crucial step during the biogenesis of OMPs is the chaperone-guided passage from the IM to the OM via the periplasm (Rollauer et al., 2015). In *Ec*, *Ye* and *Pa,* SurA represents the major chaperone for the biogenesis of the majority of OMPs, whereas Skp and DegP constitute as an alternative pathway which may compensate the loss or depletion of SurA (Klein et al., 2019; Sklar et al., 2007b; Vertommen et al., 2009; Weirich et al., 2017). In *Pa*, the deletion of *surA* seems to be even lethal as only a conditional knockout mutant strain of Δ*surA* could be created, supporting the notion of SurA as the main chaperone in *Pa* (Klein et al., 2019). However, in *Nm* Skp seems to be the main periplasmic chaperone for OMP assembly (Volokhina et al., 2011). Since periplasmic chaperones have been validated for their potential to serve as novel targets for therapeutics that reduce virulence and possibly break resistance in *Ec* (Justice et al., 2006; Watts and Hunstad, 2008), *Ye* (Weirich et al., 2017) and *Pa* (Klein et al., 2019), the aim of this work was to examine their potential as antivirulence/resistance breaker targets in *Ab*.

Single gene knockout mutants of *surA*, *skp* and *degP* were generated by allelic exchange. Every genomic deletion was verified by two PCRs, the first one using a primer pair flanking the respective target gene and delivering a shorter PCR product upon successful deletion. The second PCR using a primer pair where one primer was designed to anneal within the deleted gene region, and which should not yield a PCR product upon successful deletion “Figure 3). Additionally, the region of the gene deletion of each mutant was sequenced (Birkle et al., manuscript submitted). As mentioned before, AB5075 is able to switch between different phenotypes by phase variation (Tipton et al., 2015). To avoid high variability in assay outcomes as a result of a variable bacterial population structure caused by a phase switch, only opaque cells were used to carry out the experiments.

6.1.1 Assessment of general fitness by recording growth curves

To examine the growth behavior of the mutants, growth kinetics were recorded at 37°C. In comparison to the wild type, we did not observe significant changes in growth behavior for the Δ*surA* and Δ*skp* strain. The strain lacking DegP even reached a higher OD_{600nm} compared to the wild type. In growth kinetics using *Pa*, the deletion of the *skp* homolog *hlpA* was also comparable to the wild type. The deletion of *surA*, however, resulted in a slight but significant reduction of growth in *Pa*, indicating a role of SurA for bacterial growth in *Pa* (Klein et al., 2019). For *Ye*, no reduction of growth could be observed in the strains lacking SurA, Skp or DegP respectively (Weirich et al., 2017). As stated before, DegP is essential for growth at higher temperatures in *Ec* and strains lacking DegP display a temperature sensitive phenotype (Lipinska et al., 1989; Skorko-Glonek et al., 1995; Strauch et al., 1989). Therefore, we also performed growth curves at an elevated temperature of 42°C. The Δ*surA* and Δ*skp* mutants strain displayed only a slight reduction in growth compared to the wild type. Although the strain lacking DegP reached a higher maximum OD_{600nm} than the wild type, after ~ 17 hours the OD_{600nm} dropped slightly below the OD_{600nm} of the wild type (“Figure *4*).

Taken together, the lack of SurA, Skp or DegP in AB5075 did not result in a significantly reduced growth both at 37°C and 42°C.

6.1.2 Impact of deletions on OM barrier function

The biogenesis of β-barrel OMPs that contribute to the OM barrier function of Gram-negative pathogens generally depends on periplasmic chaperones (Rollauer et al., 2015). Hence, the mutants lacking SurA, Skp and DegP were tested for their OM integrity. One approach to test the integrity of the OM is the use of bile salts. Bile salts are located in the intestinal tract and act as detergents thereby providing protection against pathogens (Merritt and Donaldson, 2009). Therefore, serial dilutions of the wild type strain as well as the mutant strains of Δ*surA*, Δ*skp* and Δ*degP* were spotted on LB agar as a control and LB agar containing 0,3% bile salts. Surprisingly the lack of SurA had no significant effect compared to the wild type (“Figure *5*). This was in stark contrast to *Ec* (Lazar and Kolter, 1996) *Pa* (Klein et al., 2019) and *Ye (Weirich et al., 2017)* where the conditional deletion mutant of Δ*surA* resulted in the most pronounced reduction of growth. Noteworthy, the bile salt assay for *Pa* was performed as kinetic growth curves which might have slight effects on the difference of the results (Klein et al., 2019). Nevertheless, these results may indicate a minor role for SurA in *Ab*. Mutants strains of Δ*skp* showed a subtle growth reduction compared to the wild type. However, for *Ye* (Weirich et al., 2017) and *Pa* (Klein et al., 2019) no effect could be detected for mutants lacking Skp or the Skp homolog HlpA in *Pa*. Interestingly, the mutants lacking Δ*degP* showed the most pronounced effect in the bile salt assay (“Figure *5*). In contrast to this, also the deletion of *degP* had no effect for the growth of *Ye* on agar supplemented with bile salt (Weirich et al., 2017).

Compared to other species, this may indicate a more important role for DegP in *Ab* to cope with stressors like bile salts.

6.2 Generation and characterization of concurrent deletions of *surA*, *skp* and *degP* as well of a triple mutant lacking all three periplasmic chaperones

Since the deletion of SurA surprisingly resulted only in weak phenotypes compared to what has been observed before in *Ec* (Rizzitello et al., 2001) *Ye* (Weirich et al., 2017) and *Pa* (Klein et al., 2019), we attempted to create double knockouts of *surA* + *skp*, *surA* + *degP*, and *skp* + *degP*. In *Ec*, the concurrent deletion of *surA* + *skp* and *surA* + *degP* is not tolerated (Rizzitello et al., 2001). However, some synthetic phenotypes could be observed for the concurrent loss of SurA + Skp or SurA + *DegP*. This was shown in a *skp* deletion mutant were the endogenous *surA*, was disrupted by a kanamycin resistance cassette, and complementation was facilitated by a plasmid carrying an arabinose-inducible copy of wild type *surA*. The same replacement of disrupted endogenous *surA* was performed in a strain were *degP* was disrupted by a transposon insertion (*Tn*10). The simultaneous interference with *surA* and *skp* expression had a bactericidal effect, whereas interfering with *skp* and *degP* had a bacteriostatic effect. A change in cell morphology towards more filamentous growing cells, probably indicating a problem with cell division, could only be observed in the cells carrying mutations in both *surA* and *skp*. A reduction of envelope proteins was observed for both combinations, demonstrating the importance of functional chaperones in the periplasm (Rizzitello et al., 2001).

In contrast we found that a double knockout of two periplasmic chaperones in each combination was tolerated by AB5075 very well. Even a triple knockout strain, lacking all three periplasmic chaperones simultaneously, was viable. The respective gene deletions were also verified by PCR, sequencing and additionally by RT-PCR (“Figure *6*, Birkle et al., manuscript submitted). Thereby, the generation of viable double knockout mutant strains of Δ*surA*Δ*skp*, Δ*surA*Δ*degP*, Δ*skp*Δ*degP,* and even a viable triple mutant strain of Δ*surA*Δ*skp*Δ*degP* was shown for the first time in Gram-negative pathogens (Birkle et al., manuscript submitted).

6.2.1 Assessment of general fitness by recording growth curves

To assess the growth behaviour of the double and triple mutant strains, and to compare it to the single deletion mutants, their growth in LB medium was monitored over 24 hours at 37°C, as well as at 42°C. At 37°C the growth of the Δ*surA*Δ*degP* mutant strain exhibited no differences compared to the wild type. However, the Δ*surA*Δ*skp* and Δ*skp*Δ*degP* knockout strains grew slightly slower and their maximum OD_{600nm} stayed below that of the wildtype strain. In *Ec*, depletion strains of *skp* and *surA* as well as *degP* and *surA*, display a significant reduction of growth (Sklar et al., 2007b). This indicates a more important role of the periplasmic chaperones for bacterial growth in *Ec* than in *Ab* and probably the existence of a more redundant periplasmic chaperone system in *Ab*.

The growth of the triple mutant strain of AB5075 showed the most pronounced reduction in growth ("Figure *7*). Though a triple knockout of *surA*, *skp* and *degP* is not lethal in *Ab* it seems that the lack of all three chaperones causes distress that affects the growth behaviour. At 42°C all tested strains showed a reduction in growth compared to 37°C. However, Δ*surA*Δ*skp* and Δ*skp*Δ*degP* showed also slight growth defects in comparison to the wild type. Although single deletions of *surA* and *degP* showed no distinct reduction of growth, the Δ*surA*Δ*degP* mutants reached a significantly lower OD_{600nm} during growth compared to the wild type. As observed at 37°C, the highest reduction of growth could be observed in the triple mutant ("Figure *7*). Therefore, the growth phenotype of the triple mutant has to be considered when interpreting results of experiments where retarded growth of the strain plays a role.

6.2.2 Impact of deletions on OM barrier function

6.2.2.1 Sensitivity to treatment with bile salts

Periplasmic chaperones play an important role for biogenesis of OMPs (Rollauer et al., 2015). Hence, we assumed rearrangements of the OM composition especially in the double and triple mutant strains which might cause a decrease in OM integrity. Therefore, also the double and triple deletion strains were tested for sensitivity towards treatment with bile salts. We found that the double mutant strains Δ*surA*Δ*degP* and Δ*surA*Δ*skp* displayed sensitivity comparable to that of the wild type ("Figure *8*). This indicates that a loss of SurA has no impact on the sensitivity towards bile salts, which corroborates our findings for the single mutant strains, and that Skp or DegP can somehow compensate their mutual loss. Again, this was in contrast to what has been demonstrated for the lack of SurA in *Ec* (Lazar and Kolter, 1996) *Pa* (Klein et al., 2019), and *Ye* (Weirich et al., 2017).

Although the single Δ*skp* deletion mutant was only slightly impaired in growth in the presence of bile salts, the lack of Skp and DegP in parallel induced the most prominent reduction of growth. Surprisingly, the growth of the triple mutant was slightly reduced compared to the wild type, but was less inhibited than in the Δ*skp*Δ*degP* mutant ("Figure *8*). Taken together, the impact of single, double and triple knockouts of SurA, Skp and DegP induced only weak OM integrity perturbations, as assessed by the sensitivity towards treatment with bile salts. The most profound effect was seen in the Δ*skp*Δ*degP* double mutant strain. However, we currently cannot sufficiently explain why this is the case. To our surprise, it was not the triple mutant having the strongest membrane perturbations. This might indicate that *Ab* employs yet unknown mechanisms which can compensate the loss of all three periplasmic chaperones and thereby largely maintain the OM integrity.

6.2.2.2 Assessing OM barrier function using 1-N-phenylnaphthylamine (NPN)

As another test for OM integrity, an NPN assay was performed. NPN is a dye which possesses a bright fluorescence only in hydrophobic environments. Cells with an intact OM and LPS/ lipooligosaccharides (LOS) are able to prevent the intrusion of NPN (Konovalova et al., 2016). Hence, a reduction in the integrity of the OM leads to higher fluorescence reads in the assay. The single deletion mutant strains Δ*surA*, Δ*skp* and Δ*degP* showed all significantly higher fluorescence reads than the wild type. However, the Δ*surA* deletion strain showed a significantly but only slightly increased fluorescence compared to the wild type ("Figure *9*). Again, this was in stark contrast to what has been shown in *Pa*, where the conditional knockout of *surA* led to a ~3-fold increase of the fluorescence signal (Klein et al., 2019). Additionally, the knockout of the *skp* homolog *hlpA* in *Pa* showed no significantly change in the NPN assay, whereas the knockout of *skp* in *Ab* led to a significant increase of the fluorescence using the same assay system "Figure 9) (Klein et al., 2019). The results of the NPN assay do not match those of the bile salts assay, probably indicating that the two assays detect different modifications of the OM. Differing assay readouts when using two different agents (NPN and in this case EtBr) to detect permeability defects actually have been reported before (Kamischke et al., 2019). However, as the results observed in the bile salt assay, these data indicate a minor role for SurA and more important role of Skp in biogenesis of OMPs and thus membrane integrity in *Ab*. This hypothesis is also supported by the finding that we did not observe a significantly changed fluorescence in the Δ*surA*Δ*degP* mutant strain, compared to the wild type ("Figure *9*). The lack of SurA and DegP might possibly be compensated by Skp. However, the concurrent deletion of *surA* and *skp* had the greatest impact on OM integrity in the NPN assay ("Figure *9*). Though, it seems that Skp plays a more important role in *Ab* than SurA, and the loss of both proteins seems to add up. Also, the Δ*skp*Δ*degP* mutant strain demonstrated a slight increase in fluorescence, but the impact of Skp and DegP on OM integrity does not seem to be additive. Of note, although some mutants showed a significantly increased fluorescence, the fluorescence signals recorded were in general much lower than that of the positive control, where cells were treated with polymyxin B. As we had observed also in the bile salt assays ("Figure *8*), the triple mutant actually was not the one displaying the most pronounced phenotype, but revealed only a slight difference compared to the wild type, which is somewhat puzzling and we currently do not have a good explanation for this finding. In *Ab,* a mutation in the *lpxD* gene, a part of the early lipid A synthetic pathway, leads to the occurrence of lipid A and LOS deficient bacteria (Moffatt et al., 2010). In mass spectrometric analyses (MS) of the triple mutant compared to the wild type (which will be discussed in more detail below) we found a significant reduced abundancy of LpxD ("Table *15*). So, it could well be that the triple mutant strain in AB5075 has reduced LOS levels.

However, if this is really the case was not analyzed in in this work and has to be examined in further experiments. A significant reduction of the abundancy of other proteins (e.g. LpxA, LpxC, and LptD) involved in LOS synthesis could not be observed ("Table *15*). Furthermore, there could be different mechanisms which compensate the deficiency of LOS and/or prevent the intrusion of NPN in the cell. Nevertheless, the reduced abundancy of LpxD could be one reason for the observed reduction of growth, since a reduced fitness of *Ab* ATCC 19606 strains with mutations in the *lpxD* gene was observed (Beceiro et al., 2014). Still, it has to be considered that many factors exist which can affect growth and the reduced abundancy of LpxD could only be one factor contributing to a reduced growth.

6.2.3 Impact of deletions on antibiotic susceptibility

Since the OM of Gram-negative pathogens can effectively prevent antibiotics from intruding into the cell, we wondered whether the deletions of *surA*, *skp*, and *degP* changed the OM composition in a way that enhances antibiotic uptake. Therefore, microbroth dilution assays were carried out. For this assay representatives of 6 classes of antibiotics: (I) aminoglycosides (amikacin, gentamicin and tobramycin), (II) carbapenems (imipenem and meropenem), (III) penicillins (piperacillin/tazobactam), (IV) cephalosporins (ceftolozan/tazobactam and ceftazidim/avibactam) and (V) fluoroquinolones (levofloxacin) were used. Those antibiotics are typically used to fight *Ab* infections, according to the European Committee on Antimicrobial Susceptibility Testing (EUCAST) (http://www.eucast.org) as well as to the Clinical & Laboratory Standards Institute (CLSI) (http://em100.edaptivedocs.net/dashboard.aspx). Compared to the wild type, for the single deletion mutant strains of *surA* and *skp* no difference in the minimal inhibitory concentration (MIC) for most of the antibiotics could be observed. However, for amikacin a 2-fold and 4-fold reduction of the MIC values for Δ*surA* and Δ*skp*, respectively, was observed. Also, for ceftazidim/avibactam the MIC was reduced 4-fold for both mutant strains compared to the wild type. Interestingly, the Δ*surA* deletion mutant showed a break of resistance specifically for tobramycin, whereas the MIC value for this antibiotic even increased in the *skp* deletion strain. The *degP* deletion mutant showed no significant decreased MIC values. For two aminoglycosides (amikacin and tobramycin) as well as for levofloxacin, the MIC values are even higher than the values of the wild type. However, like for Δ*surA*, also for Δ*surA*Δ*degP,* Δ*surA*Δ*skp,* and Δ*surA*Δ*skp*Δ*degP* MIC values lower than the breakpoint could be observed for tobramycin ("Table *10*). In sum, for all mutant strains lacking SurA, a break of resistance against tobramycin could be shown. This indicates an important role of SurA for tobramycin resistance. In the MS of the triple mutant strain compared to the wild type, the APH (3')-VI family aminoglycoside O-phosphotransferase was reduced below detection limit in whole cell lysates of the triple mutant strain ("Table *11*).

The APH(3')-VI protein belongs to the family of aminoglycoside modifying enzymes and is encoded by the *aphA6* gene, located on the p1AB5075 of AB5075 (Gallagher et al., 2015; Ramirez and Tolmasky, 2010). As a transposable element, *aphA6* is flanked by the two IS elements IS*Aba*125 (Hamidian et al., 2014). A lack of this protein would contribute to the observed increased susceptibility against the aminoglycoside antibiotics amikacin and tobramycin in the triple mutant strain. Using whole genome sequencing (WGS), we actually found that the transposable element encoding *aphA6* had been lost in the genome of the triple mutant strain. However, a deletion of the *aphA6* gene could not be detected in the double knockout mutants, which also displayed increased susceptibility towards aminoglycosides ("Table *10*). Thus, AB5075 also must possess other and/or additional mechanisms associated with resistance against aminoglycosides which may be affected by the simultaneous deletion of two, but not all three, chaperone proteins. Recently, Gallagher et al. identified 37 genes which are associated with tobramycin resistance in AB5075. The majority of these genes was encoded in the core genome, whereas one gene encoding for a protein of unknown function was carried on p2AB5075, and two genes, *aadB* and *aacA4*, on the large plasmid p1AB5075 (Gallagher et al., 2017). Tobramycin heteroresistant subpopulations of AB5075 were observed that were characterized by a RecA-dependent increased expression of *aadB* (Anderson et al., 2018). RecA represents a protein important for stress response (Cox, 1991) and will be discussed below. Our MS analysis did not reveal significantly changed abundance of the 2'-aminoglycoside nucleotidyltransferase AadB, encoded by *aadB* (Birkle et al., manuscript submitted). Therefore, we could not draw an association of the increased susceptibility of the triple mutant for tobramycin. Anderson et al. also observed heteroresistant subpopulations of AB5075 in a *recA* deletion mutant. Also here, an increased expression of *aadB* was not detected. This indicates the existence of another mechanism causative for the heteroresistance towards treatment with tobramycin (Anderson et al., 2018). The resistance against aminoglycosides, especially tobramycin, in AB5075 is maintained by many different genes and mechanisms (Anderson et al., 2018; Gallagher et al., 2017). However, the data collected within this thesis indicate that SurA plays an important role for tobramycin resistance in AB5075 by a yet unknown mechanism.

With respect to all tested antibiotics, we found the most pronounced effect in the Δ*surA*Δ*skp* deletion strain compared to the wild type and all other mutant strains. This is consistent with the NPN assay, where the Δ*surA*Δ*skp* mutant revealed the most profound disturbance of OM barrier function ("Figure *9*), however, membrane integrity is not the only factor that influences antibiotic susceptibility and also other mechanisms may contribute to our observations. Besides for tobramycin, also the MIC value for amikacin dropped below the breakpoint in the triple mutant strain.

Nevertheless, for the other antibiotics that were tested the additional lack of DegP did not result in a further decrease of the MIC values in the triple mutant compared to the Δ*surA*Δ*skp* mutant strain ("Table *10*). This indicates that different effects caused by the lack of periplasmic chaperones are causative for a change in susceptibility to treatment with a specific antibiotic. It is obviously not only a membrane defect leading to increased susceptibility. As WGS revealed that the transposable element encoding for the aminoglycoside inactivating enzyme APH (3')-VI had been lost only in the genome of the triple mutant strain, this of course may be also an explanation for increased susceptibility towards tobramycin, but only in the triple mutant.

Interestingly, we observed a significant increase in the abundancy of the proteins AdeB and AdeC by MS analyses ("Table *11*). As mentioned before (1.3.2 Expression of efflux pumps), AdeB is the transporter part of the three-part RND efflux system AdeABC. In *Ab* strain BM4454, it was shown that AdeABC is involved in resistance against a number of antibiotics, including aminoglycosides, like tobramycin, gentamicin, and less effectively against kanamycin and amikacin as well as chloramphenicol, fluoroquinolones, and tetracycline (Magnet et al., 2001). Our MS analyses also revealed a slight though significant increase of the protein AdeJ, which is the transporter part of the AdeIJK efflux system (Damier-Piolle et al., 2008) ("Table *15*). For AdeIJK, an association with resistance to β-lactams, chloramphenicol, fluoroquinolones, and tetracycline was observed in the *Ab* strain BM4454 (Damier-Piolle et al., 2008). As presumably both systems are tightly regulated by two-component systems (Rosenfeld et al., 2012; Yoon et al., 2013), the higher abundancy of these proteins in the triple mutant strain may be the result of stimuli caused by the knockout of SurA, Skp and DegP, e.g. a stress response due to the hampered OMP biogenesis. By increasing amounts of efflux pumps, the enhanced influx of antimicrobials enabled by defects in the OM could possibly be compensated. However, the MS analyses revealed increased abundance only of parts of the systems. For AdeA, AdeI, and AdeK no significant change in the abundancy could be detected ("Table *15*). Actually, it has been shown that overexpression of AdeB is sufficient to cause an increase in MIC (Magnet et al., 2001) and that AdeC is even dispensable for the function of the AdeABC efflux system. Less is known about the AdeIJK efflux system, but also here we found only the transporter protein AdeJ more abundant ("Table *15*). Given the homology of both systems it is conceivable to assume that also overexpression of AdeJ only might result in increased efflux. However, the AdeIJK system in general is much less expressed compared to AdeABC, since its overexpression seems to be toxic for the cells (Rosenfeld et al., 2012).

A possible explanation for the increased abundancy of the OM component AdeC could be the existence of a mechanism aiming at compensating the loss of other membrane stabilizing proteins whose OM insertion dependents on SurA, Skp and/or DegP. As said, like *Nm*, *Ab* is able to survive without LOS (Moffatt et al., 2010; Steeghs et al., 1998).

One theory of how the loss of LOS may be compensated is the increased expression of lipoproteins replacing the missing proteins in the OM, and thereby reinforcing the OM (Powers and Trent, 2018). The significantly increased abundancy of AdeB, AdeC, and AdeJ could therefore also serve as a complementation of the loss of other OM proteins. Nevertheless, our data demonstrate a SurA-, Skp- or DegP-independency for several proteins belonging to RND efflux systems. Actually, in other species a SurA independency of proteins of efflux systems was already demonstrated: in *Pa*, even an increased abundancy of OprM was shown in a MS analysis of a conditional deletion strain of *surA* (Klein et al., 2019). Like AdeC and AdeK, *Pa* OprM is also an OM channel protein. In combination with MexA (MFP) and MexB (multidrug transporter) or MexX (MFP) and MexY (multidrug transporter), OprM forms efflux systems in *Pa* (Poole, 2001). This also indicates that another mechanism might exist that is responsible for efficient insertion of efflux pump associated OMPs.

In contrast to AdeB, AdeC, and AdeJ that had higher abundancy in the triple mutant strain, an AdeT-like protein was significantly less abundant ("Table *15*). AdeT is a RND type efflux pump and is involved in resistance against several antibiotics, including chloramphenicol, tetracycline and ciprofloxacin (Srinivasan et al., 2011). The *Ab* strains ATCC 17978 and AC0037 harbor two copies of *adeT* genes and insertional inactivation of these genes in *Ab* AC0037 was associated with increased susceptibility against several antibiotics (Smith et al., 2007; Srinivasan et al., 2011). However, in the genome of AB5075, three genes encoding for *adeT*-like genes can be found (Scribano et al., 2019). So, taken together, although a significant reduction of the abundance of the AdeT-like protein could be observed, a clear association with the increased susceptibility of the triple mutants to antibiotics could not be made, as the other two AdeT-like proteins could possibly compensate the reduction of the third one.

Besides the microbroth dilution assay, E-tests were used to assess the susceptibility towards treatment with vancomycin ("Table *10*). Vancomycin is typically used only for treatment of infections with Gram-positive bacteria, as it cannot pass the OM of Gram-negative bacteria. However, if membrane integrity is hampered, vancomycin sensitivity can serve as an indicator for the presence and severity of OM defects (Wu et al., 2005). Compared to the wild type, all mutant strains showed an increased susceptibility to treatment with vancomycin. Interestingly, the single deletion of *surA* led to a more profound susceptibility against vancomycin than the concurrent deletions of *surA* + *degP* or *skp* + *degP*. In contrast to the bile salt and NPN assay as well as the microbroth dilution assay using different antibiotics, the Δ*surA* deletion mutant strain shows in the vancomycin assay similar results as obtained by the deletion of *surA* in *Pa*. An increased susceptibility towards treatment with vancomycin was also observed in a conditional knockout strain of *surA* in a well-established *Pa* laboratory strain, as well as in the MDR clinical bloodstream isolate ID72 (Klein et al., 2019; Willmann et al., 2018).

For the AB5075 *degP* deletion mutant strain, an even lower vancomycin susceptibility was observed, compared to the Δ*surA*Δ*degP* and Δ*skp*Δ*degP* mutant strains. Both, the bile salt as well as the NPN assay we had carried out indicated an impaired OM integrity upon the single deletion of *degP* or in combination with *skp*. Nevertheless, the microbroth dilution assays as well as the E-test with vancomycin indicate a less important role of DegP in resistance to treatment with several antibiotics. The Δ*surA*Δ*skp* deletion strain showed the most distinct effect followed by the triple mutant. Again, this is consistent with the experimental outcomes of the microbroth dilution assay ("Table *10*) and the NPN assay ("Figure *9*) for the Δ*surA*Δ*skp* mutant strain. Since these assays probe the membrane integrity the simultaneously lack of SurA and Skp seems to cause the most pronounced membrane defects. Taken together, the concurrent deletion of the periplasmic chaperones leads to a reduction of OM integrity, permeability and hence susceptibility against antibiotics. With respect to antibiotic susceptibility, the most pronounced effect was observed for the Δ*surA*Δ*skp* as well as the triple mutant. The most striking finding, however, was that the deletion of two of the periplasmic chaperones SurA, Skp and DegP or even all three at the same time is viable in *Ab*. This could be shown for the first time in a Gram-negative bacterium (Birkle et al., manuscript submitted) and implies that *Ab* OMP biogenesis has distinct features that discern it from that of *Ec* and also *Nm*, the best-studied organisms in that respect (Rizzitello et al., 2001; Sklar et al., 2007b; Volokhina et al., 2011).

6.2.4 Mass spectrometric analyses (MS) of the triple mutant compared to the wild type

Unexpectedly, *Ab* survived the deletion of two or more periplasmic chaperones and revealed phenotypes that were rather different to what we had expected based on the data derived from *Ec*, *Ye* and *Pa*. Therefore, we wanted to better understand which rearrangements on the protein levels were induced by the knockouts of SurA, Skp and DegP in *Ab*. To this end we wanted to compare the abundancy of the major OMPs in the wild type and the triple mutant strain. As we assumed that the concurrent lack of SurA, Skp and DegP might induce the upregulation of proteins acting compensatory, we also aimed to identify protein significantly more abundant in the triple mutant strain. Furthermore, the MS data also should serve as an additionally proof for the deletion of all three periplasmic chaperones. MS analyses were performed using both whole cells lysate (WCL), as well as membrane fractions (MEM) of the wild type and Δ*surA*Δ*skp*Δ*degP* mutant strain in three independent experiments. In general, for the WCL as well as the MEM fractions more proteins were less abundant (~ 74 % of all identified proteins) in the triple mutant strain compared to the wild type ("Figure *10*). This global reduction of protein abundance indicates that the lack of SurA, Skp and DegP actually has profound global effect on the cells, either directly or indirectly. The reduction of the cellular levels of numerous proteins might be the result of a stress response, aiming to relief the stresses, such as accumulation of proteins in the periplasm, membrane stress due to problems with insertion of vital OMPs, and membrane defects.

One possible reason for the observed increased susceptibility towards treatment with different antibiotics, the reduced growth in the presence of 0,3% bile salts, and the increased uptake of the fluorescence dye NPN, could be a reduced abundancy of the major OMPs of *Ab* including OmpA and CarO. As mentioned before, those proteins are OM porins and are associated with the significant low permeability of the OM, as well as with carbapenem resistance (Limansky et al., 2002; Mussi et al., 2005; Sugawara and Nikaido, 2012). Recently, reduced membrane integrity as well as an increased susceptibility against several antibiotics could be demonstrated in isogenic mutants of $OmpA_{AB}$ in *Ab* and *A. nosocomialis* (Kwon et al., 2017; Kwon et al., 2019). However, we did not observe a significant change in the abundancy of the major OMPs of *Ab* which could explain the impaired permeability of the triple mutant strain. Nevertheless, for some OMPs, including a DcaP-like protein (ABUW_0826), an OprD family protein (ABUW_3685) and an OmpW-family protein (ABUW_3583) we observed a significantly reduced abundance ("Table *11*). However, a direct association of the reduced abundancy of those proteins with the impaired OM could not be made. This has to be investigated in further experiments.

In sum, we found a significantly reduced abundance for some OMPs, however, surprisingly not for the major OMPs of *Ab* including CarO and OmpA ("Table *11*). Nevertheless, the impaired OM integrity of the triple mutant and hence the increased susceptibility towards antibiotics may be affected by the reduced abundancy of other OMPs also contributing to membrane integrity and permeability.

Furthermore, we did find proteins that were significantly more abundant in the triple mutant, but these proteins were either of unknown function or their known function did not obviously reveal how they could facilitate or contribute to compensating the loss of the three chaperones. Since ~ 28% of the genes encoded in AB5075 are annotated as uncharacterized proteins, this was not extremely surprising (Wu et al., 2016). Highest abundancy in the triple mutant strain was found for a protein of unknown function (UniProt ID: A0A0D5YIP3) which is encoded by three copies in the genome of AB5075 and a protein (UniProt ID: A0A0D5YJ02) which is encoded five times in the genome ("Table *11*). Their organization within the genome as well as annotations for similar proteins, indicate that they are phage-derived. Although we found that the triple mutant is viable in *Ab*, our phenotypic characterization indicated that it is exposed to reasonable stress and even had a slight growth phenotype. Consistent with this assumption we observed an increased abundance of the protein RecA ("Table *15*). RecA is important for stress response and also plays an important role in SOS mutagenesis (Cox, 1991). In *Ab* the disruption of RecA leads to an increased sensitivity towards stress factors including heat shock, desiccation and chemical oxidants. Furthermore, an increased susceptibility towards antibiotics and a reduced virulence in a mouse model could be observed (Aranda et al., 2011). In our findings, the observed increased abundancy of RecA indicates that the triple mutant strain faces stress. In contrast to the literature, however, despite the higher abundancy of RecA, the triple mutant

showed an increased susceptibility towards several antibiotics, and attenuated virulence in a *Galleria mellonella* infection model (see chapter 3.2.6). Noteworthy, the disruption of RecA had the most pronounced effect on susceptibility of *Ab* ATCC 17978 towards treatment with antibiotics belonging to the class of quinolones (Aranda et al., 2011). Since quinolones damage the DNA, this observation was somewhat expected (Aranda et al., 2011; Drlica et al., 2008). However, the disruption of RecA did not affect the susceptibility of *Ab* ATCC 17978 towards the aminoglycosides tobramycin and amikacin, with which we had observed the most pronounced increase in susceptibility in the triple mutant strain (Aranda et al., 2011) ("Table *10*). Taken together, the increased abundancy of RecA indicates an increased stress level in the triple mutant, but cannot be directly associated with the observed changes in the susceptibility towards antibiotics. However, the increased abundancy of RecA may contribute to the unexpected growth behavior of the triple mutant strain we had observed in our bile salt assay ("Figure *8*). For the triple mutant strain a significant impairment of the OM was expected which should coincide with increased sensitivity towards exposure to bile salts. Nevertheless, only a slight reduction of growth could be observed in a bile salt assay ("Figure *8*). However, it is known that besides the disruption of the bacterial membrane, bile salts also induce DNA damages (Urdaneta and Casadesus, 2017). Since we found RecA already increased in the triple mutant, this might have a protective effect against bile salts-induced DNA damage. Nevertheless, this is just a speculation and an association of RecA with the observed weak growth defects of the triple mutant strain in the bile salt assay would need to be clarified by further experiments. In contrast to the significantly increased abundancy of RecA in the triple mutant strain, a decreased abundance of several other proteins involved in stress response, like the universal stress protein and the general stress protein 39 was observed ("Table *15*). Since the assumption was that at least the triple mutant strain of *Ab* suffers from increased cellular stress, this decreased abundance of proteins involved in stress response was unexpected. However, one possible explanation for this observation could be that the increased abundance of RecA is sufficient for *Ab* to cope with the stress level present, and the decreased expression of other proteins involved in stress responses is to minimize efforts of material and energy. Similar observations were made for the expression of proteins involved in iron homeostasis. The OM receptor for the acquisition of Fe(III)-coprogen, Fe(III)-ferrioxamine B and Fe(III)-rhodotrulic acid FhuE is significantly more abundant in the triple mutant whereas the abundancy of the acinetobactin receptor BauA is significantly decreased ("Table *11*) (Dorsey et al., 2004; Funahashi et al., 2012). So, from these data it is hard to judge whether *Ab* might suffer from a deficiency to acquire iron or not.

Furthermore, it is impossible to infer whether the abundancy of FhuE increased because of the reduction of BauA or because of an impaired iron acquisition in general. This needs to be clarified experimentally in the future.

Possibly, *Ab* has simply switched siderophore receptor production to that one fitting best his needs under the conditions induced by the lack of SurA, Skp and DegP, or it just produces that siderophore receptor that can be inserted into the OM more efficiently under the given situation. Very recently, the ability of *Ab* ATCC 17978 to compensate the loss of BauA was demonstrated (Sheldon and Skaar, 2020). The ability to absorb iron by sequestering of siderophores, the growth in LB as well as in human serum, could only be disrupted in *Ab* by the concurrent inactivation of the acinetobactin, baumannoferrin, and fimsbactin biosynthesis pathway (Sheldon and Skaar, 2020). As FhuE is also able interact with siderophores which are produced by other bacteria, the switch might also be indicative of a strategy of *Ab* to compensate a shortage of iron by "stealing" it from other bacteria (Tiwari et al., 2019). Furthermore, the OMP OmpW was associated with the uptake of iron in *Ab* ATCC 19606 and *Ab* ATCC 17978 (Catel-Ferreira et al., 2016; Nwugo et al., 2011). OmpW is a porin-like β-barrel protein in the OM which serves as a channel for small hydrophobic molecules in several Gram-negative bacteria (Hong et al., 2006; Touw et al., 2010). In *Ec*, OmpW was shown to be downregulated in an iron deplete environment (Lin et al., 2008), and upregulated during iron replete conditions (Nwugo et al., 2011). This association was also confirmed in *Ab* ATCC 17978, demonstrating an impaired iron-uptake by using a mutant with an inactive *ompW* gene (Catel-Ferreira et al., 2016). In our MS analyses, we identified a significant decrease of an OmpW-family protein (ABUW_3583) ("Table *11*). A multiple sequence alignment revealed that this protein shares an identity of 93% to the OmpW protein of the *Ab* strains ATCC 19606 and ATCC 17978. Therefore, we assume similar function, i.e. a role in iron homeostasis, and regulation of OmpW expression in *Ab*. However, this has to be verified in more detail in further experiments. For one thing, the observed decreased abundancy of OmpW could be the result of significantly decreased abundancy of other proteins involved in iron-acquisition, including BauA, and hence an impaired iron uptake. For an efficient iron acquisition and homeostasis, the increased abundancy of other proteins like FhuE may be more important. Furthermore, it is possible that some proteins of *Ab* which are even more efficient in iron uptake could not yet be identified.

Generally, the proteins involved in uptake, regulation as well as homeostasis of iron are affected by the concurrent deletion of *surA*, *skp* and *degP* albeit to different extent. However, if our triple mutant strain suffers from deficiency to acquire iron and thus the upkeep of iron homeostasis, has to be clarified in further experiments.

Interestingly, the majority of proteins involved in the assembly of type 4 pili as well as CsuB and CsuC, proteins of the type I chaperone-usher pilus system, showed also a significantly reduction of abundancy ("Table *11*).

A reduced expression of pili was previously observed under low iron conditions in *Ab* (Eijkelkamp et al., 2011). Hence, the low abundancy of pili proteins maybe could be associated with the decrease of BauA and the diminished iron acquisition.

6.2.5 Addressing the impact of gene deletions, on AB5075 virulence using the *Galleria mellonella* infection model

Our MS data showed a significantly reduced abundancy for some proteins which are linked to virulence in other species, including e.g. T4P in *Pa* (Hahn, 1997). For this reason, we observed the virulence of the wild type and the deletion mutants we had created in a *Galleria mellonella* infection model. 30 larvae per strain were infected with 1 x 10^5 bacterial cells (actual injected inoculum ranged from 1.1 x 10^5 to 2.3 x 10^5 cells) and incubated at 37°C for 6 days. Periodically, the survival of the larvae was examined. Infection with the wild type strain resulted in the death of all larvae within 96 h. Consistent with the previously examined outcomes of the bile salt and NPN assay as well as the examination of susceptibility towards antibiotics, the single deletion of *surA* had only weak effects by demonstrating a survival rate of 13.3% ("Figure *11*). In contrast, in *Pa*, a threefold delay of time of death could be observed by the deletion of *surA* (Klein et al., 2019). However, the deletion of *degP* or *skp* resulted in a higher survival rate. Larvae injected with the *degP* deletion strain displayed a survival rate of 36.7%. Upon infection with the *skp* deletion strain, more than half of the larvae (53.3%) survived the duration of the experiment ("Figure *11*). In *Pa* instead, the deletion of the Skp homolog HlpA did not result in significant changes of the virulence compared to the wild type. This was in line with the finding that also in a bile salt assay using the *Pa hlpA* deletion mutant did not have a significant phenotype (Klein et al., 2019). Once again, our data indicate a more important role for Skp than SurA in *Ab*, especially for virulence. This assumption was corroborated by our findings after infection of *Galleria mellonella* larvae with the double and triple mutant strains of AB5075 ("Figure *11*). As before, 30 larvae were infected with 1 x 10^5 bacterial cells (actual injected inoculum ranged from 9 x 10^4 to 1.12 x 10^5 cells) of the wild type and the double and triple mutants. Larvae were incubated at 37°C and survival was monitored for 6 days. We found that larvae infected with strains lacking Skp had high survival rates (Δ*surA*Δ*skp:* 86.7%, Δ*skp*Δ*degP*: 73.3%, and Δ*surA*Δ*skp*Δ*degP*: 70%) whereas the larvae infected with the wild type died already within 48 h. For the injection of larvae with the Δ*surA*Δ*degP* mutant, a rather low survival rate of 6.7% was observed. However, to what extent the reduced survival rate of the triple mutant is affected by the reduced growth rate we had observed earlier, remains unclear.

Other factors potentially contributing to the reduced virulence of the triple mutant can be found in the collection of proteins with decreased abundancy.

Recently, it was shown that a functional biosynthesis of the acinetobactin pathway, including BauA, is essential for the virulence of *Ab* ATCC 17978 in mice (Sheldon and Skaar, 2020). Additionally, Gebhardt et al. identified genes required for growth in *Galleria mellonella* larvae, also including *bauA* (Gebhardt et al., 2015).

In *Pa*, T4P represent one of the major factors of virulence (Hahn, 1997). For *Ab*, an association of T4P-expression and virulence could not yet be demonstrated. However, in *Ab* ATCC 17978 the injection of *Galleria mellonella* larvae with deletion mutants of *comE*C, encoding for an IM transporter protein of T4P, led to a significantly increased survival. In contrast, the deletion of *pilT* had no impact on the survival of the larvae (Wilharm et al., 2013). Since we found the majority of T4P proteins significantly less abundant in the triple mutant, an association with reduced virulence can thus not be ruled out. Furthermore, a significant decrease of the protein DcaP was observed by MS analyses ("Table *15*).

The OM porin DcaP which is also involved in the uptake of sulbactam and tazobactam, was shown to be highly abundant during an infection of rodents with *Ab* strain AB307-0294 (Bhamidimarri et al., 2019). Although a direct association of DacP with virulence was not made, the decreased abundancy of DcaP may correlate with the decreased virulence we have observed with our triple mutant strain of AB5075. However, to find out whether DcaP has any correlation with virulence here, further experiments have to be performed.

All in all, our data gained using the *Galleria mellonella* infection model indicate a more important role of Skp for *Ab* virulence than of SurA.

6.3 How could AB5075 possibly compensate the concurrent lack of SurA, Skp and DegP?

6.3.1 Compensation by an alternative mechanism facilitating the transport of nascent OMPs through the periplasm

The basic idea of this work was the characterization of single deletion mutants of the periplasmic chaperones SurA, Skp and DegP to evaluate their potential to serve as antivirulence/resistance breaker targets in *Ab*. In *Ec* (Rizzitello et al., 2001; Sklar et al., 2007b), *Ye* (Weirich et al., 2017), and *Pa* (Klein et al., 2019) the individual deletion of the periplasmic chaperone proteins SurA, Skp and DegP leads to defects of the OM composition to different extent, with the deletion of SurA causing the most severe defects. The rearrangement of the OM composition results in an increased permeability as well as an increased sensitivity towards treatment with antibiotics and bile salts. In *Ec*, the deletion of two of these periplasmic chaperones is even lethal (Rizzitello et al., 2001). However, in *Ab* AB5075, the individual deletion of SurA, Skp or DegP led to only slight phenotypes regarding the sensitivity to detergents and antibiotics as well as the permeability of the OM as judged by a NPN assay.

To our surprise, even a double or triple knockout of *surA*, *skp* and *degP* was viable in *Ab* AB5075 and also led to slight phenotypes ("Table ***12***).

"Table 12 Overview of the altered phenotypes observed in the single, double and the triple knockout strains compared to the WT strain AB5075."

Impact on phenotype compared to WT	Single K.O.			Double K.O.			Triple K.O.
	ΔsurA	*Δskp*	*ΔdegP*	*ΔsurA ΔdegP*	*ΔsurA Δskp*	*Δskp ΔdegP*	*ΔsurA Δskp ΔdegP*
OD_{600nm} in LB at 37°C after 24 h	↔	↔	↑	↔	↓	↓	↓↓
OD_{600nm} in LB at 42°C after 24 h	↔	↔	↔	↓↓	↓	↓	↓↓
Sensitivity to detergent (0.3% bile salts)	↔	↔	↑	↔	↔	↑	↑
Outer membrane permeability (NPN Assay)	↑	↑	↑	↔	↑	↑	↑
Antibiotic susceptibility	↔	↔	↔	↑	↑↑↑	↑	↑↑↑
% survival of *G. mellonella* larvae 144 h after infection (WT: 0% after 48-96 h)	↑ (~ 13%)	↑↑ (~ 53%)	↑ (~ 37%)	↑ (~ 7%)	↑↑↑ (~ 87%)	↑↑ (~ 73%)	↑↑ (~ 70%)

↑ increased
↓ reduced
↔ no change compared to WT

Consequently, this finding implies that *Ab* AB5075 is somehow able to tolerate the simultaneous loss of all three periplasmic chaperone proteins. This has not been demonstrated for Gram-negative bacteria before.

One hypothesis that might explain how *Ab* manages to survive the concurrent loss of SurA, Skp and DegP would be the existence of an alternative mechanism facilitating the transport of nascent OMPs to the BAM-complex ("Figure *12*B). This means that there are either yet uncharacterized proteins within the periplasm taking over the job of SurA, Skp and DegP, or already known periplasmic proteins do possess also chaperone activity, but this has not been recognized so far.

As mentioned before, we aimed to identify such proteins by a MS analysis of the triple mutant compared to the wild type. We hypothesized that proteins with an increased abundancy in the triple mutant might be such candidates. However, most of the proteins that were significantly increased in the triple mutant strain are entirely uncharacterized and we were not able to identify a candidate protein that obviously was a good candidate because of its already know function ("Table *15*). Nevertheless, the role of the yet uncharacterized candidate proteins of OMP biogenesis in a SurA, Skp and DegP deplete situation will be investigated in a future project. This will be done by the attempt to create an additional gene deletion in the triple knockout background. As this will only work out for candidates that obviously do not play a role for maintenance of OMP biogenesis, we will additionally create a strain with Skp and DegP knocked out and SurA under the control of an inducible promoter. This will allow us to test whether the knockout of candidate genes is possible under SurA replete conditions, but lethal under SurA depleted conditions.

Another approach to identify proteins which could compensate for the absence of SurA, Skp and DegP was the search for paralogues of the periplasmic chaperone proteins which may take over the transport of nascent OMPs. For SurA a high sequence identity with a PPI domain as well as some

homology to the N-terminal and C-terminal domains could be identified in the periplasmic protein PpiD (“Table *13*). In *Ec* it was shown that some substrates of SurA are shared with PpiD, indicating a potential compensatory role for PpiD (Stymest and Klappa, 2008). Furthermore, the lethality of a simultaneous knockout of *surA* and *skp* could be rescued by an enhanced expression of PpiD in *Ec* (Matern et al., 2010). However, if the triple knockout of *surA*, *skp* and *degP* is tolerated in *Ab* because of PpiD, acting as a periplasmic chaperone delivering substrates to the BAM-complex has to be investigated in future experiments. For DegP, the regulatory periplasmic protease DegS was identified as a paralogue because of a sequence homology of the PDZ1 domain (“Table *13*). In *Ec* and in contrast to what is known for DegP, DegS is not heat-inducible. Instead DegS initiates a multi-step process of protein degradation by the cleavage of the anti-sigma factor RseA (Alba et al., 2002; Waller and Sauer, 1996). This indirect though important role for protein degradation within the periplasm and the lack of evidence for a chaperone activity of DegS make it a rather weak candidate to compensate the loss of DegP in *Ab*. Therefore, we plan not only to investigate the candidate proteins of unknown function for their role in periplasmic shuttling of OMPs in more detail, but we also aim to globally search for and corroborate already identified candidate genes that become essential in the absence of SurA, Skp and DegP. To this end we also plan to generate a high-density transposon (Tn) insertion mutant library using the triple mutant as genetic background.

6.3.1 Compensation by the formation of a supercomplex facilitating the direct interaction of the Sec-translocon with the BAM-complex

Based on the results of the MS analysis, another hypothesis for the compensation of the concurrent loss of all three chaperones was made. Interestingly, our MS analysis revealed a significantly reduced abundancy of SecY (“Table *11*). As a component of the Sec machinery, SecY is involved in the translocation of nascent OMPs across the IM into the periplasm (Mori and Ito, 2001). Thus, we assumed a reduced abundancy of the major OMPs of *Ab*, including CarO and OmpA, as a consequence of an impaired translocation through the IM. Interestingly, the abundancy of those OMPs seemed to be unaffected by the reduced amounts of SecY and the three periplasmic chaperones. This led us to another hypothesis in which the transport of nascent proteins across the periplasm is not only independent of SurA, Skp and DegP but also independent of the Sec-machinery (“Figure *12*C). Actually, a model of a so-called super-complex has been proposed before.

In this model, SecA interacts directly with the BAM-complex and functions as the translocon for nascent OMPs (Alvira et al., 2020; Jin and Chang, 2017; Jin et al., 2018; Wang et al., 2016).

However, the distinct role of the periplasmic chaperones, including SurA, is unclear in the model of a super-complex. In one proposed model SurA is a part of the super-complex (Jin and Chang, 2017; Jin et al., 2018; Wang et al., 2016).

According to the revision history, another paper omitted some data about the role of SurA in the context of a supercomplex upon recommendation of a reviewer, as they judged these data to be inconclusive (Alvira et al., 2020). However, to validate the hypothesis of a Sec machinery-independent transport of nascent OMPs to the BAM-complex, extensive experimentation would be required, confounding an entirely new project.

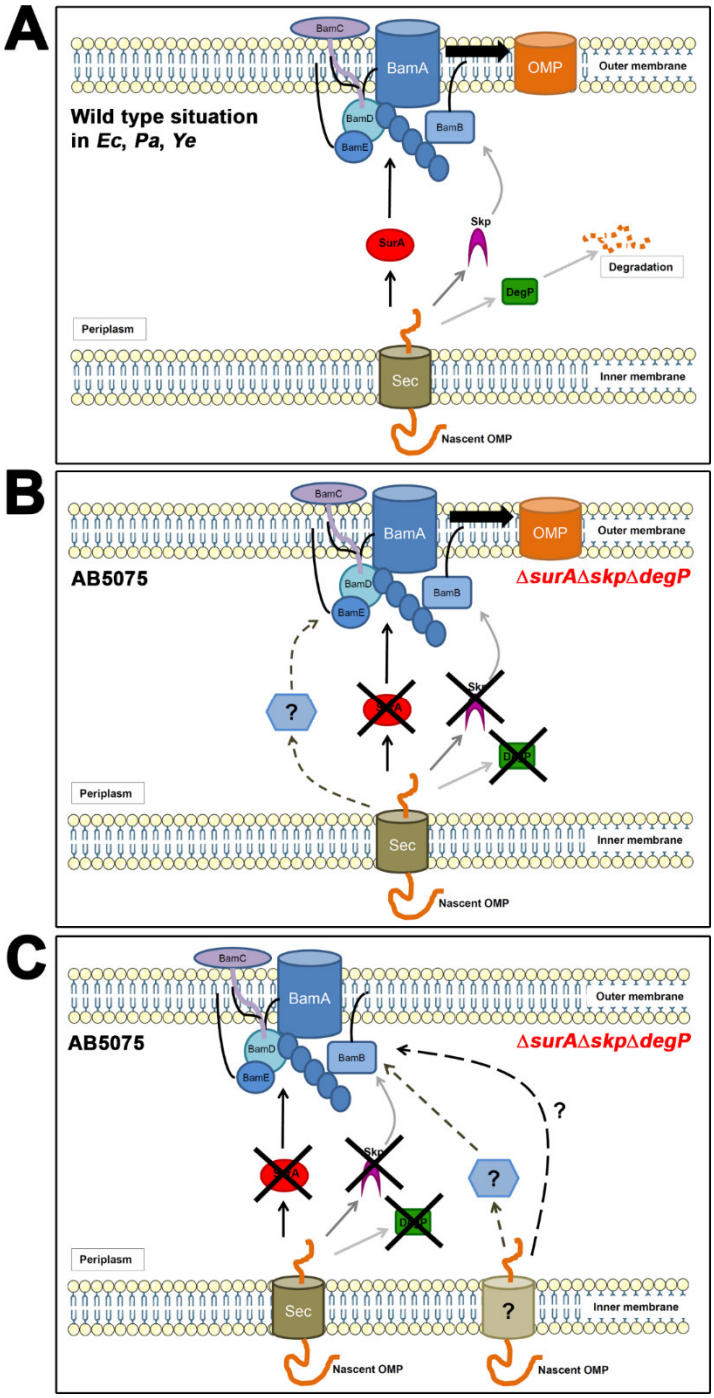

"Figure 12 Canonical periplasmic chaperone network in Gram-negative bacteria and possible compensation strategies of AB5075 in the absence of SurA, Skp and DepP. *(A) OMP biogenesis in the wild type Ec, Pa and Ye. After translocation into the periplasm though the secretory export machinery (Sec), nascent OMPs are guided through the periplasm by SurA or Skp/DegP. Misfolded or aggregated OMPs are degraded by the protease activity of DegP. After passage through the periplasm, the BAM complex facilitates insertion of the OMPs into the OM. (B) AB5075 possesses additional periplasmic factors that can transport OMPs to the BAM complex in the absence of SurA, Skp and DegP. (C) AB5075 employs a pathway independent of SecY, SurA, Skp and DegP to insert OMPs into the OM. The figure was adapted from (Noinaj et al., 2017). Certain elements such as membrane bilayers were drawn using templates from Servier Medical Art (https://smart.servier.com/)."*

7. Literature

Abdi, S.N., Ghotaslou, R., Ganbarov, K., Mobed, A., Tanomand, A., Yousefi, M., Asgharzadeh, M., Kafil, H.S., 2020. *Acinetobacter baumannii* Efflux Pumps and Antibiotic Resistance. Infect Drug Resist 13, 423-434.

Abraham, E.P., Chain, E., 1940. An Enzyme from Bacteria able to Destroy Penicillin. Nature 146, 837-837.

Adams, M.D., Goglin, K., Molyneaux, N., Hujer, K.M., Lavender, H., Jamison, J.J., MacDonald, I.J., Martin, K.M., Russo, T., Campagnari, A.A., Hujer, A.M., Bonomo, R.A., Gill, S.R., 2008. Comparative genome sequence analysis of multidrug-resistant *Acinetobacter baumannii*. J Bacteriol 190, 8053-8064.

Al Atrouni, A., Joly-Guillou, M.L., Hamze, M., Kempf, M., 2016. Reservoirs of Non-*baumannii* *Acinetobacter* Species. Front Microbiol 7, 49.

Alba, B.M., Gross, C.A., 2004. Regulation of the *Escherichia coli* sigma-dependent envelope stress response. Mol Microbiol 52, 613-619.

Alba, B.M., Leeds, J.A., Onufryk, C., Lu, C.Z., Gross, C.A., 2002. DegS and YaeL participate sequentially in the cleavage of RseA to activate the sigma(E)-dependent extracytoplasmic stress response. Genes Dev 16, 2156-2168.

Altschul, S.F., Madden, T.L., Schaffer, A.A., Zhang, J., Zhang, Z., Miller, W., Lipman, D.J., 1997. Gapped BLAST and PSI-BLAST: a new generation of protein database search programs. Nucleic Acids Res 25, 3389-3402.

Alvira, S., Watkins, D.W., Troman, L., Allen, W.J., Lorriman, J., Degliesposti, G., Cohen, E.J., Beeby, M., Daum, B., Gold, V.A.M., Skehel, J.M., Collinson, I., 2020. Inter-membrane association of the Sec and BAM translocons for bacterial outer-membrane biogenesis. bioRxiv, 589077.

Ambler, R.P., 1980. The structure of beta-lactamases. Philos Trans R Soc Lond B Biol Sci 289, 321-331.

Anderson, S.E., Sherman, E.X., Weiss, D.S., Rather, P.N., 2018. Aminoglycoside Heteroresistance in *Acinetobacter baumannii* AB5075. mSphere 3.

Andrewes, F.W., 1922. Studies in group-agglutination I. The *salmonella* group and its antigenic structure. The Journal of Pathology and Bacteriology 25, 505-521.

Andrews, S.C., Robinson, A.K., Rodriguez-Quinones, F., 2003. Bacterial iron homeostasis. FEMS Microbiol Rev 27, 215-237.

Aranda, J., Bardina, C., Beceiro, A., Rumbo, S., Cabral, M.P., Barbe, J., Bou, G., 2011. *Acinetobacter baumannii* RecA protein in repair of DNA damage, antimicrobial resistance, general stress response, and virulence. J Bacteriol 193, 3740-3747.

Asokan, G.V., Ramadhan, T., Ahmed, E., Sanad, H., 2019. WHO Global Priority Pathogens List: A Bibliometric Analysis of Medline-PubMed for Knowledge Mobilization to Infection Prevention and Control Practices in Bahrain. Oman medical journal 34, 184-193.

Ayoub Moubareck, C., Hammoudi Halat, D., 2020. Insights into *Acinetobacter baumannii*: A Review of Microbiological, Virulence, and Resistance Traits in a Threatening Nosocomial Pathogen. Antibiotics 9.

Beceiro, A., Moreno, A., Fernandez, N., Vallejo, J.A., Aranda, J., Adler, B., Harper, M., Boyce, J.D., Bou, G., 2014. Biological cost of different mechanisms of colistin resistance and their impact on virulence in *Acinetobacter baumannii*. Antimicrob Agents Chemother 58, 518-526.

Behrens, S., Maier, R., de Cock, H., Schmid, F.X., Gross, C.A., 2001. The SurA periplasmic PPIase lacking its parvulin domains functions in vivo and has chaperone activity. EMBO J 20, 285-294.

Beijerinck, M., 1911. Pigmenten als oxydatieproducten gevormd door bacterien. Versl Koninklijke Akad Wetensch Amsterdam 19, 1092-1103.

Bentancor, L.V., Camacho-Peiro, A., Bozkurt-Guzel, C., Pier, G.B., Maira-Litran, T., 2012. Identification of Ata, a multifunctional trimeric autotransporter of *Acinetobacter baumannii*. J Bacteriol 194, 3950-3960.
Benveniste, R., Davies, J., 1973. Mechanisms of antibiotic resistance in bacteria. Annu Rev Biochem 42, 471-506.
Bergogne-Berezin, E., Joly-Guillou, M.L., 1991. Hospital infection with *Acinetobacter* spp.: an increasing problem. J Hosp Infect 18 Suppl A, 250-255.
Bergogne-Berezin, E., Towner, K.J., 1996. *Acinetobacter* spp. as nosocomial pathogens: microbiological, clinical, and epidemiological features. Clin Microbiol Rev 9, 148-165.
Bernards, A.T., Harinck, H.I., Dijkshoorn, L., van der Reijden, T.J., van den Broek, P.J., 2004. Persistent *Acinetobacter baumannii*? Look inside your medical equipment. Infect Control Hosp Epidemiol 25, 1002-1004.
Bernards, A.T., van der Toorn, J., van Boven, C.P., Dijkshoorn, L., 1996. Evaluation of the ability of a commercial system to identify *Acinetobacter* genomic species. Eur J Clin Microbiol Infect Dis 15, 303-308.
Bhamidimarri, S.P., Zahn, M., Prajapati, J.D., Schleberger, C., Soderholm, S., Hoover, J., West, J., Kleinekathofer, U., Bumann, D., Winterhalter, M., van den Berg, B., 2019. A Multidisciplinary Approach toward Identification of Antibiotic Scaffolds for *Acinetobacter baumannii*. Structure 27, 268-280 e266.
Bitto, E., McKay, D.B., 2002. Crystallographic structure of SurA, a molecular chaperone that facilitates folding of outer membrane porins. Structure 10, 1489-1498.
Bojkovic, J., Richie, D.L., Six, D.A., Rath, C.M., Sawyer, W.S., Hu, Q., Dean, C.R., 2015. Characterization of an *Acinetobacter baumannii* lptD Deletion Strain: Permeability Defects and Response to Inhibition of Lipopolysaccharide and Fatty Acid Biosynthesis. J Bacteriol 198, 731-741.
Boll, J.M., Tucker, A.T., Klein, D.R., Beltran, A.M., Brodbelt, J.S., Davies, B.W., Trent, M.S., 2015. Reinforcing Lipid A Acylation on the Cell Surface of *Acinetobacter baumannii* Promotes Cationic Antimicrobial Peptide Resistance and Desiccation Survival. mBio 6, e00478-00415.
Bos, M.P., Robert, V., Tommassen, J., 2007. Biogenesis of the gram-negative bacterial outer membrane. Annu Rev Microbiol 61, 191-214.
Bos, M.P., Tefsen, B., Geurtsen, J., Tommassen, J., 2004. Identification of an outer membrane protein required for the transport of lipopolysaccharide to the bacterial cell surface. Proc Natl Acad Sci U S A 101, 9417-9422.
Bos, M.P., Tommassen, J., 2005. Viability of a capsule- and lipopolysaccharide-deficient mutant of *Neisseria meningitidis*. Infect Immun 73, 6194-6197.
Boucher, H.W., Talbot, G.H., Bradley, J.S., Edwards, J.E., Gilbert, D., Rice, L.B., Scheld, M., Spellberg, B., Bartlett, J., 2009. Bad bugs, no drugs: no ESKAPE! An update from the Infectious Diseases Society of America. Clin Infect Dis 48, 1-12.
Bouvet, P.J., Grimont, P.A., 1986. Taxonomy of the genus *Acinetobacter* with the recognition of *Acinetobacter baumannii* sp. nov., *Acinetobacter haemolyticus* sp. nov., *Acinetobacter johnsonii* sp. nov., and *Acinetobacter junii* sp. nov. and emended descriptions of *Acinetobacter calcoaceticu*s and *Acinetobacter lwoffii*. International Journal of Systematic and Evolutionary Microbiology 36, 228-240.
Brisou, J., Prevot, A.R., 1954. [Studies on bacterial taxonomy. X. The revision of species under *Acromobacter* group]. Annales de l'Institut Pasteur 86, 722-728.
Brunet, Y.R., Henin, J., Celia, H., Cascales, E., 2014. Type VI secretion and bacteriophage tail tubes share a common assembly pathway. EMBO Rep 15, 315-321.
Buxton, A.E., Anderson, R.L., Werdegar, D., Atlas, E., 1978. Nosocomial respiratory tract infection and colonization with *Acinetobacter calcoaceticus*. Epidemiologic characteristics. Am J Med 65, 507-513.
Calabrese, A.N., Schiffrin, B., Watson, M., Karamanos, T.K., Walko, M., Humes, J.R., Horne, J.E., White, P., Wilson, A.J., Kalli, A.C., Tuma, R., Ashcroft, A.E., Brockwell, D.J., Radford, S.E., 2020. Inter-

domain dynamics in the chaperone SurA and multi-site binding to its outer membrane protein clients. Nat Commun 11, 2155.
Calvert, M.B., Jumde, V.R., Titz, A., 2018. Pathoblockers or antivirulence drugs as a new option for the treatment of bacterial infections. Beilstein journal of organic chemistry 14, 2607-2617.
Camp, C., Tatum, O.L., 2010. A Review of *Acinetobacter baumannii* as a Highly Successful Pathogen in Times of War. Laboratory Medicine 41, 649-657 %@ 0007-5027.
Campos, M., Cisneros, D.A., Nivaskumar, M., Francetic, O., 2013. The type II secretion system - a dynamic fiber assembly nanomachine. Res Microbiol 164, 545-555.
Carruthers, M.D., Nicholson, P.A., Tracy, E.N., Munson, R.S., Jr., 2013. *Acinetobacter baumannii* utilizes a type VI secretion system for bacterial competition. PLoS One 8, e59388.
Catel-Ferreira, M., Coadou, G., Molle, V., Mugnier, P., Nordmann, P., Siroy, A., Jouenne, T., De, E., 2011. Structure-function relationships of CarO, the carbapenem resistance-associated outer membrane protein of *Acinetobacter baumannii*. J Antimicrob Chemother 66, 2053-2056.
Catel-Ferreira, M., Marti, S., Guillon, L., Jara, L., Coadou, G., Molle, V., Bouffartigues, E., Bou, G., Shalk, I., Jouenne, T., Vila-Farres, X., De, E., 2016. The outer membrane porin OmpW of *Acinetobacter baumannii* is involved in iron uptake and colistin binding. FEBS Lett 590, 224-231.
Catel-Ferreira, M., Nehme, R., Molle, V., Aranda, J., Bouffartigues, E., Chevalier, S., Bou, G., Jouenne, T., De, E., 2012. Deciphering the function of the outer membrane protein OprD homologue of *Acinetobacter baumannii*. Antimicrob Agents Chemother 56, 3826-3832.
Chau, S.L., Chu, Y.W., Houang, E.T., 2004. Novel resistance-nodulation-cell division efflux system AdeDE in *Acinetobacter* genomic DNA group 3. Antimicrob Agents Chemother 48, 4054-4055.
Chen, R., Henning, U., 1996. A periplasmic protein (Skp) of *Escherichia coli* selectively binds a class of outer membrane proteins. Mol Microbiol 19, 1287-1294.
Chin, C.Y., Tipton, K.A., Farokhyfar, M., Burd, E.M., Weiss, D.S., Rather, P.N., 2018. A high-frequency phenotypic switch links bacterial virulence and environmental survival in *Acinetobacter baumannii*. Nat Microbiol 3, 563-569.
Choi, C.H., Lee, E.Y., Lee, Y.C., Park, T.I., Kim, H.J., Hyun, S.H., Kim, S.A., Lee, S.K., Lee, J.C., 2005. Outer membrane protein 38 of *Acinetobacter baumannii* localizes to the mitochondria and induces apoptosis of epithelial cells. Cell Microbiol 7, 1127-1138.
Choi, C.H., Lee, J.S., Lee, Y.C., Park, T.I., Lee, J.C., 2008. *Acinetobacter baumannii* invades epithelial cells and outer membrane protein A mediates interactions with epithelial cells. BMC Microbiol 8, 216.
Chuang, Y.C., Sheng, W.H., Li, S.Y., Lin, Y.C., Wang, J.T., Chen, Y.C., Chang, S.C., 2011. Influence of genospecies of *Acinetobacter baumannii* complex on clinical outcomes of patients with acinetobacter bacteremia. Clin Infect Dis 52, 352-360.
Chusri, S., Chongsuvivatwong, V., Rivera, J.I., Silpapojakul, K., Singkhamanan, K., McNeil, E., Doi, Y., 2014. Clinical outcomes of hospital-acquired infection with *Acinetobacter nosocomialis* and *Acinetobacter pittii*. Antimicrob Agents Chemother 58, 4172-4179.
Clark, R.B., 1996. Imipenem resistance among *Acinetobacter baumannii*: association with reduced expression of a 33-36 kDa outer membrane protein. J Antimicrob Chemother 38, 245-251.
Cohen, M.L., 1992. Epidemiology of drug resistance: implications for a post-antimicrobial era. Science 257, 1050-1055.
Conway, J.R., Lex, A., Gehlenborg, N., 2017. UpSetR: an R package for the visualization of intersecting sets and their properties. Bioinformatics 33, 2938-2940.
Cortés, G., de Astorza, B., Benedi, V.J., Alberti, S., 2002. Role of the htrA gene in *Klebsiella pneumoniae* virulence. Infect Immun 70, 4772-4776.
Cosgaya, C., Mari-Almirall, M., Van Assche, A., Fernandez-Orth, D., Mosqueda, N., Telli, M., Huys, G., Higgins, P.G., Seifert, H., Lievens, B., Roca, I., Vila, J., 2016. *Acinetobacter dijkshoorniae* sp. nov., a member of the *Acinetobacter calcoaceticus-Acinetobacter baumannii* complex mainly recovered from clinical samples in different countries. Int J Syst Evol Microbiol 66, 4105-4111.

Cox, J., Mann, M., 2008. MaxQuant enables high peptide identification rates, individualized p.p.b.-range mass accuracies and proteome-wide protein quantification. Nat Biotechnol 26, 1367-1372.
Cox, M.M., 1991. The RecA protein as a recombinational repair system. Mol Microbiol 5, 1295-1299.
Damier-Piolle, L., Magnet, S., Bremont, S., Lambert, T., Courvalin, P., 2008. AdeIJK, a resistance-nodulation-cell division pump effluxing multiple antibiotics in *Acinetobacter baumannii*. Antimicrob Agents Chemother 52, 557-562.
Danese, P.N., Snyder, W.B., Cosma, C.L., Davis, L.J., Silhavy, T.J., 1995. The Cpx two-component signal transduction pathway of *Escherichia coli* regulates transcription of the gene specifying the stress-inducible periplasmic protease, DegP. Genes Dev 9, 387-398.
Dartigalongue, C., Raina, S., 1998. A new heat-shock gene, ppiD, encodes a peptidyl-prolyl isomerase required for folding of outer membrane proteins in *Escherichia coli*. EMBO J 17, 3968-3980.
Davis, K.A., Moran, K.A., McAllister, C.K., Gray, P.J., 2005. Multidrug-resistant *Acinetobacter* extremity infections in soldiers. Emerg Infect Dis 11, 1218-1224.
de Breij, A., Gaddy, J., van der Meer, J., Koning, R., Koster, A., van den Broek, P., Actis, L., Nibbering, P., Dijkshoorn, L., 2009. CsuA/BABCDE-dependent pili are not involved in the adherence of *Acinetobacter baumannii* ATCC19606(T) to human airway epithelial cells and their inflammatory response. Res Microbiol 160, 213-218.
del Mar Tomas, M., Beceiro, A., Perez, A., Velasco, D., Moure, R., Villanueva, R., Martinez-Beltran, J., Bou, G., 2005. Cloning and functional analysis of the gene encoding the 33- to 36-kilodalton outer membrane protein associated with carbapenem resistance in *Acinetobacter baumannii*. Antimicrob Agents Chemother 49, 5172-5175.
Dijkshoorn, L., Nemec, A., Seifert, H., 2007. An increasing threat in hospitals: multidrug-resistant *Acinetobacter baumannii*. Nat Rev Microbiol 5, 939-951.
Dorsey, C.W., Tolmasky, M.E., Crosa, J.H., Actis, L.A., 2003. Genetic organization of an *Acinetobacter baumannii* chromosomal region harbouring genes related to siderophore biosynthesis and transport. Microbiology (Reading) 149, 1227-1238.
Dorsey, C.W., Tomaras, A.P., Connerly, P.L., Tolmasky, M.E., Crosa, J.H., Actis, L.A., 2004. The siderophore-mediated iron acquisition systems of *Acinetobacter baumannii* ATCC 19606 and *Vibrio anguillarum* 775 are structurally and functionally related. Microbiology (Reading) 150, 3657-3667.
Douzi, B., Filloux, A., Voulhoux, R., 2012. On the path to uncover the bacterial type II secretion system. Philos Trans R Soc Lond B Biol Sci 367, 1059-1072.
Doyle, M.T., Bernstein, H.D., 2019. Bacterial outer membrane proteins assemble via asymmetric interactions with the BamA beta-barrel. Nat Commun 10, 3358.
Drlica, K., Malik, M., Kerns, R.J., Zhao, X., 2008. Quinolone-mediated bacterial death. Antimicrob Agents Chemother 52, 385-392.
Dupont, M., Pages, J.M., Lafitte, D., Siroy, A., Bollet, C., 2005. Identification of an OprD homologue in *Acinetobacter baumannii*. J Proteome Res 4, 2386-2390.
Eijkelkamp, B.A., Hassan, K.A., Paulsen, I.T., Brown, M.H., 2011. Investigation of the human pathogen *Acinetobacter baumannii* under iron limiting conditions. BMC Genomics 12, 126.
Eijkelkamp, B.A., Stroeher, U.H., Hassan, K.A., Paulsen, I.T., Brown, M.H., 2014. Comparative analysis of surface-exposed virulence factors of *Acinetobacter baumannii*. BMC Genomics 15, 1020.
Espinal, P., Marti, S., Vila, J., 2012. Effect of biofilm formation on the survival of *Acinetobacter baumannii* on dry surfaces. J Hosp Infect 80, 56-60.
Eswaran, J., Koronakis, E., Higgins, M.K., Hughes, C., Koronakis, V., 2004. Three's company: component structures bring a closer view of tripartite drug efflux pumps. Curr Opin Struct Biol 14, 741-747.
Ewels, P.A., Peltzer, A., Fillinger, S., Patel, H., Alneberg, J., Wilm, A., Garcia, M.U., Di Tommaso, P., Nahnsen, S., 2020. The nf-core framework for community-curated bioinformatics pipelines. Nat Biotechnol 38, 276-278.
Farrow, J.M., 3rd, Wells, G., Pesci, E.C., 2018. Desiccation tolerance in *Acinetobacter baumannii* is mediated by the two-component response regulator BfmR. PLoS One 13, e0205638.

Fernandez-Cuenca, F., Martinez-Martinez, L., Conejo, M.C., Ayala, J.A., Perea, E.J., Pascual, A., 2003. Relationship between beta-lactamase production, outer membrane protein and penicillin-binding protein profiles on the activity of carbapenems against clinical isolates of *Acinetobacter baumannii*. J Antimicrob Chemother 51, 565-574.
Fernandez-Cuenca, F., Smani, Y., Gomez-Sanchez, M.C., Docobo-Perez, F., Caballero-Moyano, F.J., Dominguez-Herrera, J., Pascual, A., Pachon, J., 2011. Attenuated virulence of a slow-growing pandrug-resistant *Acinetobacter baumannii* is associated with decreased expression of genes encoding the porins CarO and OprD-like. Int J Antimicrob Agents 38, 548-549.
Fitzpatrick, M.A., Ozer, E., Bolon, M.K., Hauser, A.R., 2015. Influence of ACB complex genospecies on clinical outcomes in a U.S. hospital with high rates of multidrug resistance. J Infect 70, 144-152.
Fitzsimons, T.C., Lewis, J.M., Wright, A., Kleifeld, O., Schittenhelm, R.B., Powell, D., Harper, M., Boyce, J.D., 2018. Identification of Novel *Acinetobacter baumannii* Type VI Secretion System Antibacterial Effector and Immunity Pairs. Infect Immun 86.
Fleming, A., 2001. On the antibacterial action of cultures of a penicillium, with special reference to their use in the isolation of B. influenzae. 1929. Bulletin of the World Health Organization 79, 780-790.
Frain, K.M., van Dijl, J.M., Robinson, C., 2019. The Twin-Arginine Pathway for Protein Secretion. EcoSal Plus 8.
Fu, X., Wang, Y., Shao, H., Ma, J., Song, X., Zhang, M., Chang, Z., 2018. DegP functions as a critical protease for bacterial acid resistance. FEBS J 285, 3525-3538.
Funahara, Y., Nikaido, H., 1980. Asymmetric localization of lipopolysaccharides on the outer membrane of *Salmonella typhimurium*. J Bacteriol 141, 1463-1465.
Funahashi, T., Tanabe, T., Mihara, K., Miyamoto, K., Tsujibo, H., Yamamoto, S., 2012. Identification and characterization of an outer membrane receptor gene in *Acinetobacter baumannii* required for utilization of desferricoprogen, rhodotorulic acid, and desferrioxamine B as xenosiderophores. Biol Pharm Bull 35, 753-760.
Gaddy, J.A., Arivett, B.A., McConnell, M.J., Lopez-Rojas, R., Pachon, J., Actis, L.A., 2012. Role of acinetobactin-mediated iron acquisition functions in the interaction of *Acinetobacter baumannii* strain ATCC 19606T with human lung epithelial cells, *Galleria mellonella* caterpillars, and mice. Infect Immun 80, 1015-1024.
Gaddy, J.A., Tomaras, A.P., Actis, L.A., 2009. The *Acinetobacter baumannii* 19606 OmpA protein plays a role in biofilm formation on abiotic surfaces and in the interaction of this pathogen with eukaryotic cells. Infect Immun 77, 3150-3160.
Gallagher, L.A., Lee, S.A., Manoil, C., 2017. Importance of Core Genome Functions for an Extreme Antibiotic Resistance Trait. mBio 8.
Gallagher, L.A., Ramage, E., Weiss, E.J., Radey, M., Hayden, H.S., Held, K.G., Huse, H.K., Zurawski, D.V., Brittnacher, M.J., Manoil, C., 2015. Resources for Genetic and Genomic Analysis of Emerging Pathogen *Acinetobacter baumannii*. J Bacteriol 197, 2027-2035.
Garcia-Garmendia, J.L., Ortiz-Leyba, C., Garnacho-Montero, J., Jimenez-Jimenez, F.J., Monterrubio-Villar, J., Gili-Miner, M., 1999. Mortality and the increase in length of stay attributable to the acquisition of *Acinetobacter* in critically ill patients. Crit Care Med 27, 1794-1799.
Garcia-Garmendia, J.L., Ortiz-Leyba, C., Garnacho-Montero, J., Jimenez-Jimenez, F.J., Perez-Paredes, C., Barrero-Almodovar, A.E., Gili-Miner, M., 2001. Risk factors for *Acinetobacter baumannii* nosocomial bacteremia in critically ill patients: a cohort study. Clin Infect Dis 33, 939-946.
Gayoso, C.M., Mateos, J., Mendez, J.A., Fernandez-Puente, P., Rumbo, C., Tomas, M., Martinez de Ilarduya, O., Bou, G., 2014. Molecular mechanisms involved in the response to desiccation stress and persistence in *Acinetobacter baumannii*. J Proteome Res 13, 460-476.
Gebhardt, M.J., Gallagher, L.A., Jacobson, R.K., Usacheva, E.A., Peterson, L.R., Zurawski, D.V., Shuman, H.A., 2015. Joint Transcriptional Control of Virulence and Resistance to Antibiotic and Environmental Stress in *Acinetobacter baumannii*. mBio 6, e01660-01615.

Gerner-Smidt, P., 1992. Ribotyping of the *Acinetobacter calcoaceticus-Acinetobacter baumannii* complex. J Clin Microbiol 30, 2680-2685.
Gerner-Smidt, P., Tjernberg, I., Ursing, J., 1991. Reliability of phenotypic tests for identification of *Acinetobacter* species. J Clin Microbiol 29, 277-282.
Getchell-White, S.I., Donowitz, L.G., Groschel, D.H., 1989. The inanimate environment of an intensive care unit as a potential source of nosocomial bacteria: evidence for long survival of *Acinetobacter calcoaceticus*. Infect Control Hosp Epidemiol 10, 402-407.
Giammanco, A., Cala, C., Fasciana, T., Dowzicky, M.J., 2017. Global Assessment of the Activity of Tigecycline against Multidrug-Resistant Gram-Negative Pathogens between 2004 and 2014 as Part of the Tigecycline Evaluation and Surveillance Trial. mSphere 2.
Giannouli, M., Antunes, L.C., Marchetti, V., Triassi, M., Visca, P., Zarrilli, R., 2013. Virulence-related traits of epidemic *Acinetobacter baumannii* strains belonging to the international clonal lineages I-III and to the emerging genotypes ST25 and ST78. BMC Infect Dis 13, 282.
Goemans, C., Denoncin, K., Collet, J.F., 2014. Folding mechanisms of periplasmic proteins. Biochim Biophys Acta 1843, 1517-1528.
Gomez, J., Simarro, E., Banos, V., Requena, L., Ruiz, J., Garcia, F., Canteras, M., Valdes, M., 1999. Six-year prospective study of risk and prognostic factors in patients with nosocomial sepsis caused by *Acinetobacter baumannii*. Eur J Clin Microbiol Infect Dis 18, 358-361.
Green, E.R., Juttukonda, L.J., Skaar, E.P., 2020. The Manganese-Responsive Transcriptional Regulator MumR Protects *Acinetobacter baumannii* from Oxidative Stress. Infect Immun 88.
Gribun, A., Nitzan, Y., Pechatnikov, I., Hershkovits, G., Katcoff, D.J., 2003. Molecular and structural characterization of the HMP-AB gene encoding a pore-forming protein from a clinical isolate of *Acinetobacter baumannii*. Curr Microbiol 47, 434-443.
Hahn, H.P., 1997. The type-4 pilus is the major virulence-associated adhesin of *Pseudomonas aeruginosa*--a review. Gene 192, 99-108.
Hamidian, M., Holt, K.E., Pickard, D., Dougan, G., Hall, R.M., 2014. A GC1 *Acinetobacter baumannii* isolate carrying AbaR3 and the aminoglycoside resistance transposon Tn aphA6 in a conjugative plasmid. Journal of Antimicrobial Chemotherapy 69, 955-958 %@ 1460-2091.
Hancock, R.E., Brinkman, F.S., 2002. Function of *pseudomonas* porins in uptake and efflux. Annu Rev Microbiol 56, 17-38.
Harding, C.M., Hennon, S.W., Feldman, M.F., 2018. Uncovering the mechanisms of *Acinetobacter baumannii* virulence. Nat Rev Microbiol 16, 91-102.
Harding, C.M., Kinsella, R.L., Palmer, L.D., Skaar, E.P., Feldman, M.F., 2016. Medically Relevant *Acinetobacter* Species Require a Type II Secretion System and Specific Membrane-Associated Chaperones for the Export of Multiple Substrates and Full Virulence. PLoS Pathog 12, e1005391.
Harding, C.M., Tracy, E.N., Carruthers, M.D., Rather, P.N., Actis, L.A., Munson, R.S., Jr., 2013. *Acinetobacter baumannii* strain M2 produces type IV pili which play a role in natural transformation and twitching motility but not surface-associated motility. mBio 4.
Hart, E.M., Mitchell, A.M., Konovalova, A., Grabowicz, M., Sheng, J., Han, X., Rodriguez-Rivera, F.P., Schwaid, A.G., Malinverni, J.C., Balibar, C.J., Bodea, S., Si, Q., Wang, H., Homsher, M.F., Painter, R.E., Ogawa, A.K., Sutterlin, H., Roemer, T., Black, T.A., Rothman, D.M., Walker, S.S., Silhavy, T.J., 2019. A small-molecule inhibitor of BamA impervious to efflux and the outer membrane permeability barrier. Proc Natl Acad Sci U S A 116, 21748-21757.
Henderson, I.R., Owen, P., Nataro, J.P., 1999. Molecular switches--the ON and OFF of bacterial phase variation. Mol Microbiol 33, 919-932.
Henrichsen, J., 1983. Twitching motility. Annu Rev Microbiol 37, 81-93.
Henrichsen, J., Blom, J., 1975. Correlation between twitching motility and possession of polar fimbriae in *Acinetobacter calcoaceticus*. Acta Pathol Microbiol Scand B 83, 103-115.
Herzberg, C., Friedrich, A., Averhoff, B., 2000. comB, a novel competence gene required for natural transformation of *Acinetobacter* sp. BD413: identification, characterization, and analysis of growth-phase-dependent regulation. Arch Microbiol 173, 220-228.

Higgins, P.G., Dammhayn, C., Hackel, M., Seifert, H., 2010a. Global spread of carbapenem-resistant *Acinetobacter baumannii*. J Antimicrob Chemother 65, 233-238.
Higgins, P.G., Lehmann, M., Wisplinghoff, H., Seifert, H., 2010b. gyrB multiplex PCR to differentiate between *Acinetobacter calcoaceticus* and *Acinetobacter* genomic species 3. J Clin Microbiol 48, 4592-4594.
Higgins, P.G., Wisplinghoff, H., Krut, O., Seifert, H., 2007. A PCR-based method to differentiate between *Acinetobacter baumannii* and *Acinetobacter* genomic species 13TU. Clin Microbiol Infect 13, 1199-1201.
Hong, H., Patel, D.R., Tamm, L.K., van den Berg, B., 2006. The outer membrane protein OmpW forms an eight-stranded beta-barrel with a hydrophobic channel. J Biol Chem 281, 7568-7577.
Hood, M.I., Mortensen, B.L., Moore, J.L., Zhang, Y., Kehl-Fie, T.E., Sugitani, N., Chazin, W.J., Caprioli, R.M., Skaar, E.P., 2012. Identification of an *Acinetobacter baumannii* zinc acquisition system that facilitates resistance to calprotectin-mediated zinc sequestration. PLoS Pathog 8, e1003068.
Hou, P.F., Chen, X.Y., Yan, G.F., Wang, Y.P., Ying, C.M., 2012. Study of the correlation of imipenem resistance with efflux pumps AdeABC, AdeIJK, AdeDE and AbeM in clinical isolates of *Acinetobacter baumannii*. Chemotherapy 58, 152-158.
Huang, W., Wang, S., Yao, Y., Xia, Y., Yang, X., Li, K., Sun, P., Liu, C., Sun, W., Bai, H., Chu, X., Li, Y., Ma, Y., 2016. Employing *Escherichia coli*-derived outer membrane vesicles as an antigen delivery platform elicits protective immunity against *Acinetobacter baumannii* infection. Sci Rep 6, 37242.
Huang, W., Yao, Y., Long, Q., Yang, X., Sun, W., Liu, C., Jin, X., Li, Y., Chu, X., Chen, B., Ma, Y., 2014. Immunization against multidrug-resistant *Acinetobacter baumannii* effectively protects mice in both pneumonia and sepsis models. PLoS One 9, e100727.
Huber, W., von Heydebreck, A., Sultmann, H., Poustka, A., Vingron, M., 2002. Variance stabilization applied to microarray data calibration and to the quantification of differential expression. Bioinformatics 18 Suppl 1, S96-104.
Hughes, R.B.a.A.C.S., 2019. Capsule Stain Protocols Laboratory Protocols, in: American Society for Microbiology, W., DC (Ed.), Laboratory Protocols, 2016 ed. American Society for Microbiology, Washington, DC, http://www.asmscience.org/content/education/protocol/protocol.3041.
Hunstad, D.A., Justice, S.S., Hung, C.S., Lauer, S.R., Hultgren, S.J., 2005. Suppression of bladder epithelial cytokine responses by uropathogenic *Escherichia coli*. Infect Immun 73, 3999-4006.
Imai, Y., Meyer, K.J., Iinishi, A., Favre-Godal, Q., Green, R., Manuse, S., Caboni, M., Mori, M., Niles, S., Ghiglieri, M., Honrao, C., Ma, X., Guo, J.J., Makriyannis, A., Linares-Otoya, L., Bohringer, N., Wuisan, Z.G., Kaur, H., Wu, R., Mateus, A., Typas, A., Savitski, M.M., Espinoza, J.L., O'Rourke, A., Nelson, K.E., Hiller, S., Noinaj, N., Schaberle, T.F., D'Onofrio, A., Lewis, K., 2019. A new antibiotic selectively kills Gram-negative pathogens. Nature 576, 459-464.
Infectious Diseases Society of, A., 2012. White paper: recommendations on the conduct of superiority and organism-specific clinical trials of antibacterial agents for the treatment of infections caused by drug-resistant bacterial pathogens. Clin Infect Dis 55, 1031-1046.
Jacobs, A.C., Thompson, M.G., Black, C.C., Kessler, J.L., Clark, L.P., McQueary, C.N., Gancz, H.Y., Corey, B.W., Moon, J.K., Si, Y., Owen, M.T., Hallock, J.D., Kwak, Y.I., Summers, A., Li, C.Z., Rasko, D.A., Penwell, W.F., Honnold, C.L., Wise, M.C., Waterman, P.E., Lesho, E.P., Stewart, R.L., Actis, L.A., Palys, T.J., Craft, D.W., Zurawski, D.V., 2014. AB5075, a Highly Virulent Isolate of *Acinetobacter baumannii*, as a Model Strain for the Evaluation of Pathogenesis and Antimicrobial Treatments. mBio 5, e01076-01014.
Jarchow, S., Luck, C., Gorg, A., Skerra, A., 2008. Identification of potential substrate proteins for the periplasmic *Escherichia coli* chaperone Skp. Proteomics 8, 4987-4994.
Jawad, A., Seifert, H., Snelling, A.M., Heritage, J., Hawkey, P.M., 1998. Survival of *Acinetobacter baumannii* on dry surfaces: comparison of outbreak and sporadic isolates. J Clin Microbiol 36, 1938-1941.

Jeon, J.H., Lee, J.H., Lee, J.J., Park, K.S., Karim, A.M., Lee, C.R., Jeong, B.C., Lee, S.H., 2015. Structural basis for carbapenem-hydrolyzing mechanisms of carbapenemases conferring antibiotic resistance. Int J Mol Sci 16, 9654-9692.
Jia, M., Wu, B., Yang, Z., Chen, C., Zhao, M., Hou, X., Niu, X., Jin, C., Hu, Y., 2020. Conformational Dynamics of the Periplasmic Chaperone SurA. Biochemistry 59, 3235-3246.
Jiang, J., Zhang, X., Chen, Y., Wu, Y., Zhou, Z.H., Chang, Z., Sui, S.F., 2008. Activation of DegP chaperone-protease via formation of large cage-like oligomers upon binding to substrate proteins. Proc Natl Acad Sci U S A 105, 11939-11944.
Jin, F., Chang, Z., 2017. Revealing a shortened version of SecA ($SecA^N$) that conceivably functions as a protein-conducting channel in the bacterial cytoplasmic membrane. bioRxiv, 121335.
Jin, J., Hsieh, Y.H., Chaudhary, A.S., Cui, J., Houghton, J.E., Sui, S.F., Wang, B., Tai, P.C., 2018. SecA inhibitors as potential antimicrobial agents: differential actions on SecA-only and SecA-SecYEG protein-conducting channels. FEMS Microbiol Lett 365.
Jin, J.S., Kwon, S.O., Moon, D.C., Gurung, M., Lee, J.H., Kim, S.I., Lee, J.C., 2011. *Acinetobacter baumannii* secretes cytotoxic outer membrane protein A via outer membrane vesicles. PLoS One 6, e17027.
Johnson, T.L., Waack, U., Smith, S., Mobley, H., Sandkvist, M., 2015. *Acinetobacter baumannii* Is Dependent on the Type II Secretion System and Its Substrate LipA for Lipid Utilization and In Vivo Fitness. J Bacteriol 198, 711-719.
Joly-Guillou, M.L., 2005. Clinical impact and pathogenicity of *Acinetobacter*. Clin Microbiol Infect 11, 868-873.
Jomaa, A., Damjanovic, D., Leong, V., Ghirlando, R., Iwanczyk, J., Ortega, J., 2007. The inner cavity of *Escherichia coli* DegP protein is not essential for molecular chaperone and proteolytic activity. J Bacteriol 189, 706-716.
Justice, S.S., Lauer, S.R., Hultgren, S.J., Hunstad, D.A., 2006. Maturation of intracellular *Escherichia coli* communities requires SurA. Infect Immun 74, 4793-4800.
Juttukonda, L.J., Chazin, W.J., Skaar, E.P., 2016. *Acinetobacter baumannii* Coordinates Urea Metabolism with Metal Import To Resist Host-Mediated Metal Limitation. mBio 7.
Jyothisri, K., Deepak, V., Rajeswari, M.R., 1999. Purification and characterization of a major 40 kDa outer membrane protein of *Acinetobacter baumannii*. FEBS Lett 443, 57-60.
Kamio, Y., Nikaido, H., 1976. Outer membrane of *Salmonella typhimurium*: accessibility of phospholipid head groups to phospholipase c and cyanogen bromide activated dextran in the external medium. Biochemistry 15, 2561-2570.
Kamischke, C., Fan, J., Bergeron, J., Kulasekara, H.D., Dalebroux, Z.D., Burrell, A., Kollman, J.M., Miller, S.I., 2019. The *Acinetobacter baumannii* Mla system and glycerophospholipid transport to the outer membrane. Elife 8.
Kapach, G., Nuri, R., Schmidt, C., Danin, A., Ferrera, S., Savidor, A., Gerlach, R.G., Shai, Y., 2020. Loss of the Periplasmic Chaperone Skp and Mutations in the Efflux Pump AcrAB-TolC Play a Role in Acquired Resistance to Antimicrobial Peptides in *Salmonella typhimurium*. Front Microbiol 11, 189.
Kihara, A., Ito, K., 1998. Translocation, folding, and stability of the HflKC complex with signal anchor topogenic sequences. J Biol Chem 273, 29770-29775.
Klein, K., Sonnabend, M.S., Frank, L., Leibiger, K., Franz-Wachtel, M., Macek, B., Trunk, T., Leo, J.C., Autenrieth, I.B., Schütz, M., Bohn, E., 2019. Deprivation of the Periplasmic Chaperone SurA Reduces Virulence and Restores Antibiotic Susceptibility of Multidrug-Resistant *Pseudomonas aeruginosa*. Front Microbiol 10, 100.
Knowles, T.J., Scott-Tucker, A., Overduin, M., Henderson, I.R., 2009. Membrane protein architects: the role of the BAM complex in outer membrane protein assembly. Nat Rev Microbiol 7, 206-214.
Kochar, M., Crosatti, M., Harrison, E.M., Rieck, B., Chan, J., Constantinidou, C., Pallen, M., Ou, H.Y., Rajakumar, K., 2012. Deletion of TnAbaR23 results in both expected and unexpected antibiogram changes in a multidrug-resistant *Acinetobacter baumannii* strain. Antimicrob Agents Chemother 56, 1845-1853.

Koebnik, R., Locher, K.P., Van Gelder, P., 2000. Structure and function of bacterial outer membrane proteins: barrels in a nutshell. Mol Microbiol 37, 239-253.
Konovalova, A., Mitchell, A.M., Silhavy, T.J., 2016. A lipoprotein/beta-barrel complex monitors lipopolysaccharide integrity transducing information across the outer membrane. Elife 5.
Korndorfer, I.P., Dommel, M.K., Skerra, A., 2004. Structure of the periplasmic chaperone Skp suggests functional similarity with cytosolic chaperones despite differing architecture. Nat Struct Mol Biol 11, 1015-1020.
Korotkov, K.V., Sandkvist, M., Hol, W.G., 2012. The type II secretion system: biogenesis, molecular architecture and mechanism. Nat Rev Microbiol 10, 336-351.
Krojer, T., Garrido-Franco, M., Huber, R., Ehrmann, M., Clausen, T., 2002. Crystal structure of DegP (HtrA) reveals a new protease-chaperone machine. Nature 416, 455-459.
Krojer, T., Sawa, J., Schafer, E., Saibil, H.R., Ehrmann, M., Clausen, T., 2008. Structural basis for the regulated protease and chaperone function of DegP. Nature 453, 885-890.
Kulp, A., Kuehn, M.J., 2010. Biological functions and biogenesis of secreted bacterial outer membrane vesicles. Annu Rev Microbiol 64, 163-184.
Kunin, C.M., 1983. Antibiotic resistance--a world health problem we cannot ignore. Annals of internal medicine 99, 859-860.
Kwon, H.I., Kim, S., Oh, M.H., Na, S.H., Kim, Y.J., Jeon, Y.H., Lee, J.C., 2017. Outer membrane protein A contributes to antimicrobial resistance of *Acinetobacter baumannii* through the OmpA-like domain. J Antimicrob Chemother 72, 3012-3015.
Kwon, H.I., Kim, S., Oh, M.H., Shin, M., Lee, J.C., 2019. Distinct role of outer membrane protein A in the intrinsic resistance of *Acinetobacter baumannii* and *Acinetobacter nosocomialis*. Infect Genet Evol 67, 33-37.
Kwon, S.O., Gho, Y.S., Lee, J.C., Kim, S.I., 2009. Proteome analysis of outer membrane vesicles from a clinical *Acinetobacter baumannii* isolate. FEMS Microbiol Lett 297, 150-156.
Lazar, C., 2015. imputeLCMD: a collection of methods for left-censored missing data imputation. R package, version 2.
Lazar, S.W., Kolter, R., 1996. SurA assists the folding of *Escherichia coli* outer membrane proteins. J Bacteriol 178, 1770-1773.
Lee, C.R., Lee, J.H., Park, M., Park, K.S., Bae, I.K., Kim, Y.B., Cha, C.J., Jeong, B.C., Lee, S.H., 2017. Biology of *Acinetobacter baumannii*: Pathogenesis, Antibiotic Resistance Mechanisms, and Prospective Treatment Options. Front Cell Infect Microbiol 7, 55.
Lee, J.S., Choi, C.H., Kim, J.W., Lee, J.C., 2010. *Acinetobacter baumannii* outer membrane protein A induces dendritic cell death through mitochondrial targeting. J Microbiol 48, 387-392.
Lee, Y.C., Huang, Y.T., Tan, C.K., Kuo, Y.W., Liao, C.H., Lee, P.I., Hsueh, P.R., 2011. *Acinetobacter baumannii* and *Acinetobacter* genospecies 13TU and 3 bacteraemia: comparison of clinical features, prognostic factors and outcomes. J Antimicrob Chemother 66, 1839-1846.
Lewis, J.M., Deveson Lucas, D., Harper, M., Boyce, J.D., 2019. Systematic Identification and Analysis of *Acinetobacter baumannii* Type VI Secretion System Effector and Immunity Components. Front Microbiol 10, 2440.
Li, Z.T., Zhang, R.L., Bi, X.G., Xu, L., Fan, M., Xie, D., Xian, Y., Wang, Y., Li, X.J., Wu, Z.D., Zhang, K.X., 2015. Outer membrane vesicles isolated from two clinical *Acinetobacter baumannii* strains exhibit different toxicity and proteome characteristics. Microb Pathog 81, 46-52.
Liao, Y.T., Kuo, S.C., Chiang, M.H., Lee, Y.T., Sung, W.C., Chen, Y.H., Chen, T.L., Fung, C.P., 2015. *Acinetobacter baumannii* Extracellular OXA-58 Is Primarily and Selectively Released via Outer Membrane Vesicles after Sec-Dependent Periplasmic Translocation. Antimicrob Agents Chemother 59, 7346-7354.
Limansky, A.S., Mussi, M.A., Viale, A.M., 2002. Loss of a 29-kilodalton outer membrane protein in *Acinetobacter baumannii* is associated with imipenem resistance. J Clin Microbiol 40, 4776-4778.

Lin, X.M., Wu, L.N., Li, H., Wang, S.Y., Peng, X.X., 2008. Downregulation of Tsx and OmpW and upregulation of OmpX are required for iron homeostasis in *Escherichia coli*. J Proteome Res 7, 1235-1243.
Lipinska, B., Fayet, O., Baird, L., Georgopoulos, C., 1989. Identification, characterization, and mapping of the *Escherichia coli* htrA gene, whose product is essential for bacterial growth only at elevated temperatures. J Bacteriol 171, 1574-1584.
Lipinska, B., Zylicz, M., Georgopoulos, C., 1990. The HtrA (DegP) protein, essential for *Escherichia coli* survival at high temperatures, is an endopeptidase. J Bacteriol 172, 1791-1797.
Lonergan, Z.R., Nairn, B.L., Wang, J., Hsu, Y.P., Hesse, L.E., Beavers, W.N., Chazin, W.J., Trinidad, J.C., VanNieuwenhze, M.S., Giedroc, D.P., Skaar, E.P., 2019. An *Acinetobacter baumannii*, Zinc-Regulated Peptidase Maintains Cell Wall Integrity during Immune-Mediated Nutrient Sequestration. Cell Rep 26, 2009-2018 e2006.
Luber, C.A., Cox, J., Lauterbach, H., Fancke, B., Selbach, M., Tschopp, J., Akira, S., Wiegand, M., Hochrein, H., O'Keeffe, M., Mann, M., 2010. Quantitative proteomics reveals subset-specific viral recognition in dendritic cells. Immunity 32, 279-289.
Magnet, S., Courvalin, P., Lambert, T., 2001. Resistance-nodulation-cell division-type efflux pump involved in aminoglycoside resistance in *Acinetobacter baumannii* strain BM4454. Antimicrob Agents Chemother 45, 3375-3380.
Malinverni, J.C., Werner, J., Kim, S., Sklar, J.G., Kahne, D., Misra, R., Silhavy, T.J., 2006. YfiO stabilizes the YaeT complex and is essential for outer membrane protein assembly in *Escherichia coli*. Mol Microbiol 61, 151-164.
Maneval, W.E., 1941. Staining bacteria and yeast with acid dyes. Stain Technol 16, 13–19.
Martro, E., Hernandez, A., Ariza, J., Dominguez, M.A., Matas, L., Argerich, M.J., Martin, R., Ausina, V., 2003. Assessment of *Acinetobacter baumannii* susceptibility to antiseptics and disinfectants. J Hosp Infect 55, 39-46.
Matern, Y., Barion, B., Behrens-Kneip, S., 2010. PpiD is a player in the network of periplasmic chaperones in *Escherichia coli*. BMC Microbiol 10, 251.
McConnell, M.J., Rumbo, C., Bou, G., Pachon, J., 2011. Outer membrane vesicles as an acellular vaccine against *Acinetobacter baumannii*. Vaccine 29, 5705-5710.
McQueary, C.N., Actis, L.A., 2011. *Acinetobacter baumannii* biofilms: variations among strains and correlations with other cell properties. J Microbiol 49, 243-250.
Mendez, J.A., Soares, N.C., Mateos, J., Gayoso, C., Rumbo, C., Aranda, J., Tomas, M., Bou, G., 2012. Extracellular proteome of a highly invasive multidrug-resistant clinical strain of *Acinetobacter baumannii*. J Proteome Res 11, 5678-5694.
Merritt, M.E., Donaldson, J.R., 2009. Effect of bile salts on the DNA and membrane integrity of enteric bacteria. J Med Microbiol 58, 1533-1541.
Mihara, K., Tanabe, T., Yamakawa, Y., Funahashi, T., Nakao, H., Narimatsu, S., Yamamoto, S., 2004. Identification and transcriptional organization of a gene cluster involved in biosynthesis and transport of acinetobactin, a siderophore produced by *Acinetobacter baumannii* ATCC 19606T. Microbiology (Reading) 150, 2587-2597.
Mitchell, A.L., Attwood, T.K., Babbitt, P.C., Blum, M., Bork, P., Bridge, A., Brown, S.D., Chang, H.Y., El-Gebali, S., Fraser, M.I., Gough, J., Haft, D.R., Huang, H., Letunic, I., Lopez, R., Luciani, A., Madeira, F., Marchler-Bauer, A., Mi, H., Natale, D.A., Necci, M., Nuka, G., Orengo, C., Pandurangan, A.P., Paysan-Lafosse, T., Pesseat, S., Potter, S.C., Qureshi, M.A., Rawlings, N.D., Redaschi, N., Richardson, L.J., Rivoire, C., Salazar, G.A., Sangrador-Vegas, A., Sigrist, C.J.A., Sillitoe, I., Sutton, G.G., Thanki, N., Thomas, P.D., Tosatto, S.C.E., Yong, S.Y., Finn, R.D., 2019. InterPro in 2019: improving coverage, classification and access to protein sequence annotations. Nucleic Acids Res 47, D351-D360.
Mo, E., Peters, S.E., Willers, C., Maskell, D.J., Charles, I.G., 2006. Single, double and triple mutants of *Salmonella enterica serovar Typhimurium* degP (htrA), degQ (hhoA) and degS (hhoB) have diverse phenotypes on exposure to elevated temperature and their growth in vivo is attenuated to different extents. Microb Pathog 41, 174-182.

Moffatt, J.H., Harper, M., Harrison, P., Hale, J.D., Vinogradov, E., Seemann, T., Henry, R., Crane, B., St Michael, F., Cox, A.D., Adler, B., Nation, R.L., Li, J., Boyce, J.D., 2010. Colistin resistance in *Acinetobacter baumannii* is mediated by complete loss of lipopolysaccharide production. Antimicrob Agents Chemother 54, 4971-4977.
Moon, D.C., Choi, C.H., Lee, J.H., Choi, C.W., Kim, H.Y., Park, J.S., Kim, S.I., Lee, J.C., 2012. *Acinetobacter baumannii* outer membrane protein A modulates the biogenesis of outer membrane vesicles. J Microbiol 50, 155-160.
Mori, H., Ito, K., 2001. The Sec protein-translocation pathway. Trends Microbiol 9, 494-500.
Mortensen, B.L., Rathi, S., Chazin, W.J., Skaar, E.P., 2014. *Acinetobacter baumannii* response to host-mediated zinc limitation requires the transcriptional regulator Zur. J Bacteriol 196, 2616-2626.
Mühlradt, P.F., Golecki, J.R., 1975. Asymmetrical distribution and artifactual reorientation of lipopolysaccharide in the outer membrane bilayer of *Salmonella typhimurium*. Eur J Biochem 51, 343-352.
Mulin, B., Talon, D., Viel, J.F., Vincent, C., Leprat, R., Thouverez, M., Michel-Briand, Y., 1995. Risk factors for nosocomial colonization with multiresistant *Acinetobacter baumannii*. Eur J Clin Microbiol Infect Dis 14, 569-576.
Mussi, M.A., Limansky, A.S., Viale, A.M., 2005. Acquisition of resistance to carbapenems in multidrug-resistant clinical strains of *Acinetobacter baumannii*: natural insertional inactivation of a gene encoding a member of a novel family of beta-barrel outer membrane proteins. Antimicrob Agents Chemother 49, 1432-1440.
Nairn, B.L., Lonergan, Z.R., Wang, J., Braymer, J.J., Zhang, Y., Calcutt, M.W., Lisher, J.P., Gilston, B.A., Chazin, W.J., de Crecy-Lagard, V., Giedroc, D.P., Skaar, E.P., 2016. The Response of *Acinetobacter baumannii* to Zinc Starvation. Cell Host Microbe 19, 826-836.
Nemec, A., Dolzani, L., Brisse, S., van den Broek, P., Dijkshoorn, L., 2004. Diversity of aminoglycoside-resistance genes and their association with class 1 integrons among strains of pan-European *Acinetobacter baumannii* clones. J Med Microbiol 53, 1233-1240.
Nemec, A., Krizova, L., Maixnerova, M., Sedo, O., Brisse, S., Higgins, P.G., 2015. *Acinetobacter seifertii* sp. nov., a member of the *Acinetobacter calcoaceticus-Acinetobacter baumannii* complex isolated from human clinical specimens. Int J Syst Evol Microbiol 65, 934-942.
Nemec, A., Krizova, L., Maixnerova, M., van der Reijden, T.J., Deschaght, P., Passet, V., Vaneechoutte, M., Brisse, S., Dijkshoorn, L., 2011. Genotypic and phenotypic characterization of the *Acinetobacter calcoaceticus-Acinetobacter baumannii* complex with the proposal of *Acinetobacter pittii* sp. nov. (formerly *Acinetobacter* genomic species 3) and *Acinetobacter nosocomialis* sp. nov. (formerly *Acinetobacter* genomic species 13TU). Res Microbiol 162, 393-404.
Nestorovich, E.M., Sugawara, E., Nikaido, H., Bezrukov, S.M., 2006. *Pseudomonas aeruginosa porin OprF*: properties of the channel. J Biol Chem 281, 16230-16237.
Neu, H.C., 1992. The crisis in antibiotic resistance. Science 257, 1064-1073.
Nikaido, H., 2003. Molecular basis of bacterial outer membrane permeability revisited. Microbiol Mol Biol Rev 67, 593-656.
Noinaj, N., Gumbart, J.C., Buchanan, S.K., 2017. The beta-barrel assembly machinery in motion. Nat Rev Microbiol 15, 197-204.
Nwugo, C.C., Gaddy, J.A., Zimbler, D.L., Actis, L.A., 2011. Deciphering the iron response in *Acinetobacter baumannii*: A proteomics approach. J Proteomics 74, 44-58.
Oberhettinger, P., Leo, J.C., Linke, D., Autenrieth, I.B., Schütz, M.S., 2015. The inverse autotransporter intimin exports its passenger domain via a hairpin intermediate. J Biol Chem 290, 1837-1849.
Obi, I.R., Nordfelth, R., Francis, M.S., 2011. Varying dependency of periplasmic peptidylprolyl cis-trans isomerases in promoting *Yersinia pseudotuberculosis* stress tolerance and pathogenicity. The Biochemical journal 439, 321-332.
Onufryk, C., Crouch, M.L., Fang, F.C., Gross, C.A., 2005. Characterization of six lipoproteins in the sigmaE regulon. J Bacteriol 187, 4552-4561.

Pagano, M., Martins, A.F., Barth, A.L., 2016. Mobile genetic elements related to carbapenem resistance in *Acinetobacter baumannii*. Braz J Microbiol 47, 785-792.
Parke, D., Garcia, M.A., Ornston, L.N., 2001. Cloning and genetic characterization of dca genes required for beta-oxidation of straight-chain dicarboxylic acids in *Acinetobacter sp.* strain ADP1. Appl Environ Microbiol 67, 4817-4827.
Peleg, A.Y., Seifert, H., Paterson, D.L., 2008. *Acinetobacter baumannii*: emergence of a successful pathogen. Clin Microbiol Rev 21, 538-582.
Peng, D., Hong, W., Choudhury, B.P., Carlson, R.W., Gu, X.X., 2005. *Moraxella catarrhalis* bacterium without endotoxin, a potential vaccine candidate. Infect Immun 73, 7569-7577.
Penwell, W.F., DeGrace, N., Tentarelli, S., Gauthier, L., Gilbert, C.M., Arivett, B.A., Miller, A.A., Durand-Reville, T.F., Joubran, C., Actis, L.A., 2015. Discovery and Characterization of New Hydroxamate Siderophores, Baumannoferrin A and B, produced by *Acinetobacter baumannii*. Chembiochem 16, 1896-1904.
Perez, F., Hujer, A.M., Hujer, K.M., Decker, B.K., Rather, P.N., Bonomo, R.A., 2007. Global challenge of multidrug-resistant *Acinetobacter baumannii*. Antimicrob Agents Chemother 51, 3471-3484.
Poole, K., 2001. Multidrug efflux pumps and antimicrobial resistance in *Pseudomonas aeruginosa* and related organisms. J Mol Microbiol Biotechnol 3, 255-264.
Porstendorfer, D., Drotschmann, U., Averhoff, B., 1997. A novel competence gene, comP, is essential for natural transformation of *Acinetobacter* sp. strain BD413. Appl Environ Microbiol 63, 4150-4157.
Porstendorfer, D., Gohl, O., Mayer, F., Averhoff, B., 2000. ComP, a pilin-like protein essential for natural competence in *Acinetobacter* sp. Strain BD413: regulation, modification, and cellular localization. J Bacteriol 182, 3673-3680.
Powers, M.J., Trent, M.S., 2018. Expanding the paradigm for the outer membrane: *Acinetobacter baumannii* in the absence of endotoxin. Mol Microbiol 107, 47-56.
Preston, A., Mandrell, R.E., Gibson, B.W., Apicella, M.A., 1996. The lipooligosaccharides of pathogenic gram-negative bacteria. Crit Rev Microbiol 22, 139-180.
Proschak, A., Lubuta, P., Grun, P., Lohr, F., Wilharm, G., De Berardinis, V., Bode, H.B., 2013. Structure and biosynthesis of fimsbactins A-F, siderophores from *Acinetobacter baumannii* and *Acinetobacter baylyi*. Chembiochem 14, 633-638.
Purdy, G.E., Fisher, C.R., Payne, S.M., 2007. IcsA surface presentation in *Shigella flexneri* requires the periplasmic chaperones DegP, Skp, and SurA. J Bacteriol 189, 5566-5573.
Purdy, G.E., Hong, M., Payne, S.M., 2002. *Shigella flexneri* DegP facilitates IcsA surface expression and is required for efficient intercellular spread. Infect Immun 70, 6355-6364.
Raetz, C.R., Whitfield, C., 2002. Lipopolysaccharide endotoxins. Annu Rev Biochem 71, 635-700.
Rahfeld, J.-U., Schierhorn, A., Mann, K., Fischer, G., 1994. A novel peptidyl-prolyl cisltrans isomerase from *Escherichia coli*. FEBS letters 343, 65-69 %@ 0014-5793.
Ramirez, M.S., Don, M., Merkier, A.K., Bistue, A.J., Zorreguieta, A., Centron, D., Tolmasky, M.E., 2010. Naturally competent *Acinetobacter baumannii* clinical isolate as a convenient model for genetic studies. J Clin Microbiol 48, 1488-1490.
Ramirez, M.S., Tolmasky, M.E., 2010. Aminoglycoside modifying enzymes. Drug Resist Updat 13, 151-171.
Redford, P., Welch, R.A., 2006. Role of sigma E-regulated genes in *Escherichia coli* uropathogenesis. Infect Immun 74, 4030-4038.
Repizo, G.D., Gagne, S., Foucault-Grunenwald, M.L., Borges, V., Charpentier, X., Limansky, A.S., Gomes, J.P., Viale, A.M., Salcedo, S.P., 2015. Differential Role of the T6SS in *Acinetobacter baumannii* Virulence. PLoS One 10, e0138265.
Rice, L.B., 2008. Federal funding for the study of antimicrobial resistance in nosocomial pathogens: no ESKAPE. J Infect Dis 197, 1079-1081.
Richie, D.L., Takeoka, K.T., Bojkovic, J., Metzger, L.E.t., Rath, C.M., Sawyer, W.S., Wei, J.R., Dean, C.R., 2016. Toxic Accumulation of LPS Pathway Intermediates Underlies the Requirement of LpxH for Growth of *Acinetobacter baumannii* ATCC 19606. PLoS One 11, e0160918.

Ritchie, M.E., Phipson, B., Wu, D., Hu, Y., Law, C.W., Shi, W., Smyth, G.K., 2015. limma powers differential expression analyses for RNA-sequencing and microarray studies. Nucleic Acids Res 43, e47.
Rizzitello, A.E., Harper, J.R., Silhavy, T.J., 2001. Genetic evidence for parallel pathways of chaperone activity in the periplasm of *Escherichia coli*. J Bacteriol 183, 6794-6800.
Rollauer, S.E., Sooreshjani, M.A., Noinaj, N., Buchanan, S.K., 2015. Outer membrane protein biogenesis in Gram-negative bacteria. Philos Trans R Soc Lond B Biol Sci 370.
Ronish, L.A., Lillehoj, E., Fields, J.K., Sundberg, E.J., Piepenbrink, K.H., 2019. The structure of PilA from *Acinetobacter baumannii* AB5075 suggests a mechanism for functional specialization in *Acinetobacter* type IV pili. J Biol Chem 294, 218-230.
Rose, A., 2010. Tn AbaR1: a novel Tn 7-related transposon in *Acinetobacter baumannii* that contributes to the accumulation and dissemination of large repertoires of resistance genes. Bioscience Horizons 3, 40-48 %@ 1754-7431.
Rosenfeld, N., Bouchier, C., Courvalin, P., Perichon, B., 2012. Expression of the resistance-nodulation-cell division pump AdeIJK in *Acinetobacter baumannii* is regulated by AdeN, a TetR-type regulator. Antimicrob Agents Chemother 56, 2504-2510.
Rossau, R., Van Landschoot, A., Gillis, M., De Ley, J., 1991. Taxonomy of *Moraxellaceae* fam. nov., a New Bacterial Family To Accommodate the Genera *Moraxella*, *Acinetobacter*, and *Psychrobacter* and Related Organisms. International Journal of Systematic and Evolutionary Microbiology 41, 310-319 %@ 1466-5026.
Rouviere, P.E., Gross, C.A., 1996. SurA, a periplasmic protein with peptidyl-prolyl isomerase activity, participates in the assembly of outer membrane porins. Genes Dev 10, 3170-3182.
Rowley, G., Skovierova, H., Stevenson, A., Rezuchova, B., Homerova, D., Lewis, C., Sherry, A., Kormanec, J., Roberts, M., 2011. The periplasmic chaperone Skp is required for successful *Salmonella Typhimurium* infection in a murine typhoid model. Microbiology (Reading) 157, 848-858.
Ruiz, N., Kahne, D., Silhavy, T.J., 2006. Advances in understanding bacterial outer-membrane biogenesis. Nat Rev Microbiol 4, 57-66.
Rumbo, C., Tomas, M., Fernandez Moreira, E., Soares, N.C., Carvajal, M., Santillana, E., Beceiro, A., Romero, A., Bou, G., 2014. The *Acinetobacter baumannii* Omp33-36 porin is a virulence factor that induces apoptosis and modulates autophagy in human cells. Infect Immun 82, 4666-4680.
Runci, F., Gentile, V., Frangipani, E., Rampioni, G., Leoni, L., Lucidi, M., Visaggio, D., Harris, G., Chen, W., Stahl, J., Averhoff, B., Visca, P., 2019. Contribution of Active Iron Uptake to *Acinetobacter baumannii* Pathogenicity. Infect Immun 87.
Saha, R., Saha, N., Donofrio, R.S., Bestervelt, L.L., 2013. Microbial siderophores: a mini review. J Basic Microbiol 53, 303-317.
Sandkvist, M., 2001. Type II secretion and pathogenesis. Infect Immun 69, 3523-3535.
Schulz, G.E., 2002. The structure of bacterial outer membrane proteins. Biochim Biophys Acta 1565, 308-317.
Schwanhäusser, B., Busse, D., Li, N., Dittmar, G., Schuchhardt, J., Wolf, J., Chen, W., Selbach, M., 2011. Global quantification of mammalian gene expression control. Nature 473, 337-342.
Scott, P., Deye, G., Srinivasan, A., Murray, C., Moran, K., Hulten, E., Fishbain, J., Craft, D., Riddell, S., Lindler, L., Mancuso, J., Milstrey, E., Bautista, C.T., Patel, J., Ewell, A., Hamilton, T., Gaddy, C., Tenney, M., Christopher, G., Petersen, K., Endy, T., Petruccelli, B., 2007. An outbreak of multidrug-resistant *Acinetobacter baumannii-calcoaceticus* complex infection in the US military health care system associated with military operations in Iraq. Clin Infect Dis 44, 1577-1584.
Scribano, D., Marzano, V., Levi Mortera, S., Sarshar, M., Vernocchi, P., Zagaglia, C., Putignani, L., Palamara, A.T., Ambrosi, C., 2019. Insights into the Periplasmic Proteins of *Acinetobacter baumannii* AB5075 and the Impact of Imipenem Exposure: A Proteomic Approach. Int J Mol Sci 20.
Shaw, K.J., Rather, P.N., Hare, R.S., Miller, G.H., 1993. Molecular genetics of aminoglycoside resistance genes and familial relationships of the aminoglycoside-modifying enzymes. Microbiol Rev 57, 138-163.

Sheldon, J.R., Skaar, E.P., 2020. *Acinetobacter baumannii* can use multiple siderophores for iron acquisition, but only acinetobactin is required for virulence. PLoS Pathog 16, e1008995.
Sievers, F., Wilm, A., Dineen, D., Gibson, T.J., Karplus, K., Li, W., Lopez, R., McWilliam, H., Remmert, M., Soding, J., Thompson, J.D., Higgins, D.G., 2011. Fast, scalable generation of high-quality protein multiple sequence alignments using Clustal Omega. Mol Syst Biol 7, 539.
Sievert, D.M., Ricks, P., Edwards, J.R., Schneider, A., Patel, J., Srinivasan, A., Kallen, A., Limbago, B., Fridkin, S., National Healthcare Safety Network, T., Participating, N.F., 2013. Antimicrobial-resistant pathogens associated with healthcare-associated infections: summary of data reported to the National Healthcare Safety Network at the Centers for Disease Control and Prevention, 2009-2010. Infect Control Hosp Epidemiol 34, 1-14.
Silhavy, T.J., Kahne, D., Walker, S., 2010. The bacterial cell envelope. Cold Spring Harb Perspect Biol 2, a000414.
Sipahi, O.R., 2008. Economics of antibiotic resistance. Expert Rev Anti Infect Ther 6, 523-539.
Siroy, A., Molle, V., Lemaitre-Guillier, C., Vallenet, D., Pestel-Caron, M., Cozzone, A.J., Jouenne, T., De, E., 2005. Channel formation by CarO, the carbapenem resistance-associated outer membrane protein of *Acinetobacter baumannii*. Antimicrob Agents Chemother 49, 4876-4883.
Skiebe, E., de Berardinis, V., Morczinek, P., Kerrinnes, T., Faber, F., Lepka, D., Hammer, B., Zimmermann, O., Ziesing, S., Wichelhaus, T.A., Hunfeld, K.P., Borgmann, S., Grobner, S., Higgins, P.G., Seifert, H., Busse, H.J., Witte, W., Pfeifer, Y., Wilharm, G., 2012. Surface-associated motility, a common trait of clinical isolates of *Acinetobacter baumannii*, depends on 1,3-diaminopropane. Int J Med Microbiol 302, 117-128.
Sklar, J.G., Wu, T., Gronenberg, L.S., Malinverni, J.C., Kahne, D., Silhavy, T.J., 2007a. Lipoprotein SmpA is a component of the YaeT complex that assembles outer membrane proteins in *Escherichia coli*. Proc Natl Acad Sci U S A 104, 6400-6405.
Sklar, J.G., Wu, T., Kahne, D., Silhavy, T.J., 2007b. Defining the roles of the periplasmic chaperones SurA, Skp, and DegP in *Escherichia coli*. Genes Dev 21, 2473-2484.
Skorko-Glonek, J., Wawrzynow, A., Krzewski, K., Kurpierz, K., Lipinska, B., 1995. Site-directed mutagenesis of the HtrA (DegP) serine protease, whose proteolytic activity is indispensable for *Escherichia coli* survival at elevated temperatures. Gene 163, 47-52.
Smani, Y., Dominguez-Herrera, J., Pachon, J., 2013. Association of the outer membrane protein Omp33 with fitness and virulence of *Acinetobacter baumannii*. J Infect Dis 208, 1561-1570.
Smani, Y., McConnell, M.J., Pachon, J., 2012. Role of fibronectin in the adhesion of *Acinetobacter baumannii* to host cells. PLoS One 7, e33073.
Smani, Y., Pachon, J., 2013. Loss of the OprD homologue protein in *Acinetobacter baumannii*: impact on carbapenem susceptibility. Antimicrob Agents Chemother 57, 677.
Smith, M.G., Gianoulis, T.A., Pukatzki, S., Mekalanos, J.J., Ornston, L.N., Gerstein, M., Snyder, M., 2007. New insights into *Acinetobacter baumannii* pathogenesis revealed by high-density pyrosequencing and transposon mutagenesis. Genes Dev 21, 601-614.
Southern, S.J., Scott, A.E., Jenner, D.C., Ireland, P.M., Norville, I.H., Sarkar-Tyson, M., 2016. Survival protein A is essential for virulence in *Yersinia pestis*. Microb Pathog 92, 50-53.
Spellberg, B., Rex, J.H., 2013. The value of single-pathogen antibacterial agents. Nat Rev Drug Discov 12, 963.
Spiess, C., Beil, A., Ehrmann, M., 1999. A temperature-dependent switch from chaperone to protease in a widely conserved heat shock protein. Cell 97, 339-347.
Srinivasan, V.B., Rajamohan, G., Pancholi, P., Marcon, M., Gebreyes, W.A., 2011. Molecular cloning and functional characterization of two novel membrane fusion proteins in conferring antimicrobial resistance in *Acinetobacter baumannii*. J Antimicrob Chemother 66, 499-504.
Steeghs, L., de Cock, H., Evers, E., Zomer, B., Tommassen, J., van der Ley, P., 2001. Outer membrane composition of a lipopolysaccharide-deficient *Neisseria meningitidis* mutant. EMBO J 20, 6937-6945.
Steeghs, L., den Hartog, R., den Boer, A., Zomer, B., Roholl, P., van der Ley, P., 1998. Meningitis bacterium is viable without endotoxin. Nature 392, 449-450.

Storek, K.M., Auerbach, M.R., Shi, H., Garcia, N.K., Sun, D., Nickerson, N.N., Vij, R., Lin, Z., Chiang, N., Schneider, K., Wecksler, A.T., Skippington, E., Nakamura, G., Seshasayee, D., Koerber, J.T., Payandeh, J., Smith, P.A., Rutherford, S.T., 2018. Monoclonal antibody targeting the beta-barrel assembly machine of *Escherichia coli* is bactericidal. Proc Natl Acad Sci U S A 115, 3692-3697.
Strauch, K.L., Johnson, K., Beckwith, J., 1989. Characterization of degP, a gene required for proteolysis in the cell envelope and essential for growth of *Escherichia coli* at high temperature. J Bacteriol 171, 2689-2696.
Stymest, K.H., Klappa, P., 2008. The periplasmic peptidyl prolyl cis-trans isomerases PpiD and SurA have partially overlapping substrate specificities. FEBS J 275, 3470-3479.
Su, S., Law, C.W., Ah-Cann, C., Asselin-Labat, M.L., Blewitt, M.E., Ritchie, M.E., 2017. Glimma: interactive graphics for gene expression analysis. Bioinformatics 33, 2050-2052.
Sugawara, E., Nestorovich, E.M., Bezrukov, S.M., Nikaido, H., 2006. *Pseudomonas aeruginosa* porin OprF exists in two different conformations. J Biol Chem 281, 16220-16229.
Sugawara, E., Nikaido, H., 2012. OmpA is the principal nonspecific slow porin of *Acinetobacter baumannii*. J Bacteriol 194, 4089-4096.
Sydenham, M., Douce, G., Bowe, F., Ahmed, S., Chatfield, S., Dougan, G., 2000. *Salmonella enterica* serovar typhimurium surA mutants are attenuated and effective live oral vaccines. Infect Immun 68, 1109-1115.
Tacconelli, E., Carrara, E., Savoldi, A., Harbarth, S., Mendelson, M., Monnet, D.L., Pulcini, C., Kahlmeter, G., Kluytmans, J., Carmeli, Y., Ouellette, M., Outterson, K., Patel, J., Cavaleri, M., Cox, E.M., Houchens, C.R., Grayson, M.L., Hansen, P., Singh, N., Theuretzbacher, U., Magrini, N., Group, W.H.O.P.P.L.W., 2018. Discovery, research, and development of new antibiotics: the WHO priority list of antibiotic-resistant bacteria and tuberculosis. Lancet Infect Dis 18, 318-327.
Tamayo, R., Ryan, S.S., McCoy, A.J., Gunn, J.S., 2002. Identification and genetic characterization of PmrA-regulated genes and genes involved in polymyxin B resistance in *Salmonella enterica* serovar typhimurium. Infect Immun 70, 6770-6778.
Tipton, K.A., Chin, C.Y., Farokhyfar, M., Weiss, D.S., Rather, P.N., 2018. Role of Capsule in Resistance to Disinfectants, Host Antimicrobials, and Desiccation in *Acinetobacter baumannii*. Antimicrob Agents Chemother 62.
Tipton, K.A., Dimitrova, D., Rather, P.N., 2015. Phase-Variable Control of Multiple Phenotypes in *Acinetobacter baumannii* Strain AB5075. J Bacteriol 197, 2593-2599.
Tipton, K.A., Rather, P.N., 2017. An ompR-envZ Two-Component System Ortholog Regulates Phase Variation, Osmotic Tolerance, Motility, and Virulence in *Acinetobacter baumannii* Strain AB5075. J Bacteriol 199.
Tiwari, V., Rajeswari, M.R., Tiwari, M., 2019. Proteomic analysis of iron-regulated membrane proteins identify FhuE receptor as a target to inhibit siderophore-mediated iron acquisition in *Acinetobacter baumannii*. Int J Biol Macromol 125, 1156-1167.
Tomaras, A.P., Dorsey, C.W., Edelmann, R.E., Actis, L.A., 2003. Attachment to and biofilm formation on abiotic surfaces by *Acinetobacter baumannii*: involvement of a novel chaperone-usher pili assembly system. Microbiology 149, 3473-3484.
Tormo, A., Almiron, M., Kolter, R., 1990. surA, an *Escherichia coli* gene essential for survival in stationary phase. J Bacteriol 172, 4339-4347.
Touw, D.S., Patel, D.R., van den Berg, B., 2010. The crystal structure of OprG from *Pseudomonas aeruginosa*, a potential channel for transport of hydrophobic molecules across the outer membrane. PLoS One 5, e15016.
Trebosc, V., Gartenmann, S., Royet, K., Manfredi, P., Totzl, M., Schellhorn, B., Pieren, M., Tigges, M., Lociuro, S., Sennhenn, P.C., Gitzinger, M., Bumann, D., Kemmer, C., 2016. A Novel Genome-Editing Platform for Drug-Resistant *Acinetobacter baumannii* Reveals an AdeR-Unrelated Tigecycline Resistance Mechanism. Antimicrob Agents Chemother 60, 7263-7271.

Tseng, T.T., Gratwick, K.S., Kollman, J., Park, D., Nies, D.H., Goffeau, A., Saier, M.H., Jr., 1999. The RND permease superfamily: an ancient, ubiquitous and diverse family that includes human disease and development proteins. J Mol Microbiol Biotechnol 1, 107-125.
Tsirigotaki, A., De Geyter, J., Sostaric, N., Economou, A., Karamanou, S., 2017. Protein export through the bacterial Sec pathway. Nat Rev Microbiol 15, 21-36.
Turton, J.F., Woodford, N., Glover, J., Yarde, S., Kaufmann, M.E., Pitt, T.L., 2006. Identification of *Acinetobacter baumannii* by detection of the blaOXA-51-like carbapenemase gene intrinsic to this species. J Clin Microbiol 44, 2974-2976.
Urdaneta, V., Casadesus, J., 2017. Interactions between Bacteria and Bile Salts in the Gastrointestinal and Hepatobiliary Tracts. Front Med (Lausanne) 4, 163.
Urfer, M., Bogdanovic, J., Lo Monte, F., Moehle, K., Zerbe, K., Omasits, U., Ahrens, C.H., Pessi, G., Eberl, L., Robinson, J.A., 2016. A Peptidomimetic Antibiotic Targets Outer Membrane Proteins and Disrupts Selectively the Outer Membrane in *Escherichia coli*. J Biol Chem 291, 1921-1932.
Valenzuela, J.K., Thomas, L., Partridge, S.R., van der Reijden, T., Dijkshoorn, L., Iredell, J., 2007. Horizontal gene transfer in a polyclonal outbreak of carbapenem-resistant *Acinetobacter baumannii*. J Clin Microbiol 45, 453-460.
Vashist, J., Tiwari, V., Kapil, A., Rajeswari, M.R., 2010. Quantitative profiling and identification of outer membrane proteins of beta-lactam resistant strain of *Acinetobacter baumannii*. J Proteome Res 9, 1121-1128.
Vertommen, D., Ruiz, N., Leverrier, P., Silhavy, T.J., Collet, J.F., 2009. Characterization of the role of the *Escherichia coli* periplasmic chaperone SurA using differential proteomics. Proteomics 9, 2432-2443.
Vila, J., Marti, S., Sanchez-Cespedes, J., 2007. Porins, efflux pumps and multidrug resistance in *Acinetobacter baumannii*. J Antimicrob Chemother 59, 1210-1215.
Vincent, J.L., Rello, J., Marshall, J., Silva, E., Anzueto, A., Martin, C.D., Moreno, R., Lipman, J., Gomersall, C., Sakr, Y., Reinhart, K., Investigators, E.I.G.o., 2009. International study of the prevalence and outcomes of infection in intensive care units. JAMA 302, 2323-2329.
Vollmer, W., Holtje, J.V., 2004. The architecture of the murein (peptidoglycan) in gram-negative bacteria: vertical scaffold or horizontal layer(s)? J Bacteriol 186, 5978-5987.
Volokhina, E.B., Grijpstra, J., Stork, M., Schilders, I., Tommassen, J., Bos, M.P., 2011. Role of the periplasmic chaperones Skp, SurA, and DegQ in outer membrane protein biogenesis in *Neisseria meningitidis*. J Bacteriol 193, 1612-1621.
Waller, P.R., Sauer, R.T., 1996. Characterization of degQ and degS, *Escherichia coli* genes encoding homologs of the DegP protease. J Bacteriol 178, 1146-1153.
Walton, T.A., Sousa, M.C., 2004. Crystal structure of Skp, a prefoldin-like chaperone that protects soluble and membrane proteins from aggregation. Mol Cell 15, 367-374.
Wang, N., Ozer, E.A., Mandel, M.J., Hauser, A.R., 2014. Genome-wide identification of *Acinetobacter baumannii* genes necessary for persistence in the lung. mBio 5, e01163-01114.
Wang, Y., Wang, R., Jin, F., Liu, Y., Yu, J., Fu, X., Chang, Z., 2016. A Supercomplex Spanning the Inner and Outer Membranes Mediates the Biogenesis of beta-Barrel Outer Membrane Proteins in Bacteria. J Biol Chem 291, 16720-16729.
Waterhouse, A.M., Procter, J.B., Martin, D.M., Clamp, M., Barton, G.J., 2009. Jalview Version 2--a multiple sequence alignment editor and analysis workbench. Bioinformatics 25, 1189-1191.
Watts, K.M., Hunstad, D.A., 2008. Components of SurA required for outer membrane biogenesis in uropathogenic *Escherichia coli*. PLoS One 3, e3359.
Weber, B.S., Kinsella, R.L., Harding, C.M., Feldman, M.F., 2017. The Secrets of *Acinetobacter* Secretion. Trends Microbiol 25, 532-545.
Weber, B.S., Ly, P.M., Irwin, J.N., Pukatzki, S., Feldman, M.F., 2015. A multidrug resistance plasmid contains the molecular switch for type VI secretion in *Acinetobacter baumannii*. Proc Natl Acad Sci U S A 112, 9442-9447.

Weber, B.S., Miyata, S.T., Iwashkiw, J.A., Mortensen, B.L., Skaar, E.P., Pukatzki, S., Feldman, M.F., 2013. Genomic and functional analysis of the type VI secretion system in *Acinetobacter*. PLoS One 8, e55142.
Wei, J.R., Richie, D.L., Mostafavi, M., Metzger, L.E.t., Rath, C.M., Sawyer, W.S., Takeoka, K.T., Dean, C.R., 2017. LpxK Is Essential for Growth of *Acinetobacter baumannii* ATCC 19606: Relationship to Toxic Accumulation of Lipid A Pathway Intermediates. mSphere 2.
Weidensdorfer, M., Chae, J.I., Makobe, C., Stahl, J., Averhoff, B., Muller, V., Schurmann, C., Brandes, R.P., Wilharm, G., Ballhorn, W., Christ, S., Linke, D., Fischer, D., Gottig, S., Kempf, V.A., 2015. Analysis of Endothelial Adherence of Bartonella henselae and *Acinetobacter baumannii* Using a Dynamic Human Ex Vivo Infection Model. Infect Immun 84, 711-722.
Weidensdorfer, M., Ishikawa, M., Hori, K., Linke, D., Djahanschiri, B., Iruegas, R., Ebersberger, I., Riedel-Christ, S., Enders, G., Leukert, L., Kraiczy, P., Rothweiler, F., Cinatl, J., Berger, J., Hipp, K., Kempf, V.A.J., Gottig, S., 2019. The *Acinetobacter* trimeric autotransporter adhesin Ata controls key virulence traits of *Acinetobacter baumannii*. Virulence 10, 68-81.
Weinberg, E.D., 2009. Iron availability and infection. Biochim Biophys Acta 1790, 600-605.
Weiner, L.M., Webb, A.K., Limbago, B., Dudeck, M.A., Patel, J., Kallen, A.J., Edwards, J.R., Sievert, D.M., 2016. Antimicrobial-Resistant Pathogens Associated With Healthcare-Associated Infections: Summary of Data Reported to the National Healthcare Safety Network at the Centers for Disease Control and Prevention, 2011-2014. Infect Control Hosp Epidemiol 37, 1288-1301.
Weirich, J., Bräutigam, C., Mühlenkamp, M., Franz-Wachtel, M., Macek, B., Meuskens, I., Skurnik, M., Leskinen, K., Bohn, E., Autenrieth, I., Schütz, M., 2017. Identifying components required for OMP biogenesis as novel targets for antiinfective drugs. Virulence 8, 1170-1188.
Wendt, C., Dietze, B., Dietz, E., Ruden, H., 1997. Survival of *Acinetobacter baumannii* on dry surfaces. J Clin Microbiol 35, 1394-1397.
Wickham, H., 2016. ggplot2: elegant graphics for data analysis. springer.
Wilharm, G., Piesker, J., Laue, M., Skiebe, E., 2013. DNA uptake by the nosocomial pathogen *Acinetobacter baumannii* occurs during movement along wet surfaces. J Bacteriol 195, 4146-4153.
Willmann, M., Götting, S., Bezdan, D., Maček, B., Velic, A., Marschal, M., Vogel, W., Flesch, I., Markert, U., Schmidt, A., 2018. Multi-omics approach identifies novel pathogen-derived prognostic biomarkers in patients with *Pseudomonas aeruginosa* bloodstream infection. bioRxiv, 309898.
Wisplinghoff, H., Paulus, T., Lugenheim, M., Stefanik, D., Higgins, P.G., Edmond, M.B., Wenzel, R.P., Seifert, H., 2012. Nosocomial bloodstream infections due to *Acinetobacter baumannii*, *Acinetobacter pittii* and *Acinetobacter nosocomialis* in the United States. J Infect 64, 282-290.
Wisplinghoff, H., Perbix, W., Seifert, H., 1999. Risk factors for nosocomial bloodstream infections due to *Acinetobacter baumannii:* a case-control study of adult burn patients. Clin Infect Dis 28, 59-66.
Wisplinghoff, H., Schmitt, R., Wohrmann, A., Stefanik, D., Seifert, H., 2007. Resistance to disinfectants in epidemiologically defined clinical isolates of *Acinetobacter baumannii*. J Hosp Infect 66, 174-181.
Wong, D., Nielsen, T.B., Bonomo, R.A., Pantapalangkoor, P., Luna, B., Spellberg, B., 2017. Clinical and Pathophysiological Overview of *Acinetobacter* Infections: a Century of Challenges. Clin Microbiol Rev 30, 409-447.
Wright, M.S., Haft, D.H., Harkins, D.M., Perez, F., Hujer, K.M., Bajaksouzian, S., Benard, M.F., Jacobs, M.R., Bonomo, R.A., Adams, M.D., 2014. New insights into dissemination and variation of the health care-associated pathogen *Acinetobacter baumannii* from genomic analysis. mBio 5, e00963-00913.
Wu, R., Stephenson, R., Gichaba, A., Noinaj, N., 2020. The big BAM theory: An open and closed case? Biochim Biophys Acta Biomembr 1862, 183062.
Wu, T., Malinverni, J., Ruiz, N., Kim, S., Silhavy, T.J., Kahne, D., 2005. Identification of a multicomponent complex required for outer membrane biogenesis in *Escherichia coli*. Cell 121, 235-245.
Wu, X., Chavez, J.D., Schweppe, D.K., Zheng, C., Weisbrod, C.R., Eng, J.K., Murali, A., Lee, S.A., Ramage, E., Gallagher, L.A., Kulasekara, H.D., Edrozo, M.E., Kamischke, C.N., Brittnacher, M.J., Miller,

S.I., Singh, P.K., Manoil, C., Bruce, J.E., 2016. In vivo protein interaction network analysis reveals porin-localized antibiotic inactivation in *Acinetobacter baumannii* strain AB5075. Nat Commun 7, 13414.
Xu, X., Wang, S., Hu, Y.X., McKay, D.B., 2007. The periplasmic bacterial molecular chaperone SurA adapts its structure to bind peptides in different conformations to assert a sequence preference for aromatic residues. J Mol Biol 373, 367-381.
Yamamoto, S., Okujo, N., Sakakibara, Y., 1994. Isolation and structure elucidation of acinetobactin, a novel siderophore from *Acinetobacter baumannii*. Arch Microbiol 162, 249-254.
Yoon, E.J., Courvalin, P., Grillot-Courvalin, C., 2013. RND-type efflux pumps in multidrug-resistant clinical isolates of *Acinetobacter baumannii*: major role for AdeABC overexpression and AdeRS mutations. Antimicrob Agents Chemother 57, 2989-2995.
Yorgey, P., Rahme, L.G., Tan, M.W., Ausubel, F.M., 2001. The roles of mucD and alginate in the virulence of *Pseudomonas aeruginosa* in plants, nematodes and mice. Mol Microbiol 41, 1063-1076.
Yuasa, R., Levinthal, M., Nikaido, H., 1969. Biosynthesis of cell wall lipopolysaccharide in mutants of Salmonella. V. A mutant of *Salmonella typhimurium* defective in the synthesis of cytidine diphosphoabequose. J Bacteriol 100, 433-444.
Zaffiri, L., Gardner, J., Toledo-Pereyra, L.H., 2012. History of antibiotics. From salvarsan to cephalosporins. Journal of investigative surgery : the official journal of the Academy of Surgical Research 25, 67-77.
Zahn, M., Bhamidimarri, S.P., Basle, A., Winterhalter, M., van den Berg, B., 2016. Structural Insights into Outer Membrane Permeability of *Acinetobacter baumannii*. Structure 24, 221-231.
Zahn, M., D'Agostino, T., Eren, E., Basle, A., Ceccarelli, M., van den Berg, B., 2015. Small-Molecule Transport by CarO, an Abundant Eight-Stranded beta-Barrel Outer Membrane Protein from *Acinetobacter baumannii*. J Mol Biol 427, 2329-2339.
Zgurskaya, H.I., Lopez, C.A., Gnanakaran, S., 2015. Permeability Barrier of Gram-Negative Cell Envelopes and Approaches To Bypass It. ACS Infect Dis 1, 512-522.
Zgurskaya, H.I., Nikaido, H., 2000. Multidrug resistance mechanisms: drug efflux across two membranes. Mol Microbiol 37, 219-225.
Zhang, G., Meredith, T.C., Kahne, D., 2013. On the essentiality of lipopolysaccharide to Gram-negative bacteria. Curr Opin Microbiol 16, 779-785.
Zhang, J., Yuan, D., Zhao, Q., Yan, S., Tang, S.-Y., Tan, S.H., Guo, J., Xia, H., Nguyen, N.-T., Li, W., 2018. Tunable particle separation in a hybrid dielectrophoresis (DEP)-inertial microfluidic device. Sensors and Actuators B: Chemical 267, 14-25 %@ 0925-4005.
Zhu, J., Wang, C., Wu, J., Jiang, R., Mi, Z., Huang, Z., 2009. A novel aminoglycoside-modifying enzyme gene aac(6')-Ib in a pandrug-resistant *Acinetobacter baumannii* strain. J Hosp Infect 73, 184-185.
Zimbler, D.L., Penwell, W.F., Gaddy, J.A., Menke, S.M., Tomaras, A.P., Connerly, P.L., Actis, L.A., 2009. Iron acquisition functions expressed by the human pathogen *Acinetobacter baumannii*. Biometals 22, 23-32.
Zimmermann, L., Stephens, A., Nam, S.Z., Rau, D., Kubler, J., Lozajic, M., Gabler, F., Soding, J., Lupas, A.N., Alva, V., 2018. A Completely Reimplemented MPI Bioinformatics Toolkit with a New HHpred Server at its Core. J Mol Biol 430, 2237-2243.
Zoued, A., Brunet, Y.R., Durand, E., Aschtgen, M.S., Logger, L., Douzi, B., Journet, L., Cambillau, C., Cascales, E., 2014. Architecture and assembly of the Type VI secretion system. Biochim Biophys Acta 1843, 1664-1673.
Zurawski, D.V., Thompson, M.G., McQueary, C.N., Matalka, M.N., Sahl, J.W., Craft, D.W., Rasko, D.A., 2012. Genome sequences of four divergent multidrug-resistant *Acinetobacter baumannii* strains isolated from patients with sepsis or osteomyelitis. J Bacteriol 194, 1619-1620.

8. Figures

9. Tables

10. Appendix

Declaration of contributions

“Table *13*, “Table ***14***, “Table *15* and “Figure ***13*** as well as the figures text are literally taken from Birkle et al. (manuscript submitted) and are highlighted with quotation marks as well as written in italic.
“Table *13*, “Table ***14***, “Table *15* and “Figure ***13*** as well as the figures text were generated and written by the co-author Dr. Fabian Renschler from the Institute for Medical Microbiology and Hygiene.
The manuscript Birkle et al. (manuscript submitted) was mainly written by PD Dr. Monika Schütz and me.

"Table 13 Search for SurA, Skp and DegP paralogues in AB5075. *To identify paralogues of the AB5075 proteins SurA, Skp and DegP the AB5075 proteome (UniProt ID UP000032746) (Gallagher et al., 2015) was scanned for sequences homologous to SurA (A0A077GP18), Skp (V5VCL3) and DegP (V5VAG2) using BLAST (2.10.0+) (Altschul et al., 1997). BLAST hits of the query sequences are highlighted in italic. Sequence alignments identified by BLAST were manually inspected and the homologous regions were assigned to the corresponding regions of the query proteins ("Figure 13). In addition, their (predicted) localization was retrieved from the InterPro database (Mitchell et al., 2019). Finally, BLAST hits were qualified as highly probable (green) depending on whether all three criteria were met and less probable (yellow) paralogues if at least one criterion was not met. First, they must have a sequence identity >= 30% and an as high as possible percentage of positives. Secondly, the sequence identity must be in a substantial sequence range (>=60 aa). Third, they must be (predicted to) localize to the periplasm. However, the search for paralogues by simple sequence homology search algorithms such as BLAST does not allow identifying functional paralogues with no or limited sequence homologies. Therefore, the existence of additional paralogues cannot be ruled out."*

accession number	name	score (Bits)	E value	localisation	size (aa)	% identity	% positives	domain homology	possible orthologes	comments
SurA										
A0A077GP18	*Chaperone SurA*	*893*	*0*	*periplasm*	*436*	*100*			*n/a*	
V5VA69	Peptidylprolyl isomerase PpiC	60,5	2,00E-12	cytoplasm	96	37	51	93 aa, PPI2	no	PPI2 domain
A0A0E1JKW1	Peptidylprolyl isomerase PpiD	65,1	3,00E-12	inner membrane transmembrane protein, mostly periplasmic	621	35	61	110 aa, PPI2	yes	PPI2 domain
A0A0D5YFT8	Uncharacterized protein	25,8	2,4	cytoplasm	110	24	40	86 aa, N	no	
A0A0D5YFC4	Patatin-like phospholipase family protein	26,6	3,6	lipoprotein	305	28	47	79 aa, PPI1	maybe	
A0A0D5YCP6	Cation efflux system protein (EsvF1)	26,2	4,6	inner membrane transmembrane protein, mostly periplasmic	405	52	71	21 aa, N	no	
A0A0D5YG98	AMP-binding protein	25,8	5,8	cytoplasm	547	36	50	28 aa, N	no	
A0A0D5YHN3	Transaldolase	25,4	6,7	cytoplasm	329	27	50	45 aa, PPI1	no	
A0A0D5YJX4	3-oxoadipyl-CoA thiolase	25,4	8,2	inner membrane protein, mostly cytoplasmic	401	28	52	87 aa, N	no	
A0A0D5YK63	Capsule assembly Wzi family protein	25,4	8,7	outer membrane protein	481	28	52	46 aa, C	no	
A0A0D5YFQ2	Rhombotarget A	25,4	9	outer membrane protein	617	31	51	39 aa, N-PPI1	no	
Skp										
V5VCL3	*OmpH family outer membrane protein Skp*	*331*	*2,00E-119*	*periplasm*	*167*	*100*			*n/a*	
A0A0D5YDF1	NAD-dependent succinate-semialdehyde dehydrogenase	26,9	0,6	cytoplasm	482	27	50	52 aa, tentacle	no	
A0A0D5YKR2	Uncharacterized protein	25	1,7	?	136	25	48	60 aa, tentacle	no	
A0A077GFJ9	4-hydroxybenzoate octaprenyltransferase	25,4	1,8	inner membrane transmembrane protein	292	30	45	47 aa, tentacle	no	
V5VAP2	ABC transporter ATP-binding protein	25,4	2,1	inner membrane transmembrane protein	553	36	64	44 aa, body-tentacle	no	
A0A0D5YIG3	Bifunctional (P)ppGpp synthase/hydrolase SpoT	24,6	2,5		146	29	50	84 aa, tentacle	no	
V5VI16	Arginine--tRNA ligase	25	2,9	cytoplasm	596	29	53	34 aa, tentacle	no	
A0A0J8W8F3	Heat shock protein HtpX	23,5	8,1	inner membrane transmembrane protein	629	34	62	29 aa, tentacle	no	
DegP										
V5VAG2	*Periplasmic serine endoprotease DegP-like*	*919*	*0*	*periplasm*	*458*	*100*			*n/a*	
A0A0D5YGS6	Peptidase S1 and S6/ DegS	187	8,00E-56	inner membrane transmembrane protein, mostly periplasmic	391	39	57	293 aa, protease-PDZ1	yes	protease and PDZ1 domain
A0A0D5YFR0	M61 family peptidase	36,6	0,003	cytoplasm	567	29	45	139 aa, protease-PDZ1	no	
A0A086HVC9	General secretion pathway protein	34,7	0,008	inner membrane transmembrane protein, mostly periplasmic	278	32	52	65 aa, PDZ1	maybe	PDZ1 domain
A0A0D5YI62	Zinc metalloprotease	33,1	0,033	inner membrane transmembrane protein, mostly periplasmic	451	34	51	61 aa, PDZ1	maybe	PDZ1 domain, contains 2 PDZ domains
V5VCS2	Ribose-5-phosphate isomerase A	28,9	0,57	cytoplasm	223	46	69	26 aa, PDZ2	no	
G1D8S2	APH(3')-VI family aminoglycoside O-phosphotransferase	26,2	4	cytoplasm	259	28	53	47 aa, protease	no	
A0A0D5YKM0	Endonuclease/exonuclease/phosphatase	26,2	4,8	cytoplasm	783	26	42	95 aa, protease	no	
A0A0D5YJ06	Urea amidolyase	26,2	5,7	cytoplasm	1201	42	67	24 aa, PDZ2	no	
V5VI16	Arginine--tRNA ligase	25,4	8	cytoplasm	596	33	21	43 aa, PDZ1-PDZ2	no	

"Table 14 Pairwise identities (%) of SurA, Skp and DegP from various species. *Domain nomenclature as in "Figure* ***13****."*

Protein	SurA					Skp					DegP				
	Full length					Full length					Full length				
	Ab AB5075	*Pa* PA14	*Kp* p	*Nm* H44/76	*Eco* K12	*Ab* AB5075	*Pa* PA14	*Kp* p	*Nm* H44/76	*Eco* K12	*Ab* AB5075	*Pa* PA14	*Kp* p	*Nm* H44/76	*Eco* K12
Ab AB5075		35,57	27,67	24,68	27,44		20,83	18,79	16,27	18,79		41,35	32,92	38,48	33,05
Pa PA14			39,02	26,75	38,41			23,49	22,16	25,15			38,65	47,07	39,05
Kp p				21,98	89,49				25,00	90,06				34,21	90,78
Nm H44/76					23,15					23,17					32,19
Eco K12															
Domain	NC-core					Body					Protease				
Ab AB5075		37,64	29,61	22,60	29,61		21,15	14,00	19,61	12,00		50,00	36,88	47,83	37,16
Pa PA14			35,80	22,86	36,36			29,09	30,36	27,27			42,75	56,52	43,68
Kp p				20,57	93,22				21,82	90,91				38,93	93,87
Nm H44/76					20,00					16,36					37,45
Eco K12															
Domain	PPI1					Tentacle					PDZ1				
Ab AB5075		26,88	19,79	n/a	19,15		20,21	20,83	14,13	18,95		36,36	34,34	36,36	35,35
Pa PA14			41,41	n/a	41,41			22,34	17,02	22,34			37,37	48,48	37,37
Kp p				n/a	87,88				23,91	86,81				37,37	87,88
Nm H44/76					n/a					20,65					34,34
Eco K12															
Domain	PPI2					-					PDZ2				
Ab AB5075		45,19	37,14	38,46	36,19							27,88	25,00	25,96	26,09
Pa PA14			42,86	34,62	41,90								30,93	29,36	31,96
Kp p				37,14	85,71									25,56	84,44
Nm H44/76					38,10										22,22
Eco K12															

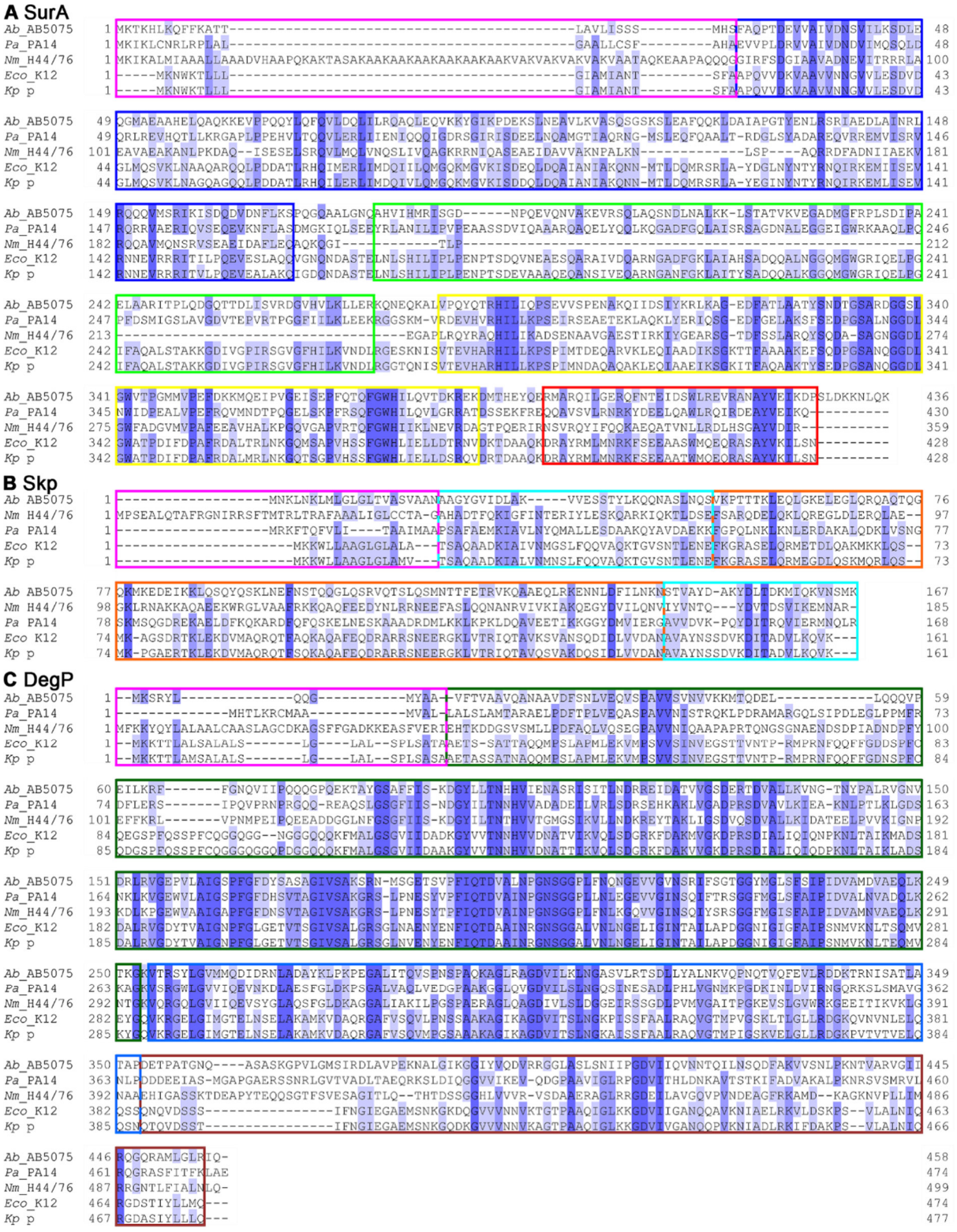

"Figure 13 Amino acid sequence alignment and sequence conservation analysis of SurA, Skp and DegP of various Gram-negative species. *(A) Sequence alignment of SurA from Acinetobacter baumannii strain AB5075 (Ab AB5075; A0A077GP18), Pseudomonas aeruginosa strain PA14 (Pa PA14; A0A0H2ZLB3), Neisseria meningitidis strain H44/76 (Nm H44/76; E6MWH2), Klebsiella pneumoniae subsp. pneumoniae (Kp p; A0A2X3H098) and Escherichia coli strain K12 (Eco K12; P0ABZ6).*

Sequences were aligned using clustalΩ (Sievers et al., 2011; Zimmermann et al., 2018) and color coded according to conservation from white (no conservation) to blue (100% conservation). Sequence identities for the full-length proteins as well as the individual domains are summarized in "Table ***14****. The domains are deduced from the crystal structure of the Eco K12 protein (pdb ID: 1m5y) and are indicated as a magenta box for the N-terminal signal sequence, as a dark blue box for the N-terminal domain, as a green box for the peptidyl-prolyl isomerase (PPI) domain 1, as a yellow box for the PPI2 domain and as a red box for the C-terminal domain. Of note, the N-terminal and C-terminal domains form a single structural domain, called the NC-core. The sequence alignment view was prepared with Jalview (Waterhouse et al., 2009). (B) Sequence alignment of Skp as in A (Ab AB5075: V5VL3; Nm H44/76: E6MUY6; Pa PA14: A0A0H2ZEQ6; Eco K12: P0AEU7; Kp p: A0A1Y0Q2G3). The domains were deduced from the crystal structure of the Eco K12 protein (pdb IDs: 1sg2, 1u2m) and are indicated as magenta box for the N-terminal signal sequence, as cyan box for the body domain and as orange box for the tentacle domain of Skp. (C) Sequence alignment of DegP as in A (Ab AB5075: V5VAG2; Pa PA14: A0A0H2Z7B2; Nm H44/76: E6MVM8; Eco K12 P0C0V0; Kp p: A0A422Y8P3). The domains are deduced from the crystal structure of the Eco K12 protein (pdb IDs: 1ky9) and are indicated as a magenta box for the N-terminal signal sequence, as a dark green box for the DegP protease domain, as a blue box for the Postsynaptic density protein-95, Disk large, Zonula occludens 1 (PDZ) domain 1 and as a brown box for the PDZ2 domain."*

"Table 15 Overview of all proteins the abundance of which was significantly changed in the triple mutant (ΔΔΔ) compared to the wild type (WT) at least 2-fold in samples of the whole cell lysate (WCL) and/or membrane fractions (MEM). *n.a.= gene name not available."*

No.	Functional Category	Subcategory	Function	UniProt Entry	Gene ID	Gene Name, Synonym	Presence (0/1) and change of expression (+/-) in ΔΔΔ/WT	Mean LFQ ΔΔΔ	Mean LFQ WT	log2-fold change LFQ ΔΔΔ/WT	-log10 adjusted p-value ΔΔΔ/WT	Presence (0/1) and change of expression (+/-) in ΔΔΔ/WT	Mean LFQ ΔΔΔ	Mean LFQ WT	log2-fold change LFQ ΔΔΔ/WT	-log10 adjusted p-value ΔΔΔ/WT	SignalP Sec/SPI	SignalP Tat/SPI	SignalP Sec/SPII Lipoprotein	Other	SecP non classical secretion (Cutoff 0,5)	LipoP Score	LipoP Class/ *known classification*
							WCL					MEM					Signal P 5.0				SecP 2.0a	LipoP 1.0	
1	Uncharacterized proteins		Uncharacterized	A0A0D5YIP3	**ABUW_2034**	*n.a.*	1+	3,61E+09	0,00E+00	9,83	7,05	0					0,0334	0,0031	0,0044	**0,9591**	**0,8637**	-0,2009	non-classically secreted
2	Uncharacterized proteins		Uncharacterized	A0A0D5YJ02	**ABUW_1997**	*n.a.*	1+	1,87E+09	0,00E+00	8,55	7,42	0					0,0209	0,0009	0,0025	**0,9757**	**0,5177**	-0,2009	non-classically secreted
3	Enzymes	Dehydrogenase	Succinate dehydrogenase hydrophobic membrane anchor subunit	V5VAK8	**ABUW_0869**	*sdhD*	1+	1,02E+08	0,00E+00	4,71	1,60	0					0,0012	0,0002	0,0035	**0,9951**	0,1492	**6,9770**	TMH
4	Secreted proteins/ surface antigen	Surface antigens	17 kDa surface antigen family protein	V5VDE2	**ABUW_1563**	*n.a.*	1+	1,28E+08	0,00E+00	4,24	10,15	1+	1,16E+08	0,00E+00	2,88	3,18	**0,9972**	0,0007	0,0012	0,0010	**0,6280**	**20,5669**	SpI
5	Enzymes	Hydrolases	Indoleacetamide hydrolase	A0A0D5YH92	**ABUW_1948**	*iaaH*	1+	6,78E+07	0,00E+00	4,17	4,75	0					0,0089	0,0034	0,0005	**0,9872**	0,2678	-0,2009	cytoplasmic
6	Uncharacterized proteins		Uncharacterized	V5VBW4	**ABUW_1652**	*n.a.*	1+	2,24E+07	0,00E+00	3,93	13,38	0					0,0113	0,0050	0,0062	**0,9776**	0,1072	-0,2009	cytoplasmic
7	Enzymes	Phosphatases	Histidine phosphatase family protein	A0A0D5YH36	**ABUW_1852**	*n.a.*	1+	1,23E+07	0,00E+00	3,41	4,85	0					0,0094	0,0013	0,0014	**0,9880**	0,0658	-0,2009	cytoplasmic
8	Other		Glycine cleavage system H protein	V5VDJ8	**ABUW_2283**	*gcvH*	1+	6,20E+07	0,00E+00	2,97	4,76	0					0,0035	0,0017	0,0004	**0,9945**	0,3257	-0,2009	cytoplasmic
9	Uncharacterized proteins		Uncharacterized	A0A0D5YDI9	**ABUW_0607**	*n.a.*	1+	1,13E+09	2,06E+08	2,44	9,24	1+	6,14E+08	1,77E+08	1,79	4,58	0,0030	0,0001	**0,9968**	0,0001	**0,9358**	**11,9776**	SpII
10	Enzymes	Ribonucleases	Endoribonuclease L-PSP	A0A0D5YLA1	**ABUW_3316**	*n.a.*	1+	1,25E+08	2,54E+07	2,28	3,54	0					0,0286	0,0010	0,0014	**0,9690**	0,3133	-0,2009	cytoplasmic
11	Enzymes	Hydrolases	Isochorismatase hydrolase	A0A059ZTU2	**ABUW_1905**	*ycaC_1*	1+	1,02E+09	2,16E+08	2,23	3,07	0					0,0424	0,0091	0,0003	**0,9482**	0,1646	-0,2009	cytoplasmic
12	Uncharacterized proteins		Uncharacterized	A0A059ZT62	**ABUW_1298**	*n.a.*	1+	1,94E+07	0,00E+00	2,10	1,59	0					0,0790	0,0015	0,0032	**0,9163**	**0,7912**	-0,2009	non-classically secreted
13	Stress response/ DNA repair	Stress response	SOS-response	V5VDZ0	**ABUW_1748**	*recA*	1+	1,26E+10	4,31E+09	1,53	5,28	1+	3,4E+09	1,25E+09	1,48	2,04	0,0063	0,0294	0,0006	**0,9638**	0,1340	-0,2009	cytoplasmic
14	Micronutrient acquisition	Iron acquisition	Outer-membrane receptor for Fe(III)-coprogen,Fe(III)-ferrioxamine B and Fe(III)-rhodotrulic acid	A0A0D5YJ17	**ABUW_2165**	*fhuE_1*	1+	5,11E+08	1,84E+08	1,46	4,84	1+	2,95E+08	0,00E+00	6,22	1,56	**0,9826**	0,0012	0,0097	0,0065	**0,9455**	**10,8422**	SpI
15	Enzymes	Nucleosidases	5'-methylthioadenosine nucleosidase	A0A0D5YKU5	**ABUW_3145**	*mtnN*	1+	6,10E+08	2,32E+08	1,38	2,31	0					0,0004	0,0001	**0,9993**	0,0002	**0,5824**	**17,6419**	SpII
16	Enzymes	Oxidoreductases	SDR family NAD(P)-dependent oxidoreductase	A0A0D5YGP1	**ABUW_1721**	*galE_2*	1+	1,35E+09	5,41E+08	1,30	5,46	1+	1,09E+09	3,62E+08	1,62	2,85	**0,6092**	0,0033	0,0813	0,3063	0,1227	-0,2009	cytoplasmic
17	Efflux / Transport	RND efflux pump family	Efflux transporter, RND family, MFP subunit	Q2FD52	**ABUW_3362**	*macA*	1+	9,28E+08	3,99E+08	1,20	4,50	1+	1,09E+09	3,8E+08	1,53	4,74	0,0214	0,0003	0,0029	**0,9754**	**0,9643**	**3,2464**	SpI
18	Lipoproteins	Lipoproteins	Lipoprotein	V5VJ35	**ABUW_3730**	*n.a.*	1+	2,77E+08	1,20E+08	1,19	2,33	0					0,0013	0,0001	**0,9983**	0,0003	0,4964	**11,8555**	SpII
19	Enzymes	Cyclase	PqqA peptide cyclase	A0A0D5YJ35	**ABUW_2067**	*pqqE*	1+	1,94E+08	8,51E+07	1,17	4,72	0					0,1090	0,0014	0,0634	**0,8261**	0,0714	-0,2009	cytoplasmic
20	Uncharacterized proteins		DUF2797 domain-containing protein	A0A0D5YJC3	**ABUW_2163**	*n.a.*	1+	2,00E+08	8,91E+07	1,15	7,27	1					0,0205	0,0049	0,0056	**0,9690**	0,0831	-0,2009	cytoplasmic
21	Antibiotic Resistance	Beta-lactamase family	Beta-lactamase enzyme family protein	G1C783	**ABUW_1070**	*dacD*	1+	4,87E+08	2,22E+08	1,11	3,12	1					**0,9347**	0,0005	0,0492	0,0156	0,3068	**7,9430**	SpI
22	Enzymes	Synthases	Pyrroloquinoline-quinone synthase	A0A081GZA3	**ABUW_2069**	*pqqC*	1+	4,87E+08	2,28E+08	1,08	4,18	0					0,0054	0,0010	0,0005	**0,9931**	0,0959	-0,2009	cytoplasmic
23	Efflux / Transport	RND efflux pump family	AdeC/AdeK/OprM family multidrug efflux complex outer membrane factor	A0A0D5YL63	**ABUW_3364**	*adeC*	1+	7,88E+08	3,77E+08	1,04	2,58	1+	4,34E+08	1,37E+08	1,66	2,93	0,0050	0,0001	**0,9944**	0,0005	**0,6610**	**17,4731**	SpII
24	Enzymes	Dehydrogenase	L-sorbosone dehydrogenase	A0A0D5YIN1	**ABUW_1902**	*sndH2*	1+	7,07E+08	3,48E+08	1,01	2,10	0					0,0007	0,0001	**0,9989**	0,0003	**0,9413**	**12,4124**	SpII
25	Enzymes	Dehydrogenase	Quinoprotein glucose dehydrogenase	A0A0D5YIN6	**ABUW_1907**	*gdhB1*	1+	1,89E+09	9,74E+08	1,01	4,59	0					**0,9926**	0,0020	0,0025	0,0029	**0,9350**	**5,5086**	SpI
26	Micronutrient acquisition		TonB-dependent siderophore receptor	A0A0D5YFB1	**ABUW_0661**	*n.a.*	1-	3,13E+08	6,19E+08	-1,01	4,61	1-	0,00E+00	1,63E+08	-4,02	1,83	**0,9172**	0,0114	0,0690	0,0024	**0,9434**	**7,7978**	SpI
27	Stress response/ DNA repair	Stress response	Trehalose 6-phosphate phosphatase	A0A0D5YLK1	**ABUW_3122**	*otsB*	1-	4,56E+08	9,06E+08	-1,01	2,61	0					0,0043	0,0006	0,0009	**0,9943**	0,0469	-0,2009	cytoplasmic
28	Secreted proteins/ surface antigen	Secreted proteins	Polyisoprenoid-binding protein (YecI)	V5XWY4	**ABUW_2293**	*n.a.*	1-	1,57E+09	3,18E+09	-1,03	2,87	1					**0,9982**	0,0002	0,0012	0,0004	**0,9237**	**20,2370**	SpI
29	Signal Peptides		Signal peptide	A0A0D5YCG8	**ABUW_0135**	*n.a.*	1-	8,18E+08	1,67E+09	-1,05	4,15	1-	4,76E+08	1,21E+09	-1,34	2,88	**0,9977**	0,0005	0,0014	0,0004	**0,9373**	**20,2295**	SpI
30	Efflux / Transport	ABC transporter family	Glutamate/aspartate transport protein	V5VDN7	**ABUW_2333**	*gltI*	1-	6,30E+08	1,29E+09	-1,05	1,77	0					**0,9947**	0,0005	0,0045	0,0004	**0,9573**	**12,9430**	SpI
31	Antibiotic Resistance	Copper resistance/detoxifiaction	Copper resistance protein A	A0A0D5YLC8	**ABUW_3321**	*copA*	1-	4,52E+08	9,28E+08	-1,05	1,48	0					**0,9565**	0,0040	0,0082	0,0314	**0,9252**	**5,5460**	SpI
32	Signal Peptides		Signal peptide	V5VE93	**ABUW_1844**	*n.a.*	1-	5,37E+08	1,11E+09	-1,07	1,82	1-	0,00E+00	3,16E+08	-4,92	3,32	0,0045	0,0001	**0,9952**	0,0002	**0,9415**	**12,5699**	SpI

No.	Functional Category	Subcategory	Function	UniProt Entry	Gene ID	Gene Name, Synonym	Presence (0/1) and change of expression (+/-) in ΔΔΔ/WT	Mean LFQ ΔΔΔ	Mean LFQ WT	log2-fold change LFQ ΔΔΔ/WT	-log10 adjusted p-value ΔΔΔ/WT	Presence (0/1) and change of expression (+/-) in ΔΔΔ/WT	Mean LFQ ΔΔΔ	Mean LFQ WT	log2-fold change LFQ ΔΔΔ/WT	-log10 adjusted p-value ΔΔΔ/WT	SignalP Sec/SPI	SignalP Tat/SPI	SignalP Sec/SPII Lipoprotein	Other	SecP non classical secretion (Cutoff 0,5)	LipoP Score	LipoP Class/ *known classification*
									WCL					MEM				Signal P 5.0				SecP 2.0a	LipoP 1.0	
33	Stress response/ DNA repair	Stress response	Trehalose-6-phosphate synthase	T2HTY7	**ABUW_3123**	*otsA*	1-	6,70E+08	1,41E+09	-1,09	2,34	1					0,2713	0,0348	0,0092	**0,6846**	0,1037	**2,9144**	cytoplasmic
34	Fatty acid metabolism		Long-chain fatty acid transporter	A0A0D5YDU5	**ABUW_0724**	*n.a.*	1-	2,85E+09	6,05E+09	-1,10	4,18	1-	1,45E+09	5,36E+09	-1,88	4,49	**0,9930**	0,0012	0,0043	0,0015	**0,9481**	**15,2200**	Spl
35	OMPs/ Porins		Outer membrane porin, OprD family	A0A059ZTU7	**ABUW_3685**	*oprD_3*	1-	1,27E+09	2,72E+09	-1,11	2,15	1-	7,43E+08	1,74E+09	-1,22	2,93	**0,9949**	0,0006	0,0040	0,0005	**0,9450**	**14,7531**	Spl
36	Enzymes	Hydratases	3-methylglutaconyl-CoA hydratase	A0A0D5YK55	**ABUW_2454**	*mgh*	1-	5,81E+07	1,27E+08	-1,15	2,50	0					0,0022	0,0013	0,0004	**0,9961**	0,1575	-0,2009	cytoplasmic
37	Enzymes	Glyoxylase activity	VOC family protein	A0A0D5YF96	**ABUW_0646**	*n.a.*	1-	1,46E+08	3,24E+08	-1,17	4,85	0					0,0094	0,0010	0,0007	**0,9889**	**0,5562**	-0,2009	non-classically secreted
38	Efflux / Transport	RND efflux pump family	Putative RND type efflux pump involved in aminoglycoside resistance (AdeT)	V5V8J3	**ABUW_0009**	*adeT*	1-	5,48E+08	1,24E+09	-1,20	5,50	0					**0,9984**	0,0004	0,0009	0,0003	**0,7959**	**23,7603**	Spl
39	Efflux / Transport	ABC transporter family	Sulfate ABC transporter substrate-binding protein	V5VAT6	**ABUW_1021**	*spb_2*	1-	5,92E+07	1,34E+08	-1,20	2,91	0					**0,9970**	0,0003	0,0022	0,0006	**0,8482**	**13,9335**	Spl
40	Enzymes	Dehydrogenase	Alanine dehydrogenase/PNT, N-terminal domain protein	V5VGF5	**ABUW_3314**	*pntAA*	1-	4,69E+07	1,07E+08	-1,21	1,51	0					0,0164	0,0066	0,0018	**0,9752**	0,2434	-0,2009	cytoplasmic
41	Stress response/ DNA repair	DNA binding/repair	NAD-dependent DNA ligase, DNA polymerase III subunit epsilon	A0A0D5YEA9	**ABUW_0553**	*n.a.*	1-	2,36E+08	5,44E+08	-1,22	2,48	1-	0,00E+00	7,76E+07	-3,03	1,93	0,0024	0,0010	0,0004	**0,9962**	0,0773	-0,2009	cytoplasmic
42	Uncharacterized proteins		Uncharacterized	V5VDH6	**ABUW_1601**	*n.a.*	1-	2,35E+08	5,42E+08	-1,22	2,70	0					0,0030	0,0006	0,0007	**0,9958**	0,0614	-0,2009	cytoplasmic
43	Uncharacterized proteins		Uncharacterized	A0A0D5YDA8	**ABUW_0118**	*n.a.*	1-	1,68E+08	3,88E+08	-1,23	4,24	1					0,0586	0,0001	**0,9409**	0,0004	0,2930	**6,1846**	SpII
44	Signal Peptides		Signal peptide	A0A0D8GMG5	**ABUW_1060**	*n.a.*	1-	5,09E+08	1,18E+09	-1,23	2,45	0					**0,9651**	0,0122	0,0048	0,0179	**0,8094**	**14,5314**	Spl
45	DNA binding	Transcriptional regulation	HTH-type transcriptional regulator DmlR	A0A0D7QWA3	**ABUW_1132**	*dmlR_7*	1-	2,87E+08	6,62E+08	-1,23	3,33	1-	9,64E+07	3,24E+08	-1,75	1,53	0,0492	0,0392	0,0109	**0,9007**	0,1143	-0,2009	cytoplasmic
46	Micronutrient acquisition	Heme acquisition	Heme oxygenase-like protein	A0A0D5YJQ1	**ABUW_2437**	*n.a.*	1-	1,46E+08	3,34E+08	-1,23	1,55	0					0,0013	0,0004	0,0001	**0,9982**	0,2242	-0,2009	cytoplasmic
47	Enzymes	Epimerases	Aldose 1-epimerase	A0A0D5YK99	**ABUW_2933**	*n.a.*	1-	9,42E+08	2,19E+09	-1,24	3,19	0					**0,9984**	0,0002	0,0010	0,0004	**0,9489**	**17,3396**	Spl
48	Enzymes	Transferases	Aminotransferase class I/II-fold pyridoxal phosphate-dependent enzyme	A0A0D5YEA2	**ABUW_0261**	*metY*	1-	1,33E+08	3,14E+08	-1,26	7,16	0					0,0279	0,0118	0,0025	**0,9578**	0,0926	-0,2009	cytoplasmic
49	Enzymes	Dehydrogenase	Acyl-CoA dehydrogenase	A0A0D5YFZ2	**ABUW_1467**	*n.a.*	1-	5,37E+07	1,28E+08	-1,28	2,68	0					0,0383	0,0023	0,0009	**0,9585**	0,1458	-0,2009	cytoplasmic
50	Uncharacterized proteins		Uncharacterized	A0A0D5YIF1	**ABUW_1994**	*n.a.*	1-	1,06E+08	2,61E+08	-1,32	3,09	0					**0,9954**	0,0008	0,0029	0,0009	0,0735	**12,3109**	Spl
51	Uncharacterized proteins		Uncharacterized	A0A059ZTG3	**ABUW_4122**	*n.a.*	1-	7,74E+07	1,92E+08	-1,32	1,50	0					**0,9984**	0,0003	0,0012	0,0002	0,3083	**19,7567**	Spl
52			BapA prefix-like domain-containing protein	A0A0D5YEY6	**ABUW_1120**	*n.a.*	1-	4,73E+08	1,19E+09	-1,35	2,62	0					0,0029	0,0004	0,0004	**0,9963**	**0,9145**	-0,2009	non-classically secreted
53	Secreted proteins/ surface antigen	Surface antigens	17 kDa surface antigen	A0A0D5YJG3	**ABUW_2678**	*n.a.*	1-	4,39E+07	1,11E+08	-1,35	3,50	0					0,0394	0,0164	0,0213	**0,9229**	**0,9417**	-0,2009	non-classically secreted
54	Uncharacterized proteins		Uncharacterized	A0A0D5YJ96	**ABUW_2599**	*n.a.*	1-	3,13E+07	7,92E+07	-1,36	2,17	0					0,0006	0,0001	**0,9991**	0,0003	0,2544	**12,3739**	SpII
55	Enzymes	Catalases	Catalase	A0A0E1JRA6	**ABUW_2436**	*katE*	1-	6,36E+09	1,61E+10	-1,36	2,70	1					0,0312	0,0363	0,0047	**0,9278**	0,1122	-0,2009	cytoplasmic
56	Efflux / Transport	ABC transporter family	ABC transporter glutamine-binding protein	A0A0D5YIS6	**ABUW_2420**	*glnH*	1-	2,60E+07	6,68E+07	-1,39	1,50	0					0,0017	0,0002	**0,9975**	0,0006	**0,9022**	**16,2398**	SpII
57	Stress response/ DNA repair	Stress response	Universal stress protein	A0A0D5YEG1	**ABUW_0890**	*n.a.*	1-	2,39E+08	6,45E+08	-1,45	5,88	0					0,0035	0,0006	0,0004	**0,9954**	0,0771	-0,2009	cytoplasmic
58	Uncharacterized proteins		Uncharacterized	V5V8F1	**ABUW_0181**	*n.a.*	1-	1,44E+08	3,91E+08	-1,46	4,54	0					0,0038	0,0027	0,0005	**0,9930**	0,0789	-0,2009	cytoplasmic
59	Biofilm formation/ adhesion /motility	Type IV pili	Type IV pilus response regulator protein	V5V9M9	**ABUW_0679**	*pilH*	1-	1,22E+08	3,34E+08	-1,46	1,62	0					0,0026	0,0014	0,0003	**0,9957**	0,0440	-0,2009	cytoplasmic
60	Enzymes	Dehydrogenase	3-hydroxy-2-methylbutyryl-CoA dehydrogenase	A0A0D5YG92	**ABUW_1572**	*n.a.*	1-	6,60E+07	1,80E+08	-1,47	2,27	0					0,3018	0,0273	0,0289	**0,6419**	0,0804	-0,2009	cytoplasmic
61	Enzymes	Hydrolases	Putative hydrolase YdeN	A0A0D5YN66	**ABUW_3575**	*n.a.*	1-	1,12E+08	3,18E+08	-1,52	8,83	0					0,0229	0,0004	0,0032	**0,9736**	0,3869	-0,2009	cytoplasmic
62	OMPs/ Porins		DcaP-like protein	A0A0B9X9I7	**ABUW_0826**	*n.a.*	1-	2,84E+09	8,09E+09	-1,53	9,93	1-	1,54E+09	6,4E+09	-2,05	9,78	**0,8204**	0,1407	0,0309	0,0080	**0,9572**	**13,4453**	Spl
63	Stress response/ DNA repair	DNA binding / repair	DNA breaking-rejoining protein	A0A0D5YGH9	**ABUW_1659**	*n.a.*	1-	6,38E+07	1,82E+08	-1,54	1,81	0					**0,9922**	0,0007	0,0053	0,0018	**0,5910**	**12,6278**	Spl
64	DNA binding	Transcriptional regulation	AsnC family protein	V5V8Y9	**ABUW_0177**	*lrpB*	1-	0,00E+00	1,65E+07	-1,54	1,43	0					0,0020	0,0013	0,0003	**0,9965**	0,1857	-0,2009	cytoplasmic

65	Uncharacterized proteins		Uncharacterized	A0A0D5YDS1	**ABUW_0263**	*n.a.*	1-	9,05E+08	2,63E+09	-1,55	2,55	1-	0,00E+00	1,55E+08	-4,43	12,27	0,0035	0,0001	**0,9961**	0,0004	**0,9453**	**15,8890**	SpII
66	Uncharacterized proteins		Uncharacterized	A0A0D5YK33	**ABUW_2434**	*n.a.*	1-	1,30E+08	3,76E+08	-1,56	3,78	0					0,0054	0,0004	0,0018	**0,9924**	0,0830	-0,2009	cytoplasmic
67	Enzymes	Dehydrogenase	Glucose sorbosone dehydrogenase	A0A0D5YC96	**ABUW_0055**	*n.a.*	1-	2,20E+08	6,66E+08	-1,61	5,64	0					0,0004	0,0001	**0,9992**	0,0003	**0,9209**	**19,4270**	SpII
68	Uncharacterized proteins		DUF4468 domain-containing protein	A0A0C2LH01	**ABUW_1314**	*n.a.*	1-	2,70E+08	8,10E+08	-1,61	3,86	1					0,0005	0,0001	**0,9992**	0,0002	**0,9466**	**20,9383**	SpII
69	Uncharacterized proteins		Uncharacterized	A0A0D5YIW1	**ABUW_2145**	*n.a.*	1-	3,67E+07	1,11E+08	-1,61	2,05	0					0,0017	0,0030	0,0003	**0,9951**	0,0702	-0,2009	cytoplasmic
70	Enzymes	Hydrolases	Alpha/beta hydrolase	A0A0D5YD54	**ABUW_0104**	*n.a.*	1-	1,21E+08	3,71E+08	-1,63	2,83	0					**0,9964**	0,0009	0,0021	0,0006	**0,9317**	**16,1113**	SpI
71	Enzymes	Transferases	Glutathione S-transferase	A0A0D5YHJ7	**ABUW_1635**	*ligE_1*	1-	5,33E+07	1,64E+08	-1,65	2,86	0					0,0054	0,0010	0,0006	**0,9929**	0,0815	-0,2009	cytoplasmic
72	Enzymes	Lyases	Hydroxymethylglutaryl-CoA lyase	A0A0D5YJW1	**ABUW_2456**	*n.a.*	1-	4,67E+07	1,45E+08	-1,65	2,34	0					0,0027	0,0060	0,0003	**0,9910**	0,3379	-0,2009	cytoplasmic
73	Enzymes	Transferases	Methyltransferase	A0A0D5YF88	**ABUW_0782**	*n.a.*	1-	0,00E+00	2,52E+07	-1,66	2,60	0					0,0029	0,0006	0,0002	**0,9963**	0,4766	-0,2009	cytoplasmic
74	Stress response/ DNA repair	Stress response	General stress protein 39	V5VEG3	**ABUW_2435**	*ydaD*	1-	9,77E+08	3,05E+09	-1,67	2,65	0					0,0149	0,0067	0,0025	**0,9760**	**0,8171**	-0,2009	non-classically secreted
75	Uncharacterized proteins		Uncharacterized	V5VES2	**ABUW_2621**	*n.a.*	1-	5,04E+07	1,74E+08	-1,80	1,90	0					0,0035	0,0001	0,0008	**0,9956**	0,2989	-0,2009	cytoplasmic
76	Stress response/ DNA repair	Stress response	NirD/YgiW/YdeI family stress tolerance protein/ DNA binding protein	A0A0E1FH39	**ABUW_1471**	*n.a.*	1-	2,95E+08	1,03E+09	-1,82	2,36	0					**0,9950**	0,0002	0,0044	0,0004	0,0958	**17,9899**	SpI
77	LPS biosynthesis, transport and assembly	Biosynthesis of lipid A	UDP-3-O-acylglucosamine N-acyltransferase	V5VDY4	**ABUW_1743**	*lpxD*	1-	7,33E+07	2,67E+08	-1,88	13,38	1					0,0035	0,0028	0,0004	**0,9933**	0,0591	-0,2009	cytoplasmic
78	Enzymes	Transaminases	4-aminobutyrate transaminase	A0A0D5YDJ8	**ABUW_0203**	*gabT*	1-	2,52E+08	9,99E+08	-2,02	2,06	0					0,0095	0,0015	0,0024	**0,9866**	0,0844	-0,2009	cytoplasmic
79	Micronutrient acquisition	heme acquisition	Bacterichemerythrin	A0A0Q2HWF1	**ABUW_3037**	*n.a.*	1-	1,13E+08	4,63E+08	-2,05	4,68	0					0,0038	0,0022	0,0011	**0,9929**	0,1003	-0,2009	cytoplasmic
80	Peptidases/Proteases	Aminopeptidase	Aminopeptidase	A0A0D5YG57	**ABUW_1203**	*pepN_2*	1-	7,23E+07	3,01E+08	-2,10	1,49	0					**0,9839**	0,0014	0,0127	0,0021	**0,6516**	**12,2716**	SpI
81	Antibiotic Resistance	Beta-lactamase family	Metal-dependent hydrolase of the beta-lactamase superfamily	A0A0D5YEE4	**ABUW_0920**	*n.a.*	1-	2,85E+08	1,21E+09	-2,11	4,83	1					0,1474	0,0022	0,0014	**0,8489**	**0,9318**	-0,2009	non-classically secreted
82	Enzymes	Transposases	ISAba125 transposase	I0CDW4	**ABUW_4086**	*n.a.*	1-	3,62E+07	1,66E+08	-2,22	8,47	0					0,0025	0,0007	0,0011	**0,9958**	0,0817	-0,2009	cytoplasmic
83	Stress response/ DNA repair	Stress response	LemA family protein	A0A0E1FJA9	**ABUW_0534**	*n.a.*	1-	2,20E+07	1,06E+08	-2,29	4,24	0					0,0148	0,0004	0,0101	**0,9747**	0,1286	-0,2009	cytoplasmic
84	Uncharacterized proteins		DUF4142 domain-containing protein	A0AD5YKI0	**ABUW_2679**	*n.a.*	1-	8,60E+08	4,19E+09	-2,32	4,65	0					**0,9812**	0,0007	0,0106	0,0075	**0,8765**	**7,9626**	SpI
85	Enzymes	Synthases	Anthranilate synthase	A0A077GKT8	**ABUW_2349**	*n.a.*	1-	5,96E+07	3,04E+08	-2,39	1,55	0					0,0011	0,0005	0,0003	**0,9981**	0,0548	-0,2009	cytoplasmic
86	Secreted proteins/ surface antigen	Surface antigens	Surface antigen	A0AD5YIU7	**ABUW_2440**	*n.a.*	1-	1,17E+09	6,12E+09	-2,41	12,04	0					0,0051	0,0023	0,0013	**0,9913**	**0,8941**	-0,2009	non-classically secreted
87	Uncharacterized proteins		Uncharacterized	A0A059ZHC9	**ABUW_3579**	*n.a.*	1-	3,29E+08	1,75E+09	-2,43	13,38	1-	0,00E+00	7,03E+08	-5,76	13,54	**0,8973**	0,0079	0,0888	0,0061	**0,8752**	**13,2856**	SpI
88	Uncharacterized proteins		Uncharacterized	A0AD5YEX4	**ABUW_0514**	*n.a.*	1-	8,70E+07	4,93E+08	-2,51	7,00	1-	0,00E+00	1,4E+08	-4,59	13,54	0,0008	0,0000	**0,9989**	0,0002	**0,9387**	**20,7542**	SpII
89	Enzymes	Transferases	Acetyltransferase	V5VBK4	**ABUW_1603**	*n.a.*	1-	0,00E+00	2,20E+07	-2,60	1,54	0					0,0027	0,0018	0,0004	**0,9952**	0,0783	-0,2009	cytoplasmic
90	Biofilm formation/ adhesion /motility	Type IV pili	Fimbrial assembly protein	A0AD5YCR0	**ABUW_0291**	*pilN, comN*	1-	0,00E+00	3,51E+07	-2,64	1,41	0					0,0015	0,0003	0,0009	**0,9973**	0,2678	-0,2009	cytoplasmic
91	Enzymes	Oxoprolinases	5-oxoprolinase subunit A	A0AD5YK59	**ABUW_2606**	*pxpA*	1-	0,00E+00	2,66E+07	-2,66	1,99	0					0,0079	0,0063	0,0017	**0,9842**	0,0822	-0,2009	cytoplasmic
92	Biofilm formation/ adhesion /motility	Biofilm	Csu pilus subunit CsuB	V5VC75	**ABUW_1631**	*csuB_2*	1-	1,33E+09	1,92E+08	-2,80	1,62	0					**0,9960**	0,0012	0,0024	0,0004	**0,9262**	**19,3031**	SpI
93	Protein export	Central subunit of translocase SecYEG	Protein translocase subunit	A0A090B767	**ABUW_0426**	*secY*	1-	0,00E+00	5,19E+07	-2,84	8,54	1					0,0277	0,0115	0,0048	**0,9559**	0,1624	**7,2011**	TMH
94	Uncharacterized proteins		Uncharacterized	A0AD5YKD4	**ABUW_2686**	*n.a.*	1-	0,00E+00	2,19E+07	-2,86	1,36	0					0,0047	0,0001	0,0007	**0,9944**	0,0429	-0,2009	cytoplasmic
95	Enzymes	Oxidoreductases	NADH-quinone oxidoreductase subunit N	V5VG26	**ABUW_3165**	*nuoN*	1-	0,00E+00	2,60E+07	-2,88	1,42	1					0,0006	0,0001	0,0010	**0,9983**	0,4108	**9,4754**	TMH
96	Uncharacterized proteins		Uncharacterized	A0AD5YKJ4	**ABUW_2598**	*n.a.*	1-	0,00E+00	6,26E+07	-2,92	10,28	0					0,2128	0,0091	0,0256	**0,7525**	**0,7815**	**0,5909**	TMH

97	Biofilm formation/ adhesion /motility	Type I pili	type I pilus chaperone usher secretion system	A0A0D5YGE2	**ABUW_1632**	*csuC*	1-	2,86E+08	2,21E+09	-2,96	13,38	0					0,9954	0,0003	0,0027	0,0016	0,9363	13,5890	Spl
98	Secretion	Type VI secretion	Type VI secretion system effector, Hcp1 family protein	R9RIP4	**ABUW_2578**	*hcp*	1-	5,61E+07	4,60E+08	-3,07	3,14	0					0,0106	0,0032	0,0037	0,9825	0,9540	-0,2009	non-classically secreted
99	Enzymes	Isomerases	2-(1,2-epoxy-1,2-dihydrophenyl)acetyl-CoA isomerase	A0A077GPV7	**ABUW_2529**	*paaB*	1-	0,00E+00	3,91E+07	-3,25	5,33	0					0,0044	0,0006	0,0008	0,9942	0,0971	-0,2009	cytoplasmic
100	Secretion	Type II secretion	Type II secretion system protein N	A0A0D5YMW5	**ABUW_3608**	*gspN*	1-	0,00E+00	2,42E+07	-3,26	1,38	0					0,0265	0,0004	0,0059	0,9672	0,3420	12,0189	TMH
101	Biofilm formation/ adhesion /motility	Type IV pili	Pilus assembly protein tip-associated adhesin	A0A0D5YDX1	**ABUW_0317**	*pilY1*	1-	0,00E+00	6,20E+07	-3,31	6,35	0					0,9502	0,0037	0,0040	0,0420	0,9421	17,2010	Spl
102	OMPs/ Porins		TMF family protein	A0A0D5YIM2	**ABUW_2448**	*n.a.*	1-	0,00E+00	7,76E+07	-3,34	11,68	0					0,9820	0,0010	0,0146	0,0024	0,8997	14,4194	Spl
103	Efflux / Transport	ABC transporter family	ABC transporter ATP-binding protein	A0A0D5YJC8	**ABUW_2280**	*n.a.*	1-	0,00E+00	1,94E+07	-3,35	1,38	0					0,0158	0,0006	0,0017	0,9820	0,1942	-0,2009	cytoplasmic
104	Uncharacterized proteins		Uncharacterized	A0A0D5YMD1	**ABUW_3337**	*n.a.*	1-	0,00E+00	4,16E+07	-3,53	6,03	1					0,0077	0,0067	0,0008	0,9849	0,1141	-0,2009	cytoplasmic
105	Enzymes	Hydrolases	Amidohydrolase	A0A0D5YKP8	**ABUW_3204**	*n.a.*	1-	0,00E+00	7,35E+07	-3,62	13,38	0					0,9014	0,0084	0,0680	0,0222	0,9383	4,9212	Spl
106	Uncharacterized proteins		DUF1176 domain-containing protein	A0A0D5YDS8	**ABUW_0709**	*n.a.*	1-	0,00E+00	7,93E+07	-3,87	1,64	0					0,9987	0,0002	0,0008	0,0003	0,9275	17,9895	Spl
107	Biofilm formation/ adhesion /motility	Type IV pili	Type IV pilus hybrid sensor kinase/response regulator PilL	A0A0D5YFD1	**ABUW_0682**	*pilL*	1-	0,00E+00	6,73E+07	-3,89	2,07	0					0,0071	0,0009	0,0002	0,9918	0,1335	-0,2009	cytoplasmic
108	Micronutrient acquisition	Iron acquisition	Ferric acinetobactin receptor	A0A0D5YG89	**ABUW_1177**	*bauA*	1-	0,00E+00	4,42E+07	-3,94	3,55	0					0,2736	0,1966	0,0121	0,5176	0,9501	-0,2009	non-classically secreted
109	Lipoproteins	Lipoproteins	Lipoprotein, putative	A0A0D7R2P7	**ABUW_0797**	*n.a.*	1-	0,00E+00	7,68E+07	-3,96	3,08	0					0,0202	0,0001	0,9790	0,0007	0,8544	9,9231	SpII
110	Biofilm formation/ adhesion /motility	Type IV pili	Type IVa pilus ATPase	A0A086HYC5	**ABUW_3032**	*pilU, pilT*	1-	0,00E+00	4,60E+07	-4,11	2,57	0					0,0041	0,0066	0,0011	0,9882	0,0697	-0,2009	cytoplasmic
111	Biofilm formation/ adhesion /motility	Type IV pili	Type IV-A pilus assembly ATPase	A0A0D5YLN2	**ABUW_3549**	*pulE, pilB*	1-	0,00E+00	9,04E+07	-4,69	1,60	0					0,0038	0,0050	0,0005	0,9906	0,0692	-0,2009	cytoplasmic
112	Uncharacterized proteins		DUF805 domain-containing protein	A0A0D5YCT2	**ABUW_0248**	*n.a.*	1-	0,00E+00	1,41E+08	-4,74	1,78	0					0,0035	0,0015	0,0010	0,9940	0,1586	6,6543	TMH
113	Uncharacterized proteins		Uncharacterized	A0A059ZLS5	**ABUW_2442**	*n.a.*	1-	0,00E+00	4,73E+07	-4,79	2,20	0					0,0018	0,0002	0,0002	0,9978	0,1772	-0,2009	cytoplasmic
114	Uncharacterized proteins		Uncharacterized	V5VF22	**ABUW_2700**	*n.a.*	1-	0,00E+00	1,59E+08	-5,24	13,38	0					0,0073	0,0011	0,0012	0,9903	0,0978	-0,2009	cytoplasmic
115	Biofilm formation/ adhesion /motility	Type IV pili	Type IV pilin structural subunit	A0A0D5YCX7	**ABUW_0304**	*pilA*	1-	6,87E+07	2,86E+09	-5,41	13,38	1-	0,00E+00	6,69E+08	-5,87	11,61	0,2278	0,0040	0,0331	0,7351	0,9507	-0,2009	non-classically secreted
116	Biofilm formation/ adhesion /motility	Type IV pili	Fimbrial assembly protein	A0A0D5YCW8	**ABUW_0294**	*pilQ, comQ*	1-	0,00E+00	2,82E+08	-6,09	1,75	1-	0,00E+00	2,07E+08	-5,10	1,35	0,9053	0,0610	0,0260	0,0077	0,9340	8,2619	Spl
117	Uncharacterized proteins		Uncharacterized	A0A0D5YMI4	**ABUW_3453**	*n.a.*	1-	0,00E+00	2,05E+08	-6,79	2,90	1-	0,00E+00	1,7E+08	-5,24	3,23	0,0674	0,0024	0,1366	0,7936	0,8761	-0,2009	non-classically secreted
118	Biofilm formation/ adhesion /motility	Biofilm	Biofilm-associated protein	A0A0D5YFJ5	**ABUW_0916**	*n.a.*	1-	0,00E+00	6,82E+08	-7,87	1,36	0					0,0241	0,0035	0,0085	0,9639	0,9130	-0,2009	non-classically secreted
119	**OMP biogenesis**	**Chaperone proteins**	**Periplasmic serine endoprotease DegP-like**	**V5VAG2**	**ABUW_1027**	***mucD_1, degP***	1-	0,00E+00	1,41E+09	-8,25	4,62	1-	0,00E+00	2,13E+08	-4,32	6,72	0,9812	0,0109	0,0034	0,0045	0,8877	9,1970	Spl
120	Antibiotic Resistance	Aminoglycoside−modifying Enzyme	APH(3')-VI family aminoglycoside O-phosphotransferase	G1D8S2	**ABUW_4087**	*aphA6*	1-	0,00E+00	3,02E+09	-9,02	8,53	1					0,0060	0,0010	0,0011	0,9919	0,1261	-0,2009	cytoplasmic
121	**OMP biogenesis**	**Chaperone proteins**	**OmpH family outer membrane protein**	**V5VCL3**	**ABUW_1742**	***skp***	1-	0,00E+00	3,69E+09	-9,04	13,38	1-	0,00E+00	1,79E+08	-3,69	4,10	0,9938	0,0013	0,0040		0,9511	17,1670	Spl
122	**OMP biogenesis**	**Chaperone proteins**	**Unfolded protein binding**	**A0A077GP18**	**ABUW_2268**	***surA***	1-	0,00E+00	5,11E+09	-10,10	13,38	0					0,9729	0,0208	0,0048	0,0015	0,4247	-0,2009	Spl
123	Peptidases/Proteases	M15 family peptidase	Peptidase M15 family protein	A0A0M3F9E6	**ABUW_2637**	*n.a.*	1					1+	1,15E+08	0,00E+00	4,17	2,71	0,0013	0,0001	0,9980	0,0006	0,2036	-0,2009	SpII
124	Enzymes	Hydroxylases	Aspartyl beta-hydroxylase	A0A059ZCV8	**ABUW_3570**	*lpxO*	1					1+	1,06E+08	0,00E+00	4,10	4,51	0,0139	0,0002	0,0494	0,9364	0,1820	-0,2009	cytoplasmic/*TMH*
125	Signal Peptides		Signal peptide	A0A059ZKY2	**ABUW_0603**	*n.a.*	1					1+	1,14E+08	0,00E+00	3,98	2,98	0,9977	0,0002	0,0019	0,0002	0,7746	15,0506	Spl
126	DNA binding	Transcriptional regulation	Bacterial regulatory, Fis family protein	V5VDB2	**ABUW_1533**	*fis*	1					1+	1,38E+08	0,00E+00	3,95	2,63	0,0039	0,0010	0,0005	0,9946	0,1256	-0,2009	cytoplasmic
127	Efflux / Transport		Efflux pump membrane transporter	A0A0D5YHB7	**ABUW_1975**	*adeB*	1					1+	9,65E+07	0,00E+00	3,54	2,74	0,0438	0,0053	0,0115	0,9394	0,0954	7,4768	TMH
128	Enzymes	Transferases	Homoserine O-succinyltransferase	A0A0D5YLM4	**ABUW_3406**	*metX*	1					1+	6,01E+07	0,00E+00	3,53	13,54	0,0039	0,0008	0,0003	0,9950	0,3493	-0,2009	cytoplasmic

129	Efflux / Transport	Efflux of Ni and Co	RcnB family protein	V5VJF6	**ABUW_3851**	*n.a.*	1					1+	1,40E+08	0,00E+00	3,50	1,57	**0,9982**	0,0003	0,0013	0,0003	**0,7673**	**16,5668**	Spl
130	Enzymes	Hydrolases	Alpha/beta hydrolase	A0A0D5YNT3	**ABUW_3873**	*estA*	1					1+	1,06E+08	0,00E+00	3,36	2,00	0,0136	0,0040	0,0007	**0,9817**	0,1727	-0,2009	cytoplasmic
131	Stress response/ DNA repair	DNA binding / repair	UvrABC system protein C	A0A0D5YMT2	**ABUW_3568**	*uvrC*	1					1+	9,17E+07	0,00E+00	3,34	3,39	0,0032	0,0010	0,0004	**0,9954**	0,0897	-0,2009	cytoplasmic
132	Enzymes	Hydratases	Class II fumarate hydratase	A0A0B4A3C4	**ABUW_2104**	*aspA*	1					1+	7,56E+08	0,00E+00	3,30	13,54	0,0062	0,0054	0,0009	**0,9875**	0,1114	-0,2009	cytoplasmic
133	Enzymes	Dehydratases	Delta-aminolevulinic acid dehydratase	A0A0D5YK70	**ABUW_3022**	*hemB*	1					1+	7,75E+07	0,00E+00	3,30	1,32	0,0060	0,0020	0,0016	**0,9904**	0,1214	-0,2009	cytoplasmic
134	Lipoproteins	Biosynthesis / assembly	Lipoprotein releasing system transmembrane protein LolC/E family	A0A0D5YFP2	**ABUW_0974**	*lolC*	1					1+	8,95E+07	0,00E+00	3,01	6,14	0,0034	0,0002	0,0011	**0,9953**	0,0826	-0,2009	cytoplasmic/ *TMH*
135	DNA binding	Transcriptional regulation	LysR family transcriptional regulator	A0A0D7QWZ7	**ABUW_1906**	*dmlR_5*	1					1+	9,37E+07	0,00E+00	2,95	3,85	0,0042	0,0029	0,0008	**0,9922**	0,0624	-0,2009	cytoplasmic
136	Enzymes	Transferases	tRNA (guanine-N(7)-)-methyltransferase	V5VGG6	**ABUW_2727**	*trmB_2*	1					1+	3,19E+07	0,00E+00	1,43	1,35	0,0016	0,0032	0,0002	**0,9950**	0,0751	-0,2009	cytoplasmic
137	Peptidoglycan biosynthesis/ peptidoglycan organization	Synthesis of cross-linked peptidoglycan from lipid intermediates	Penicillin-binding protein 1B	A0A0D5YGT7	**ABUW_1358**	*mrcB*	1					1+	1,17E+09	5,25E+08	1,15	1,96	0,0017	0,0003	0,0022	**0,9958**	**0,8569**	**4,6339**	TMH
138	Efflux / Transport	RND- efflux pump family	Efflux pump membrane transporter	Q2FD94	**ABUW_0843**	*adeJ*	1					1+	1,66E+09	7,89E+08	1,08	1,31	0,0732	0,0032	0,0332	**0,8904**	0,1465	**6,4880**	TMH
139	Degradation		Membrane protease subunit/ Band 7 protein	A0A090B7T1	**ABUW_0821**	*gmcA*	1					1-	2,18E+08	4,50E+08	-1,04	2,20	0,0135	0,0005	0,0094	**0,9766**	0,0911	-0,2009	cytoplasmic/*TMH*
140	Uncharacterized proteins		uncharacterized	A0A0D5YEL0	**ABUW_0375**	*n.a.*	1					1-	1,25E+09	2,68E+09	-1,11	1,51	0,0051	0,0001	**0,9944**	0,0003	**0,8438**	**20,4377**	SpII
141	OMPs/ Porins	OmpW familiy	OmpW family protein	A0A0D5YMU6	**ABUW_3583**	*n.a.*	1					1-	5,09E+09	1,25E+10	-1,28	2,13	**0,9738**	0,0003	0,0127	0,0132	**0,8388**	**15,1168**	Spl
142	Lipoproteins	Biosynthesis / assembly	incorporation of lipoproteins in the outer membrane after release by LolA	A0A0D5YKQ1	**ABUW_3091**	*lolB*	1					1-	0,00E+00	3,49E+07	-2,09	2,17	0,0006	0,0001	**0,9990**	0,0003	**0,9236**	**10,5007**	SpII
143	Efflux / Transport	RND- efflux pump family	Outer membrane efflux family protein	V5VEI6	**ABUW_2644**	*bepC_2*	1					1-	6,23E+07	2,76E+08	-2,13	3,35	0,1777	0,0018	0,0400	**0,7805**	**0,6573**	-0,2009	non-classically secreted
144	Protein transport / folding/ Chaperone proteins	disulfide bond formation	Thiol:disulfide interchange protein	A0A0D5YDT4	**ABUW_0665**	*n.a.*	1					1-	0,00E+00	4,98E+07	-2,15	3,19	**0,9988**	0,0001	0,0007	0,0004	**0,8387**	**24,2797**	Spl
145	Enzymes	Dehydrogenase	Aldehyde dehydrogenase	A0A0D5YL10	**ABUW_2794**	*n.a.*	1					1-	0,00E+00	9,09E+07	-2,27	3,96	0,0038	0,0057	0,0009	**0,9896**	0,0708	-0,2009	cytoplasmic
146	Biofilm Formation	Type IV pili	Pilus assembly protein	A0A0D5YDP9	**ABUW_0293**	*pilP, comL*	1					1-	0,00E+00	6,31E+07	-2,28	1,38	0,0015	0,0002	**0,9980**	0,0004	0,1346	**16,9045**	SpII
147	Biofilm Formation	Type IV pili	Pilus assembly protein	V5V999	**ABUW_0292**	*pilO, comO*	1					1-	0,00E+00	5,05E+07	-2,42	1,14	0,0004	0,0002	0,0027	**0,9967**	**0,6198**	-0,2009	non-classically secreted
148	Secretion	Type VI secretion	Type IV secretion protein Rhs	A0A0D5YJ30	**ABUW_2617**	*rhs*	1					1-	0,00E+00	4,29E+07	-2,54	1,60	0,0075	0,0011	0,0005	**0,9909**	0,4796	-0,2009	cytoplasmic
149	Uncharacterized proteins		uncharacterized	A0A0D5YPB6	**ABUW_4120**	*n.a.*	1					1-	0,00E+00	3,10E+07	-2,61	2,63	0,0005	0,0001	0,0182	**0,9813**	0,0839	**16,6156**	TMH
150	OMPs/ Porins	OmpA family	OmpA family protein	A0A0D5YJK8	**ABUW_2730**	*arfA*	1					1-	0,00E+00	9,01E+07	-2,65	5,71	0,0034	0,0038	0,0008	**0,9920**	**0,9480**	-0,2009	non-classically secreted
151	Lipoproteins	Lipoproteins	NLPA lipoprotein	A0A0D5YJY5	**ABUW_2820**	*n.a.*	1					1-	0,00E+00	8,07E+07	-3,43	1,45	0,0013	0,0001	**0,9984**	0,0002	**0,9472**	**23,4721**	SpII
152	Efflux / Transport	RND- efflux pump family	HlyD family efflux transporter periplasmic adaptor subunit	Q2FD85	**ABUW_0967**	*n.a.*	1					1-	0,00E+00	1,13E+08	-3,47	1,84	0,0141	0,0028	0,0082	**0,9749**	**0,9534**	-0,2009	non-classically secreted
153	Membrane fusion protein		Membrane fusion protein (MFP) family protein	Q2FD77	**ABUW_2642**	*prsE*	1					1-	0,00E+00	9,50E+07	-3,52	1,31	0,0003	0,0002	0,0004	**0,9990**	0,0835	**4,0947**	TMH
154	Enzymes	Dehydratases	Imidazoleglycerol-phosphate dehydratase	V5VAN2	**ABUW_0250**	*hisB*	1					1-	0,00E+00	1,38E+08	-3,60	2,64	0,0031	0,0005	0,0005	**0,9959**	0,0602	-0,2009	cytoplasmic
155	DNA binding	Repressors	HTH-type transcriptional repressor YvoA	V5V8J4	**ABUW_0075**	*hutC*	1					1-	0,00E+00	1,38E+08	-3,76	2,80	0,0075	0,0021	0,0008	**0,9896**	0,0613	-0,2009	cytoplasmic
156	Enzymes	Hydratases	Crotonase/enoyl-CoA hydratase family protein	A0A0D5YM79	**ABUW_3307**	*n.a.*	1					1-	0,00E+00	1,87E+08	-4,00	10,00	0,0033	0,0044	0,0004	**0,9919**	0,0648	-0,2009	cytoplasmic
157	Enzymes	Reductases	Dihydrofolate reductase	B0FND5	**ABUW_4050**	*dfrVII*	1					1-	0,00E+00	7,70E+07	-5,14	3,25	0,0285	0,0011	0,0045	**0,9660**	0,1054	-0,2009	cytoplasmic
158	Enzymes	Reductases	Acyl coenzyme A reductase	V5V971	**ABUW_0260**	*acr1_1*	1					1-	0,00E+00	2,76E+08	-5,46	2,31	0,0535	0,2329	0,0066	**0,7070**	0,1022	-0,2009	cytoplasmic
159	Biofilm Formation	Chemotaxis	Chemotaxis protein	V5VA86	**ABUW_0681**	*pctA, pilJ*	1					1-	0,00E+00	4,90E+08	-5,59	5,77	0,0013	0,0003	0,0059	**0,9925**	0,1213	-0,2009	cytoplasmic/*TMH*
160	Uncharacterized proteins		uncharacterized	A0A0C0BBP5	**ABUW_0812**	*n.a.*	1					1-	0,00E+00	1,76E+08	-6,73	1,75	0,0044	0,0005	0,0010	**0,9941**	0,1766	-0,2009	cytoplasmic

11. Danksagung

Obwohl mir die Arbeit mit *Acinetobacter baumannii* am Institut für medizinische Mikrobiologie und Hygiene Tübingen sehr viel Spaß gemacht hat, gab es einige Rückschläge und Hürden an denen ich ohne Hilfe und Unterstützung verzweifelt wäre.

Mein ganz besonderer Dank (der diese Thesis um einiges verlängern würde, wenn ich alles aufschreiben würde) gilt Frau PD Dr. Monika Schütz. Ich danke Dir für die warmherzige Aufnahme in die Arbeitsgruppe und den Glauben und das Vertrauen in mich, obwohl ich mich davor nicht viel mit Mikrobiologie auseinandergesetzt hatte. Deine fachlichen aber auch freundschaftlichen Ratschläge haben mir immer geholfen, dass ich an unserem lieben *Acinetobacter* nicht verzweifelt bin. Du hattest für jedes Problem ein offenes Ohr und zusätzlich eine passende Lösung parat.

Ebenso möchte ich mich herzlich bei PD Dr. Erwin Bohn bedanken. Zum einen für die vielen hilfreichen fachlichen Ratschläge und auch Verbesserungsvorschläge, die das Projekt stetig vorangetrieben haben. Aber auch für deine kreativen und unterhaltsamen Geschichten und Anekdoten, die triste Labortage bunter gemacht haben.

Bei der gesamten AG Schütz/Bohn: Tanja Späth, Fabian Renschler, Annette Mayer, Janes Krusche, Elena Weber, Katharina Astfalk, Kathrin Vöhringer, Valentin Egle und Ole Eggers möchte ich mich für das freundschaftliche und sehr gute Arbeitsklima bedanken. Ich kann mich an keinen Tag erinnern, an dem wir nicht zusammen gelacht haben und interessante Gespräche geführt haben.

Auch bei den ehemaligen Mitgliedern der AG Schütz/Bohn: Janina Geißert, Michael Sonnabend, Malte Schweers und besonders Kristina Klein möchte ich mich für die warmherzige Aufnahme in die Arbeitsgruppe sowie die entgegengebrachte Hilfe und Geduld bedanken.

Bei den Ärzten und Fachmikrobiologen Elias Walter, Michael Buhl, Johannes Zens, Philipp Oberhettinger und Annika Schmidt bedanke ich mich rechtherzlich für die vielen Diagnosen und Ratschläge. Besonders Annika und Philipp danke ich für die große und ständige Hilfsbereitschaft und die vielen interessante und auch lustige Diskussion beim Blutspenden oder im Auto.

Des Weiteren möchte ich mich noch bei allen anderen Kollegen des 2. Stocks für die große Hilfsbereitschaft und das freundliche Arbeitsklima bedanken.
Mein ganz besonderer Dank gilt Christina Engesser und Manuela Löffler für die ständige, hilfsbereite und warmherzige Unterstützung, das Aufmuntern und das Wissen das ihr mir beigebracht habt.

Meinem Mann Arthur möchte ich für die grenzenlose Liebe und Unterstützung danken. Du hast mich ständig aufgebaut und ermutigt weiter zu machen und immer an mich geglaubt.

Meiner Familie, besonders meinen Eltern, danke ich für die jahrelange und unermüdliche Unterstützung, Ermutigung und die Möglichkeit meiner Leidenschaft zur Wissenschaft nachzugehen.

12. Eidesstattliche Erklärung

Hiermit erkläre ich an Eides Statt, dass ich die vorliegende Arbeit zum Thema

„The role of the periplasmic chaperones SurA, Skp and DegP in fitness, outer membrane integrity, antibiotic susceptibility and virulence of *Acinetobacter baumannii*: same-same, but different?"

eigenständig, ohne unerlaubte Hilfe und nur unter Verwendung der angegebenen Hilfsmittel angefertigt habe. Alle sinngemäß und wörtlich übernommenen Textstellen aus Veröffentlichungen oder aus anderwärtigen, fremden Äußerungen habe ich als solche erkenntlich gemacht.

Tübingen, den 06.04.2021